A STRUCTURAL AND COMPUTATIONAL ANALYSIS OF MOLECULAR MECHANISMS FOR MEMBRANE ADAPTATION TO EXTREME STRESS

By

Seunho Jung

A DISSERTATION

Submitted to

Michigan State University

in partial fulfillment of requirements

for the degree of

DOCTOR OF PHILOSOPHY

Department of Biochemistry

1993

ABSTRACT

A STRUCTURAL AND COMPUTATIONAL ANALYSIS OF MOLECULAR MECHANISMS FOR MEMBRANE ADAPTATION TO EXTREME STRESS

By

Seunho Jung

One of the most complex systems in cells is the biological membrane. This system displays a very sensitive, highly tuned adaptive mechanism to changes in environmental parameters. This adaptive response includes changes in the composition of lipids as well as changes in their structure. The lipid biosynthetic machinery is intimately coupled to the dynamic state of the membrane.

A new adaptive system was discovered in *Sarcina ventriculi* and its molecular mechanism was studied. In this response, a family of transmembrane lipid species is formed in response to any perturbation which increases the dynamical state of the membrane. This response, in effect, resulted in a transition from a bilayer to a bipolar monolayer membrane system. A similar phenomenon was observed in *Clostridium thermohydrosulfuricum*. It was determined that this transition is a spontaneous event which does not require new protein synthesis and that the pairing partners is selected on a strict probability basis. The possible effects of transmembrane species are capable of significantly reducing the motional freedom of regular chain length species which are in close proximity. They also lead to increased packing of the void which usually exists in the area between the bilayer leaflets.

To my parents, Mr. Takban Jung and Mrs. Joongson Jun Jung

and my wife, Wonjae

and my son

Sungmo

ACKNOWLEDGMENTS

I thank Rawle I. Hollingsworth for being an excellent guidance and precious advice during my graduate studies. His enthusiastic passion for the truth is a great role model to me. I also thank my wife, Wonjae Rho Jung, for her tolerance, love and prayer. I also thank Drs. Ester McGroarty, Zach Burton, Ned Jackson and William Wells for their kind service as members of my guidance committee. I thank those persons who have helped me in this endeavor. Thank to Drs. Gregory Zeikus and Susan Lowe for helping and allowing me to use of their cell culture facilities; to Dr. YounSuk Jang for helping me about FAB-MS experiments; to Dr. Long Le for the NMR training. I also thank our lab. colleagues, Debbie, Chuck, Maria, Rob, Luc, Ben and Ying. Particularly, I thank K. Kim for his kindness throughout the research. I also thank my friends, Jaeman Lee, JaeNeung Kim and Dongkuy Choi for their encouragement and friendship.

I thank my parents for their love, support, encouragement and prayer during this endeavor. Most importantly, I thank my Lord, Jesus Christ for His grace for every moments that I have met since I came here.

TABLE OF CONTENTS

TABLE OF CONTENTS (cont'd)

TABLE OF CONTENTS (cont'd)

PAGE

TABLE OF CONTENTS (cont'd)

PAGE

TABLE OF CONTENTS (cont'd)

PAGE

TABLE OF CONTENTS (cont'd)

PAGE

TABLE OF CONTENTS (cont'd)

PAGE

LIST OF TABLES

PAGE

CHAPTER II

CHAPTER III

CHAPTER IV

LIST OF TABLES (cont'd)

PAGE

CHAPTER V

CHAPTER VI

LIST OF FIGURES

PAGE

CHAPTER I

CHAPTER II

PAGE

CHAPTER III

LIST OF FIGURES (cont'd)

PAGE

CHAPTER IV

CHAPTER V

PAGE

PAGE

CHAPTER VI

LIST OF FIGURES (cont'd)

PAGE

CHAPTER VII

LIST OF FIGURES (cont'd)

PAGE

LIST OF ABBREVIATIONS

ACP	Acyl Carrier Protein
AMU	Atomic Mass Unit
BD	Brownian Dynamics
CL	Cardiolipin
DEPT	Distortionless Enhanced by Polarization Transfer
DQF-COSY	Double Quantum Filtered-Correlation Spectroscopy
EI-MS	Electron Impact-Mass Spectrometry
ev	electron volt
FA	Fatty Acids
FAB-MS	Fast Atom Bombardment-Mass Spectrometry
FTIR	Fourier Transform Infrared
GC	Gas Chromatography
GC/MS	Gas Chromatography/Mass Spectrometry
MC	Monte Carlo
MD	Molecular Dynamics
NBA	Nitro Benzyl Alcohol
NL	Neutral Lipids
NMR	Nuclear Magnetic Resonance
PC	Phosphatidyl choline
PE	Phosphatidyl ethanolamine
PS	Phosphatidyl serine

LIST OF ABBREVIATIONS (cont'd)

RCM	Random Coupling Model
RMS	Root Mean Square
TFA	Trifluoroacetic acid
TLC	Thin Layer Chromatography

CHAPTER I

INTRODUCTION

Membrane Dynamics

All biological structures are dynamic, and the extent of the rate and motion are important in considering biological function. This is true most certainly for membranes. The fluid mosaic model (1, 2) has helped focus attention on the mobility of membrane components by conceptualizing the membrane as a sea of lipid in which embedded proteins are freely floating. The basic motivation of membrane dynamics is its relevance to biological functions. Figure 1 shows the characteristic frequencies of molecular motions of membrane proteins and lipids. Very wide ranges of motions are observed; from molecular vibrations occurring in about 10^{-14} sec (0.01 ps) to transbilayer flip-flop of lipids (3, 4) which can take many days to occur. The small frequencies of molecular vibrations indicate that there are always vibrational motions of the lipid chains. Furthermore, this vibrational motion would be very sensitive to subtle changes of external energy. Lipid rotation (5) and trans/gauche isomerization (6) also show the small frequency ranges (10 ps - 1 ns). Therefore, the relative impacts by environmental challenges can be explained by this wide range of motional frequency. For real time motional dynamics, 10 ps can cover the range from vibration to lipid rotation, including trans/gauche isomerization. There are some other motions for membrane components. Isotropic rotation (7) implies equivalent rotation in all directions with no favored rotational axis. This would be expected for a sphere rotating in a continuum and has been applied to the interpretation of the rotational properties of small hydrophobic probes dissolved in a bilayer. Conical constraint (8) describes the motion of amphipathic probes such as fatty acid derivatives. These can be considered in simple models as rigid rods tethered at the membrane surfaces.

All the motions of membrane components work under three general forces. These three long range forces (9) are the electrostatic forces, polarization (or induction) forces and London-van der Waals dispersion forces. Electrostatic forces are due to the mutual Coulomb attraction or repulsion of the net charges, or electric moments, carried by two

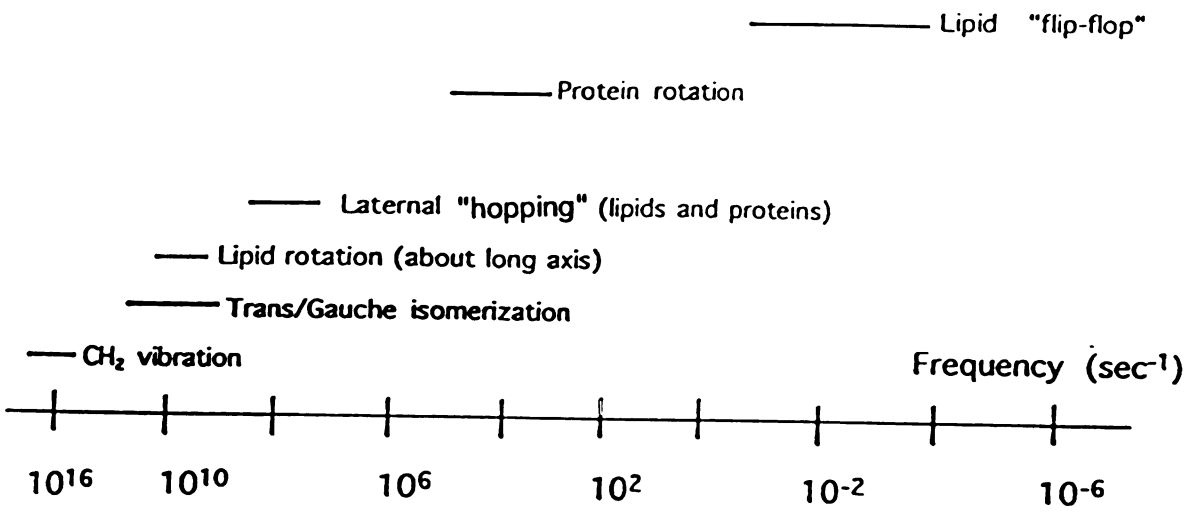

Figure 1. The characteristic frequencies of molecules of molecular motions of membrane proteins and lipids compared with the frequency ranges. The characteristic times are obtained by taking the reciprocal of the indicated frequencies. Boundaries are very approximate.

interacting molecules. Polarization forces arise from the charge separation on one molecule by the charges or permanent electric moments of the other. Typical examples are interactions between polar groups on one molecule and polarized groups on the other. London-van der Waals forces arise between all molecules, even between neutral non-polar molecules, and are due to the average interaction of an instantaneous electric moment on one molecule, brought about by charge density fluctuations, and the moment it induces on the other molecule. These forces have a purely quantum-mechanical nature. This dispersion force is of paramount importance in holding the lipid chains together through additive interactions.

For an ordinary liquid, the term "fluidity" is defined as the inverse of viscosity. This is a well-defined and easily measured physical characteristic. Viscosity is essentially a measure of the frictional resistance encountered when adjacent "layers" of fluid are moving with different velocities. Viscosity can be measured by simply observing the velocity with which a marble falls through the liquid. As applied to the membranes, the term "fluidity" is usually thought of in a more qualitative sense. It is generally meant to represent a measure of the resistance to various types of movements in the membrane. Generally, fluidity is measured by observing the motion of spin probes or fluorescent probes incorporated in the bilayer. Since the measurements are sensitive to both the rate of motion and any constraints to that motion, information about the dynamics and molecular order gets intermixed (10). Biological membranes are generally in the liquid crystalline phase, and it appears that the maintenance of membrane fluidity is critical to their function. A decrease in the fluidity of a biological membrane can cause a phase transition to a gel phase. The gel phase has different dynamic and functional properties (11). It does not allow biological function. The most dramatic evidence is from studies showing adaptations of various organisms to environmental stress.

Membrane Adaptation Mechanism of the Bacteria to Environmental Stress

The biological membrane is one of the most vulnerable components of bacteria to environmental stress. Many studies have been performed on the thermal and alcoholic stress in relation to the membrane. As for thermal stress, most bacteria develop an adaptive response system which involves fatty acid synthesis. *E. coli*, along with most (if not all) other microorganisms, synthesizes lipids with a greater proportion of unsaturated fatty acids when grown at low temperature (e.g. 25^{o}C) rather than at high temperatures (e.g. 42^{o}C) (12). This regulatory system is believed to be designed to ameliorate the effects of the temperature change on the physical state of all membrane lipids. In fact, lowering the temperature deprives the system's (membrane) energy. This low-energized system requires the disordering components (unsaturated fatty acids) to maintain the motional functionality of the membrane. Membrane functionality depends on the motional dynamics of the membrane components, particularly lipid components. In terms of that, the proportion of disordered (unsaturated) lipids to ordered (saturated) lipids in cell membranes plays a major role in membrane function. Increased incorporation of unsaturated fatty acids into the lipids decreases the temperature at which transition from ordered to disordered membrane lipids occurs, whereas increased incorporation of saturated fatty acids has the opposite effect (13). The thermal regulatory system can thus adapt the membrane lipids for optimal functioning at the new growth temperature.

Figure 2 shows the thermal regulation of fatty acid biosynthesis. According to the *in vitro* studies on purified enzymes (14, 15), the decreased growth temperature alters the activity of 3-Ketoacyl -ACP synthase II, which in turn regulates the fatty acid composition by producing more *cis*-vaccenoyl-ACP for incorporation into the lipids (16). Interestingly, the thermal regulation of the membrane depends on the activity of this one enzyme and occurs independently of new gene synthesis.

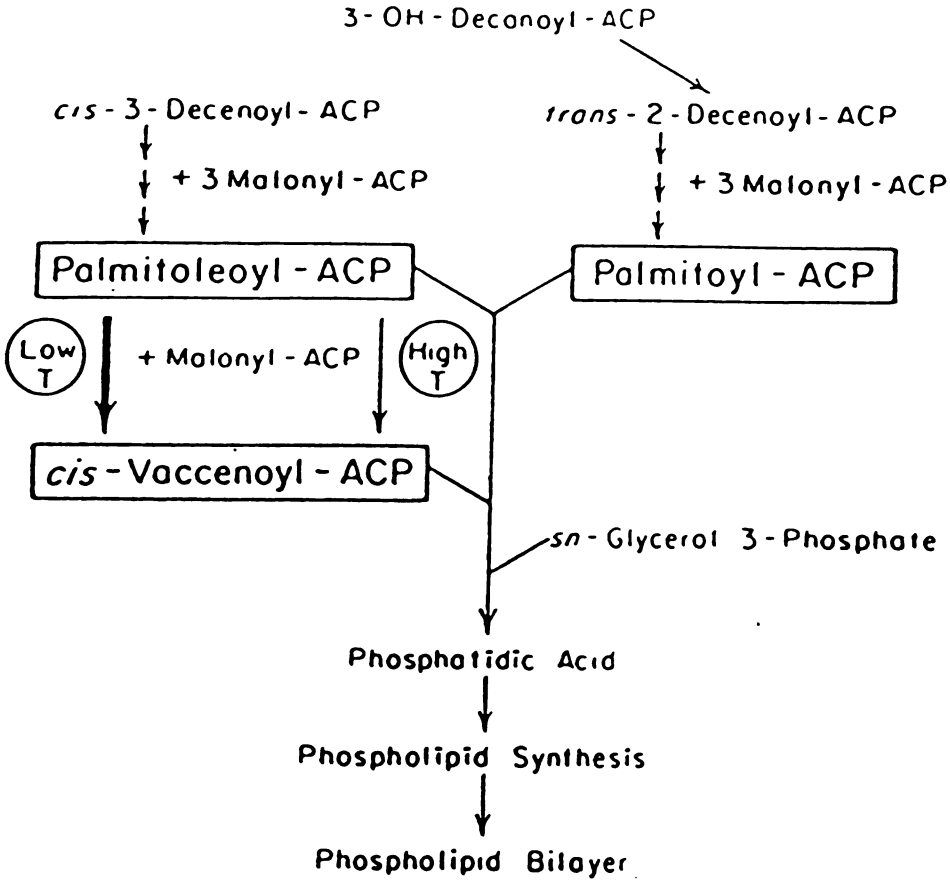

Figure 2. Thermal regulation of fatty acid biosynthesis. 3-Ketoacyl-ACP synthase II is primarily responsible for the temperature control of *E. coli* fatty acid composition by being more active in the conversion of palmitoleate to *cis*-vaccenate at lower temperatures than at higher temperatures

As another regulation to thermal stress, fatty acid chain length can be regulated. The 3-ketoacyl-ACP synthase I and II are the likely candidates for the site of chain length regulation in that both enzymes catalyze the elongation reaction. Substrate specificity studies *in vitro* indicates that one reason why membrane lipids are devoid of chains of more than 18 carbons is in part the reduced activity of synthases I and II on C_{18} substrates (59,60). Furthermore, synthase II mutants are defective in the elongation of palmitoleate to *cis*-vaccenate (61). It indicates, therefore, that synthase II plays an important role in determining the amount of C_{18} fatty acids in the membrane. Although these data indicated that condensing enzymes play a significant role in determining the chain length, physiological experiments indicate that the level of G3P (glycerol-3-phosphate) acyltransferase activity is also important. When phospholipid biosynthesis is slowed or arrested at the acyltransferase step, the fatty acids synthesized have abnormally long chains compared with the normal distribution of the fatty acids synthesized in the presence of G3P (glycerol-3-phosphate) acyltransferase activity (17). These data indicate that competition between the rate of elongation and the rate of utilization of the acyl-ACPs by the acyltransferase is a significant determinant of fatty acid chain length in *E.coli*.

Many studies (18, 19) have been performed focusing on ethanol effect on the membrane. Alcohol is an amphipathic molecule that affects microbial processes at high molar concentrations. These changes appear to be caused by colligative effects on the aqueous medium and within the membrane rather than being mediated by specific receptors. Colligative properties altered by alcohol include changes in dielectric properties, replacement of water by alcohol as a hydrogen bonding partner, and a weakening of the strength of hydrophobic bonds (20, 21). Alcohols decrease the effectiveness of the hydrophobic core of the membrane as a barrier, increasing membrane permeability and membrane leakage. Cells compensate for this effect in part by increasing the average acyl

chain length of membrane lipids, increasing the thickness of the hydrophobic core and restoring this essential barrier function (22, 23).

A membrane adaptive response to thermal or alcoholic stress in *E. coli* is to change the lipid composition by regulating the ratio of unsaturated to saturated fatty acids or by the changing chain length by two or four carbons. Besides temperature or alcohol, there are other forms of environmental stress such as pH, nutrient concentrations, osmotic pressure and pressure. However, the relevance of these factors to the membrane architecture is not known in detail.

Physiology and Biochemistry of Anaerobic Eubacteria *Sarcina ventriculi*

As a model system for membrane adaptive response to various forms of environmental stress, anaerobic facultative acidophilic eubacteria, *Sarcina ventriculi* was studied. *Sarcina ventriculi* was first observed in 1842 by Goodsir (24) in the contents of human stomach. The organism has been cultivated from the garden soil (25, 26) and the stomach contents (27), and it has also been enriched and isolated from sand (28), river mud (29), and peat bog sediments (30). The prevalence of this organism in sedimentary environments and acid or alkaline soils that have been stored for months to years (31) suggests the presence of resistant structures or spores.

Sarcina ventriculi is an obligate anaerobe capable of growth from pH 8.0 to 2.0. When grown at pH 3.0, the internal pH was 4.3, and this increased to 7.1 with an environmental pH 7.0 (32). Distinct morphological changes in the ultrastructure of *S. ventriculi* were observed when cells were grown in a medium of constant composition at pH extremes of 3.0 and 8.0. (33). Figure 3 shows the proposed biochemical pathway for glucose metabolism in *S. ventriculi* (34). The organism changed carbon and electron flow from acetate, formate and ethanol production at neutral pH, to predominantly ethanol production at pH 3.0. Increased level of pyruvate dehydrogenase (relative to pyruvate decarboxylase) and acetaldehyde dehydrogenase occurred when the cells were grown at

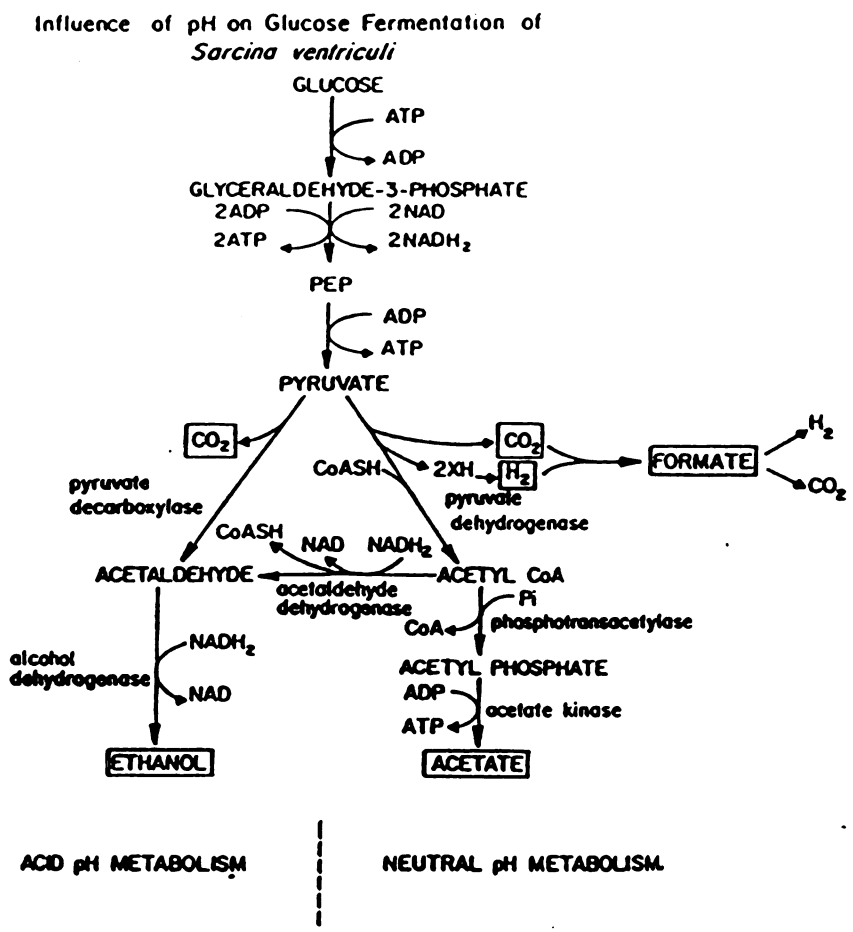

Figure 3. The proposed biochemical pathway for glucose metabolism in *S. ventriculi*.

neutral pH, indicating the predominance of carbon flux through the oxidative branch of the pathway for pyruvate metabolism. When the organism was grown at acidic pH, there was a significant increase in pyruvate decarboxylase levels and a decrease in acetaldehyde dehydrogenase, causing flux through the non-oxidative branch of the pathway.

Of interest is that *S. ventriculi* predominantly produced ethanol when the organism was grown at pH 3.0. External perturbation such as excess proton concentration (acidic condition) was involved in increasing alcohol concentration inside the cell by changing some metabolic pathway. *S. ventriculi* shows a wide dynamic life cycles since it survives from pH 2.0 to pH 8.0.

Membrane Lipid Structures in Eubacterial Thermophiles

As another model for membrane adaptation study, anaerobic thermophilic eubacteria, *Clostridium themohydrosulfuricum* was investigated. The optimum temperature for growth of the organism is 67-69^{o}C; the maximum temperature at which growth occurs is 76-78^{o}C; the minimum temperature is 42^{o}C (35). *Clostridium thermohydrosulfuricum* was isolated from Octopus Spring at Yellowstone National Park (36). It ferments starch and a wide variety of hexose- or pentose-derived saccharides including xylose and glucose into ethanol as the major reduced end product (37). In terms of the fact that it produced ethanol and experienced constantly high thermal stress, membrane adaptation mechanism was studied.

The apolar hydrocarbon chains, which are capable of hydrophobic interaction and provide the core of the membrane, have been the most extensively studied components of thermophile lipids. The majority of the hydrocarbon chains, usually pairs, are bound to glycerol molecules through one of three classes of chemical bonds : acyl esters (fatty acids), vinyl ethers (fatty aldehyde), or alkyl ether (alcohols). The derived glycerolipids in turn are known to provide the typical bilayer assembly (38). Thermophiles tend to possess

longer hydrocarbon chains and methyl (*iso-* and *anteiso-*) branched chains (39, 40). Unsaturated hydrocarbon chains, which significantly lower melting points, are rare (41). In comparison to the number of reports dealing with the nature and function of the apolar chains of thermophilic bacteria, little is really known about the structure or the function of the complex lipids. The question on inherent stability of the membrane in thermophiles remains an enigma because methyl-branching as a characteristic of the apolar chains acts as a "fluidizer" rather than "stabilizer" (42, 43, 44). A complete understanding of the molecular basis for thermostable membranes requires structural studies on the new and unique lipids.

Computational Studies on the Membrane Lipids

Model monolayers and bilayers of the chain molecules have been a popular subject of computer simulations over the years. These simulations have been performed either by Monte Carlo (MC)(45), molecular dynamics (MD)(46,47), or Brownian dynamic (BD)(48,49) simulations, at various levels of detail, on ensembles of chain molecules of varying lengths and packing densities. This has resulted in a growing understanding of the structures of real, complex systems such as the biological membrane (50, 51). One of the first detailed MD simulations of a smectic liquid crystal was reported by van der Ploeg and Beredsen (52, 53) on a system consisting of multilayers of the three component decanoate-decanol-water system. Recently Schurmann et al., (46) performed MD simulation on a model bilayer of 48 chain molecules with fixed head groups. The effects of packing density and temperature on the extent of spatial and temporal correlation in the ensemble have been studied by analyzing the trajectories from the MD simulation. The structure and dynamics of water between the bilayers was also studied by MD simulation (54). This research showed that the thermal motion of the polar head groups has no influence on the orientational polarization of water but had a large influence on the dynamics of the water interface. Large scale motional simulations in membrane lipids have been performed with

the M

the lip

the m

chain

instan

inform

calcul

most c

They

mak-n

substa

polar

prefra

viewpo

lipids

perfor

anisot

molec

very la

OVER

structu

always

viewpo

the Monte Carlo method (55) as models of lipid-protein interactions in bilayers (56) or for the lipid-cholesterol interaction in a model membrane (47). In general the results of both the molecular dynamics (MD) and the Monte Carlo (MC) simulations of systems consist of chain order, RMS (Root Mean Square) distance parameters and "snapshots" of instantaneous configurations of the systems (the MD simulation also give some dynamical information over very small time scales). The general agreement between the MC and MD calculations and experimental data indicates that the computer calculations have included most of the relevant interactions for the study of chain packing issues.

The MD simulation of a lipid micelle was also performed by Salemme et al. (57). They used 85 LPE (lysophosphatidylethanolamine) and 1591 water molecules in a 100 ps real-time simulation. Throughout the comparison of the initial and equilibrated micelles, substantial differences were proposed both in LPE hydrocarbon chain conformation and polar head-group-solvent interactions. Their work could predict the polymorphic pretransition from a spherical toward a cylindrical micelle structure with a molecular viewpoint.

Computer simulations were also performed for a large class of phenomenon of lipids such as fluctuating membranes with a simplified lipid model. Leibler et al. performed MD simulations with simplified membrane-like objects (58). They chose anisotropic, multibody forces so as to mimic real interactions between amphiphilic molecules. Their research showed the possibility of the successful MD simulations of a very large system such as a phase transition or membrane fusion.

OVERVIEW

The biological membrane is the most vulnerable cellular component since it is the structure most directly exposed to the challenges of environmental stress. External stress always accompanies a change in the "external input energy to the organism". Another viewpoint is that, molecular adaptation is the converting process of "external input energy"

to "cellular output energy" such as the regulation of lipid biosynthesis. This energy flow around the membrane causes changes in the motional dynamics of membrane components. The bacterial membrane should maintain an optimal dynamic state of the lipids for its proper function. Lipid components respond to external energy perturbations by changing the motional dynamics of the membrane. Therefore, the structural studies on the lipid components induced during the stress response should be performed from the standpoint of motional dynamics.

The basic approach throughout this thesis work was to elucidate membrane adaptive mechanisms of extremophiles such as *S. ventriculi* or *Cl. thermohydrosulfuricum* from the standpoint of membrane dynamics. New adaptive mechanisms of membranes to various forms of environmental stress will be discussed in detail. In Chapter II, the general membrane adaptive mechanism in *S. ventriculi* will be discussed. The detailed chemical and mathematical proofs for this mechanism will be discussed in Chapters III and IV. Studies on the head groups of transmembrane lipids of *S. ventriculi* cells will be discussed in Chapter V. Studies on the generality of this phenomenon and descriptions of unusual structures of the membrane components of *Cl. thermohydrosulfuricum* cells will be presented in Chapter VI. Finally, the possible structural and physiological roles of transmembrane chains will be examined by using the computational approaches such as molecular mechanics and molecular dynamics (Chapter VII).

REFERENCES

1. Singer, S.J., and Nicolson, G. L. (1972) *Science* **175**, 720-731
2. Singer, S. J. (1974) *Ann. Rev. Bioch.* **43**, 805-833
3. Op den Kamp, J.A.F. (1981) In *The Asymmetric Architecture of Membranes* (J.B. Finean and Michell, R.H. Eds.) pp83-126, Elsevier, New York
4. Op den Kamp, J.A.F. (1979) *Ann. Rev. Bioch.* **48**, 47-71
5. Ameloot, M.H., Hendrickx, H., Herreman, W., Pottel, H.,Cauwelaert, V. F., and Van Der Meer, W. (1984) *Biophy. J.* **46**, 525-539
6. Govil, G., and Hosur, R. V. (1982) In *Conformation of Biological Molecules: New Results for NMR*. Springer-Verlag, New York
7. Chapman, D., and Benga, G. (1984) In *Biomembrane Fluidity-Studies of Model and Natural Biomembranes. Biological Membranes* (D. Chapman, Ed.) Vol. **5**, pp1-56 Academic Press, New York
8. Kinosita, K., Kawato, S., and Ikegami, A. (1977) *Biophys. J.* **20**, 289-305
9. Salem, L. (1962) *Can. J. Biochem. and Physiol.* **40**, 1287-1298
10. Shinitzky, M. (1984) In *Membrane fluidity and Cellular Functions* (M. Shintzky, Ed.) vol. **1**, pp1-51 CRC Press, Boca Raton
11. Lee, A.G. (1983) In *Lipid Phase Transitions and Mixtures. Membrane Fluidity in Biology*. (R.C. Aloia, Ed.) vol. **2** pp43-88 Academic Press, New York
12. Marr, A.G., and Ingraham, J.L. (1962) *J. Bacteriol.* **84**, 1260-1267
13. Cronan, J.E., Jr., and Gelmann, E.P. (1975) *Bacteriol. Rev.* **39**, 232-256
14. Garwin, J.L., Klages, A.L., and Cronan, J.E., Jr. (1980) *J. Biol. Chem.* **255**, 3263-3265
15. Garwin, J.L., Klages, A.L., and Cronan, J.E., Jr. (1980) *J. Biol. Chem.* **255**, 11949-11956
16. de Mendoza, D., and Cronan, J.E., Jr. (1983) *Trends Biochem. Sci.* **8**, 49-52

17. Cronan, J.E., Jr., Welsberg, L.J., and Allen R.G. (1975) *J. Biol. Chem.* **250**,5835-5840

18. Ingram, L. O. (1990) *Crit. Rev. Biotechnol.* **9**, 305-319

19. Ingram, L. O., and N. S. Vreeland. (1980) *J. Bacteriol.* **144**, 481-488

20. Yaacobi, M., and Ben-Naim, A. (1974) *J. Phys. Chem.* **78**, 175-182

21. Ben-Naim, A. (1980) In *Hydrophobic Interactions*, plenum Press, New York

22. Buttke, T. M., and Ingram, L. O. (1978) *Biochemistry* **17**, 637 - 644

23. Ingram, L. O. (1980) *J. Bacteriol.* **149**, 166-172

24. Goodsir, J. (1842) *Edinb. Med. Surg. J.* **57**, 430-443

25. Beijerinck, M.W. (1905) *Amsterdam* **13**, 608-614

26. Beijerinck, M.W. (1906) *Arch. Neerl. Sci. Exact. Natur. Ser. 2*, **11**, 608 - 614

27. Beijerinck, M.W. (1911) *Amsterdam* **19**, 1412-1415

28. Smit, J. (1933) J. *Pathol. Bacteriol.* **36**, 455-468

29.Canale-Parola, E., and Wolfe, R.S. (1960) *J. Bacteriol.* **79**, 857-859

30.Goodwin, S., and J. G. Zeikus. (1987) *Appl. Environ. Microbiol.* **53**, 57-64

31. Knoll, H. (1965) *Monatsber. Dtsch. Akad. Wiss. Berl.* **7**, 475-477

32. Goodwin, S., and J. G. Zeikus. (1987) *J. Bacteriol.* **169**, 2150-2157

33. Lowe, S.E., Pankratz, H.S., and Zeikus, J. G. (1989) *J. Bacteriol.* **171**, 3775-3781

34. Lowe, S.E., and Zeikus, J. G. (1991) *Arch. Microbiol.* **155**, 325-329

35. Lovitt. R. W, Longin, R., and Zeikus, J. G. (1984) *Appl. Environ. Microbiol.* **48**, 171-177

36. Zeikus, J.G., Ben-Bassat, A., and Hegge, P. (1980) *J. Bacteriol.* **143**, 432-440

37. Ng, T.K., Ben-Bassat, A., and Zeikus, J.G. (1981) *Appl. Environ. Microbiol.* **41**, 1337-1343

38. J. Isrelachvili (1978) In *Light Transducing Membranes* (D.W. Deamer, Ed.) Academic Press, New York

39. Goldfine, H. (1982) *Curr. Top. Membr. Transp.* **17**, 1-9

40. Kaneda, T. (1991) *Microbiol. Rev.* **55**, 288-302

41. Langworhty, T.A. (1982) In *Methods Enzymol.* **88**, 396-416

42. Silvius, J. R., and McElhaney, R. N. (1979) *Chem. Phys. Lipids* **24**, 287-296

43. Silvius, J. R., and McElhaney, R. N. (1980) *Chem. Phys. Lipids* **26**, 67-77

44. Kannenberg, E., Blume, A., McElhaney, R. N. and Poralla, K. (1983) *Biochim. Biophys. Acta* **733**, 111-116

45. Quinn, P.J. , and Chapman, D. (1980) *Crit. Rev. Biochem.* **8**, 1-12

46. Biswas, A., and Schurmann, B.L. (1991) *J. Chem. Phys.* **95**, 5377-5386

47. Scott, H.L., and Kalaskar, S. (1989) *Biochemistry* **28**, 3687-3691

48. Pastor, R, Venable, R.M., and Karplus, M. (1988) *J.Chem.Phys.* **89**, 1112-1127

49. Pastor, R, Venable, R.M., Karplus, M., and Szabo, A. (1988) *J. Chem. Phys.* **89**, 1128-1140

50. Egberts, B., van Gunstern, W. F., and H.J.C. (1988) *J. Chem. Phys.* **89**, 3718-3732

51. Watanabe, K., Kelin M. L. (1989) *J. Phys. Chem.* **93**, 6987-6901

52. van der Ploeg, P., and Berendsen, H.J.C. (1982) *J. Chem. Phys.* **76**, 3271-3279

53. van der Ploeg, P., and Berendsen, H.J.C.(1983) *Mol. Phys.* **49**, 233-241

54. Raghavan, K., Reddy, M.R., and Berkowitz, M.L. (1992) *Langmuir*, **8**, 233-240

55.Metropolis, N., Rosenbluth, A., Rosenbluth, M., Teller,A., and Teller, E. (1953) *J. Chem. Phys.* **21**, 1087-1096

56. Scott, H.L. (1986) *Biochemistry*, **25**, 6122-6126

57. Wendoloski, J.J., Kimatian, S.J., Schutt,C.E., and Salemme, F.R. (1989) *Science*,

243, 636-638

58. Droufff,J-M., Maggs, A., and Leibler, S. (1991) *Science*, **254**, 1353-1356

CHAPTER II

STUDY ON THE NEW FAMILY OF THE VERY LONG CHAIN DICARBOXYLIC FATTY ACIDS IN THE MEMBRANE OF THE *SARCINA VENTRICULI* IN RESPONSE TO DIFFERENT FORMS OF ENVIRONMENTAL STRESS

INTRODUCTION

Bacterial membranes are extremely dynamic, complex systems which interface directly with the environment and carry out many important functions. They provide compartmentalization, transport, and acts as a matrix for cytoplasmic macromolecules and membrane proteins.

Bacteria in their natural ecosystem may experience many changes in environmental factors, including temperature, pH, solvent concentration, nutrient levels and oxygen concentration. In this respect, the membrane, which is directly exposed to the environment, is one of the most critical and vulnerable components of the cell and must adapt to and survive these changes.

Sarcina ventriculi is a strictly anaerobic bacterium which can grow on sugars over a wide pH range, from pH 2 to 8 (3,4). Detailed physiological studies have been done on the influence of environmental pH range on growth, fermentation product formation and the proton motive force in this organism (9, 25, 39).

S. ventriculi also undergoes morphological adaptations in response to changes in environmental pH. Regular tetrads are formed at low pH, whereas cells are irregular in shape with higher numbers of cells within each packet at neutral pH, and spores are formed at alkaline pH (24).

The purpose of this report is to examine the effect of perturbation of environmental parameters (specifically of proton and solvent concentrations, and temperature) on membrane composition and structure. We report that the lipid composition and fatty acid structure dramatically change in response to these perturbations resulting in the synthesis of a family of long chain α,ω-dicarboxylic fatty acids. These new lipids are believed to be important for maintaining membrane integrity under the new conditions.

MATERIALS AND METHODS

Organism and Culture Conditions

All chemicals were reagent grade or better and were obtained from Sigma Chemical Co., St. Louis, Mo., or Mallinckrodt, Inc., Paris, Ky. All gases were at least 99.9% pure and were passed over copper-filled Vycor furnaces (Sargent Welch Scientific Co., Skokie, Ill.) to remove oxygen. *S. ventriculi* JK was cultivated as described previously (9). For growth under pH control, 4 liter Kimax jars (Baxter Scientific Products, Romulus, Mich.) containing 3 liters of medium were used. The jars were equipped with a pH probe, and the culture mixed by placing the jars on a magnetic stirrer. When the organism was grown at pH 3.0, the initial pH did not change during the fermentation; at pH 7.0 the pH was controlled by the addition of 5 M NaOH. Cultures were harvested as outlined previously (24) under aerobic conditions.

For temperature shift experiments and growth in the presence of solvents, 750 ml fermentation vessels (New Brunswick Sci., New Brunswick, NJ) containing 350 ml of medium were used. The vessels were agitated at 200 rpm and pH maintained either at pH 3.0 or pH 7.0. To determine the effect of solvents on membrane composition, vessels containing medium with 0.25 M ethanol or 0.05 M butanol at pH 7.0, were inoculated with a 5 % (v/v) inoculum of cells grown at pH 7.0 in the absence of solvent. The cells were harvested at midexponential phase, washed twice with distilled water and stored at -70°C for further analysis.

Membrane Preparations

Cells were disrupted by passage through a French Pressure cell (American Instruments Co., Inc., Silver Spring, Md.) at 20,000 lb/in^2. The disrupted cells were centrifuged at 20,000 x g to remove unbroken cells, and the supernatant was centrifuged at 110,000 x g to sediment the membranes, which were washed twice with distilled water.

Total Fatty Acids Analysis

Fatty acid analyses were performed on whole cells or isolated membrane fractions by treatment with methanolic HCl using either of two procedures. Procedure (a) was employed for whole cells and procedure (b) for isolated membranes. (a) cells (1-5 mg) suspended with 0.3 ml chloroform and 1.5 ml 5% methanolic HCl solution, were sealed in a teflon-lined screw-capped vial, and heated in a water bath or oven at 72°C for 24 hrs. Chloroform (3 ml) was added every 8 hrs followed by mild sonication for 5 minutes. After concentration to dryness under nitrogen gas, samples were partitioned between water and chloroform and the aqueous layer washed several times with chloroform or hexane. The combined solutions were filtered through glass wool. (b) Three(3) ml of chloroform was added to 1 ml of membrane suspension followed by 15 ml 5% methanolic-HCl solution. The flask was sealed and heated in an oven at 72°C for 12 hrs. Three (3) ml of chloroform was added every 6 hrs followed by mild sonication for 5 minutes. The mixture was then concentrated on the rotary evaporator to dryness and extracted with chloroform. The combined organic fraction was redissolved in 1 ml of hexane. The fatty acid methyl esters prepared by either procedure (a) or (b) were subjected to Gas Chromatography analysis on a 25 M J&W Scientific DB1 capillary column using helium as the carrier gas and a temperature program of 150°C initial temperature, 0.00 min hold time and 3.0 deg/min rate, to a temperature of 200°C. A second ramp of 4.0 deg/min was then immediately started until the final temperature of 300°C was obtained. This temperature was held for 30 min. The relative proportion of lipid components were calculated from the integrated peak areas. The fatty acid identification and molecular weight were determined using GC/MS analysis using a Jeol JMS-AX505H spectrometer interfaced with a Hewlett-Packard 5890A Gas Chromatograph.

Extraction of Lipids

Lipids were extracted from the isolated membrane or whole cells using procedures (a) and (b) respectively. (a) To each 5-10 ml membrane suspension 30 vol. of chloroform/methanol (5:1,v/v) was added and then mixed to produce a single phase. The mixture was shaken or stirred vigorously, with intermittent sonication (approximately 5 min every 30 min), for 2 hrs at 45°C. The combined extracts were taken to dryness in a rotary evaporator. The residue was partitioned between 10 ml chloroform/methanol (5:1,v/v) and 2.5 ml water. The lower phase was taken to dryness and redissolved in 1 ml chloroform/methanol (9:1,v/v). (b) Cells of *S. ventriculi* from 50 liters of culture medium were harvested by centrifugation at 10,000 x g for 10 min. Lipids from approximately 50 g wet weight of cells were extracted at 45°C with 400 ml of a mixture of chloroform/methanol/water (15: 3: 2, by vol.) for 2 hrs, followed by 200 ml of chloroform / methanol (5:1, v/v). Extraction was performed with intermittent sonication for 2 hrs. After centrifugation at 20,000 x g the pellet (cell debris) was extracted again with the same solvent systems. After centrifugation, the supernatant was taken to dryness in a rotary evaporator, dissolved in 10 ml of chloroform/methanol (5:1,v/v) and then shaken with 2.5 ml water. The lower phase containing the lipids was taken to dryness and dissolved in 1 ml of chloroform.

Analysis of Lipids

As a preliminary step for comparing the total lipid profiles between cells of *S. ventriculi* growing at pH 3.0 versus pH 7.0, the lipids were separated by 2-dimensional TLC using chloroform/ methanol/ ammonia/ water (3.3:1.0:0.1: 0.05, by vol.) for the first dimension and chloroform /methanol / water (7:1.6:0.2, by vol.) for the second dimension. Analyses were performed on silica-gel plates (Merck). Spots were made visible either by spraying with 50% ethanolic-sulfuric acid and heating at 250°C to char the organic components, or by spraying with a 0.1% solution of 2',7,-dichlorofluorescein in aqueous ethanol (1:1) and viewing under ultraviolet light (29). Standard phospholipids such as

phosphatidylcholine (PC), phosphatidylethanolamine (PE), phosphatidylserine (PS) and cardiolipin (CL) and neutral lipids (NL) were used as standards in addition to free fatty acids (FA). Spraying agents (30) for the detection of components included ninhydrin for PE or PS, dragendorff agent for PC, orcinol for glycolipid, and molybdenum blue for phosphate.

Isolation of the α,ω-Dicarboxylic Acid Dimethyl Ester

The total lipids (100 mg) extracted from the cells as described before were methanolysed with 5 % (w/v) HCl in methanol (5 ml) for 12 hrs at 72°C. Chloroform (1 ml) was added every 4 hrs followed by mild sonication for 5 minutes. The mixture was then concentrated on the rotary evaporator to dryness and extracted with chloroform. The combined organic fraction was redissolved in 1 ml of hexane. This fraction was applied to a silica flash chromatography column and eluted with chloroform/hexane (1:1, by vol). Fractions were assayed by Gas Chromatography. Fractions containing very long chain fatty acid methyl esters were then concentrated and rechromatographed on 5% $AgNO_3$ impregnated-preparative thin layer silica chromatography plates which were eluted with petroleum ether/ diethyl ether /acetone (10:1:0.5, by vol). Spots were made visible either by spraying with 50% ethanolic-sulfuric acid and heating at 250°C to char the organic components, or by spraying with a 0.1% solution of 2',7,-dichlorofluorescein in aqueous ethanol (1:1) and viewing under ultraviolet light (29). Bands were scraped from the plate into a column fitted with a sintered disc and the material was eluted from the silca gel with methanol and chloroform. Each fraction was concentrated by evaporation and redissolved in choloroform for further analysis. Purity of each fraction was assayed by GC/MS. One band containing the pure α,ω–15,16-dimethyltricotanedioate dimethyl ester was subjected to NMR and FTIR analysis.

Isotope Labeling

Isotope labeling was used to aid in deducing the structures of esterified lipid components using GC/MS. Methyl esters of fatty acids obtained by acid methanolysis were further treated with 5% deuterated methanolic-HCl for 6 hrs at 72°C. Deuterated methyl esters of fatty acids were extracted and analyzed as described for the natural abundance samples.

^{1}H NMR and ^{13}C NMR Spectroscopy

Proton NMR spectra were recorded at 300 MHz on solutions in $CDCl_3$. Fourier transform ^{13}C NMR spectra were recorded at 125 MHz on solutions in $CDCl_3$. Chemical shifts are quoted relative to the chloroform resonances taken at 7.24 ppm for proton and 77 ppm for ^{13}C measurements, respectively.

Fourier Transform Infrared Spectroscopy

Spectra were obtained with a Nicolet model 710 FT-IR spectrometer on a 10% (w/v) solution of dicarboxylic acid dimethyl ester in chloroform.

RESULTS AND DISCUSSION

Two Dimensional TLC Analysis on Lipids

Experiments were initiated to examine lipid composition changes when cells of *S. ventriculi* were grown at pH 7.0 versus 3.0. Two dimensional TLC analyses on the lipids from intact cells or isolated membrane of cells are shown in Figure 1. Analysis of the components for specific lipids such as PE, PS and CL indicated that only traces of these are present and the major components are glycolipids. There are markedly different proportions of phospholipids and glycolipids in the cells grown at the two pH values.

In order to ensure efficient extraction of membrane lipids from the cells of *S. ventriculi* grown at pH 3.0, a relatively non-polar solvent system was selected and used to solubilize the strong hydrophobic lipid groups at elevated temperature of 45^{o}C.

Compositional Analyses of Isolated Lipids

GC analyses of fatty acid methyl esters extracted from cells grown at pH 7.0 versus 3.0 are shown in Figure 2A and 2B respectively. Most of the fatty acids in the membrane of *S. ventriculi* grown at pH 7.0 were between 14 and 18 carbon atoms long (Figure 2A) but when cells were grown at pH 3.0, a family of novel lipid components appeared (Figure 2B). The relative proportion of the unusual and unique lipid components was more than 50% by mass at pH 3.0, and only trace levels (< 7%) were present during growth at pH 7.0. Further analysis of these lipids from pH 3.0 cells using GC after methanolysis revealed that peaks a, f, i, and j of Figure 1A contained unusual fatty acid groups. This is a major difference between the cells grown at acid versus neutral pH. This indicated that the unusual fatty acids are integral lipid components and do not occur in free uncombined form.

Figure 1. Two dimensional TLC analyses of the lipids extracted from the cell of *Sarcina ventriculi* grown at pH 7 (A) versus pH 3 (B). Equal amounts (~ 0.8 mg) of total lipids of the membranes isolated from the cells of *S. ventriculi* grown at different pH values were compared in 2D-TLC plates. A(a,b,c,j), B(a,b,k); phospholipids, A(e,f,g,h,i), B(c,d,f,g,h,i,j); glycolipids. Spots A(a,f,i,j) contained unusual fatty acids with long retention times on GC/MS.

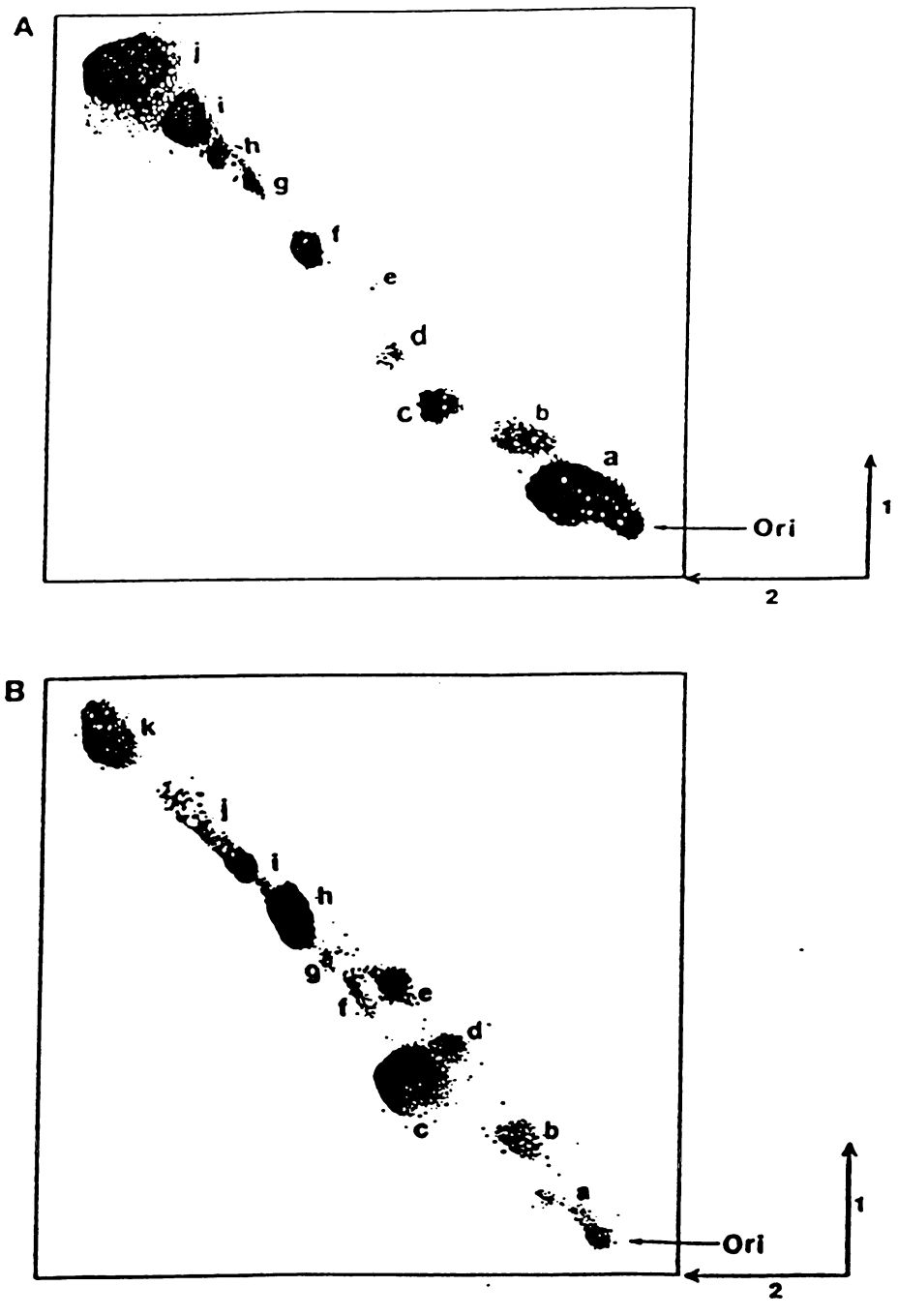

Figure 1

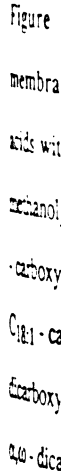

Figure 2. Gas chromatographic analyses of lipid components in the membrane of *S. ventriculi* grown at pH 7 (A) versus pH 3 (B). Total fatty acids within the membrane were analyzed as fatty acid methyl ester derivatives after methanolysis. 1. $C_{14:0}$ - carboxylic acid methyl ester, 2. $C_{17:1}$ - fatty aldehyde, 3. $C_{15:1}$ - carboxylic acid methyl ester, 4. C16:0 - carboxylic acid methyl ester, 5. unknown, 6. $C_{18:1}$ - carboxylic acid methyl ester, 7. $C_{18:0}$ - carboxylic methyl ester, 8. $C_{32:0}$ - α,ω-dicarboxylic dimethyl ester (α,ω-15,16-dimethyltricotanedioate dimethyl ester), 9. $C_{34:1}$ - α,ω - dicarboxylic dimethyl ester , 10. C36:2 - α,ω - dicarboxylic dimethyl ester .

Detector response

8

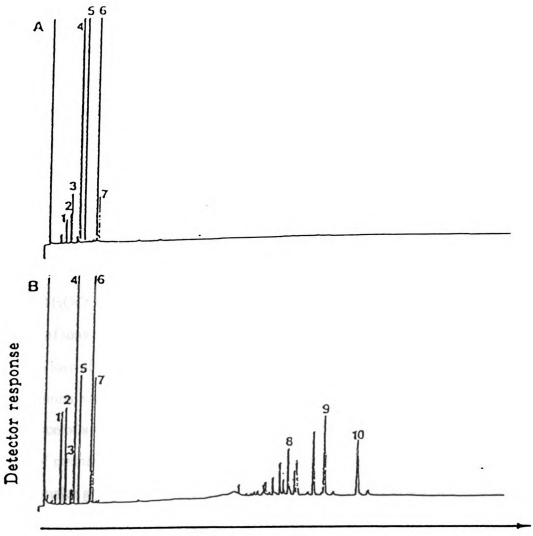
A
B
1
2
3
4
5
6
7
8
9
10
Detector response
Retention time (effective boiling points)

Figure 2

which

3.0.

alcoh

GC

and 4

the m

of me

repres

$(CH_2$

was C

series

due to

mass

presen

loss o

other

$(CH_2$

metho

molecu

deuter

mass u

molecu

Figure 3A and 3B show the mass spectra of one of the unusual lipid components which appeared in the membrane of *S. ventriculi* grown at high proton concentration (pH 3.0). The same lipid components were also present in cells grown in the presence of high alcohol or higher temperatures at pH 7.0.

GC/MS Analyses of Dicarboxylic Dimethyl Esters

The electron impact mass spectrum in Figure 3A shows major ions at m/z 538, 506 and 475 including characteristic McLafferty fragment ions 74, 87. These corresponded to the molecular ion of a C_{32}-α,ω-dicarboxylic dimethyl ester (M^+) with the sequential losses of methanol (CH_3OH) and a methoxy (CH_3O) group respectively. The ion 464 m/z represents the structure obtained by sequential losses of methanol (CH_3OH) and ketene (CH_2CO) (Figure 4, Table 1).

The mass spectrum also contained a series of ions the general structure of which was CH_3OCO-$(CH_2)n$, begining at m/z 73, charateristic of a saturated methyl ester. This series of ions continued up to and included two prominent ions at m/z 269 and 297 (296 is due to loss of one hydrogen from m/z the 297 fragment). The intense clusters of ions 28 mass units apart centered at m/z 269 (n=15) and m/z 297 (n=17) strongly indicated the presence of a vicinal dimethyl group (Figure 4). The ions at m/z 237 and 265 represent the loss of methanol (CH_3OH) from the m/z 269 and 297 ion fragments respectively. Two other major group of ions at m/z 238 and 266 were assigned to acylium ions (m/z 238; OC-$(CH_2)_{13}$-$CH(CH_3)$, m/z 266; OC-$(CH_2)_{13}$-$CH(CH_3)CH(CH_3)$) corresponding to loss of methoxy groups from the ions of m/z 269 and 297 ions respectively.

Figure 3B shows the electron impact mass spectrum of the deuterium labeled molecule obtained by methanolysis with the D-4 methanol/HCl solution (to produce the tri-deuterated methyl ester). The most striking change was the shift of the molecular ion by 6 mass units which confirmed methanol (CD_3OH) and a methoxy group (CD_3O) from the molecular ion (544 m/z) to give ions at m/z 509 and 510 were also observed in addition to

Figure 3. Electron impact mass spectrum (70ev) of α,ω-15,16-dimethyltricotanedioate dimethyl ester without (A) and with isotope labeling (B) (A) EI spectrum contained major ions at m/z 538, 506 and 475. These corresponded to molecular ion (M^+) with the sequential losses of methanol and methoxy group respectively. (B) It shows the EI spectrum of deuterium labeled molecules obtained by deuteration with D-4 methanolic-HCl solution. The presence of two carboxylic and two branching methyl groups was confirmed by isotope labeling.

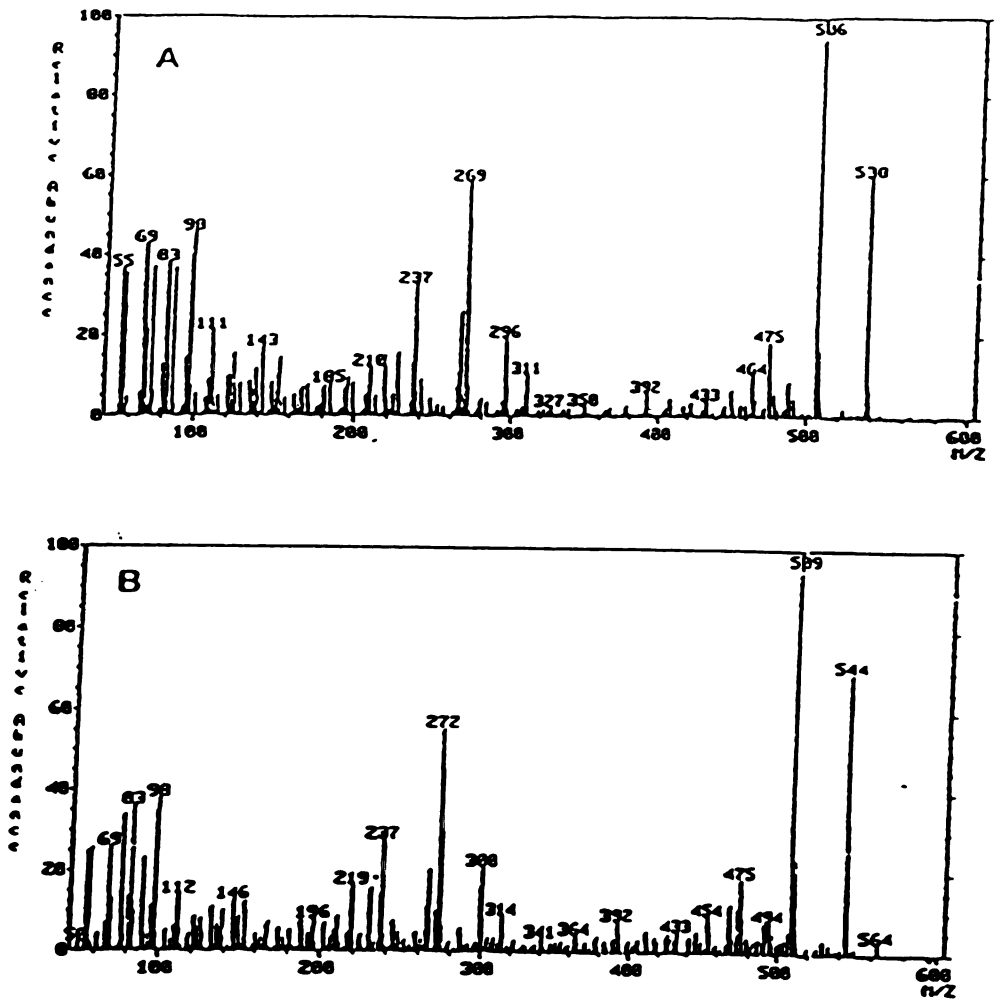
A
100
80
60
40
20
0
55
69
83
98
111
143
185
216
237
269
296
311
327
358
392
433
464
475
506
530
100
200
300
400
500
600
m/z
B
100
80
60
40
20
0
69
82
98
112
146
196
219
227
272
288
314
341
364
392
433
454
475
494
509
544
564
100
200
300
400
500
600
m/z

Figure 3

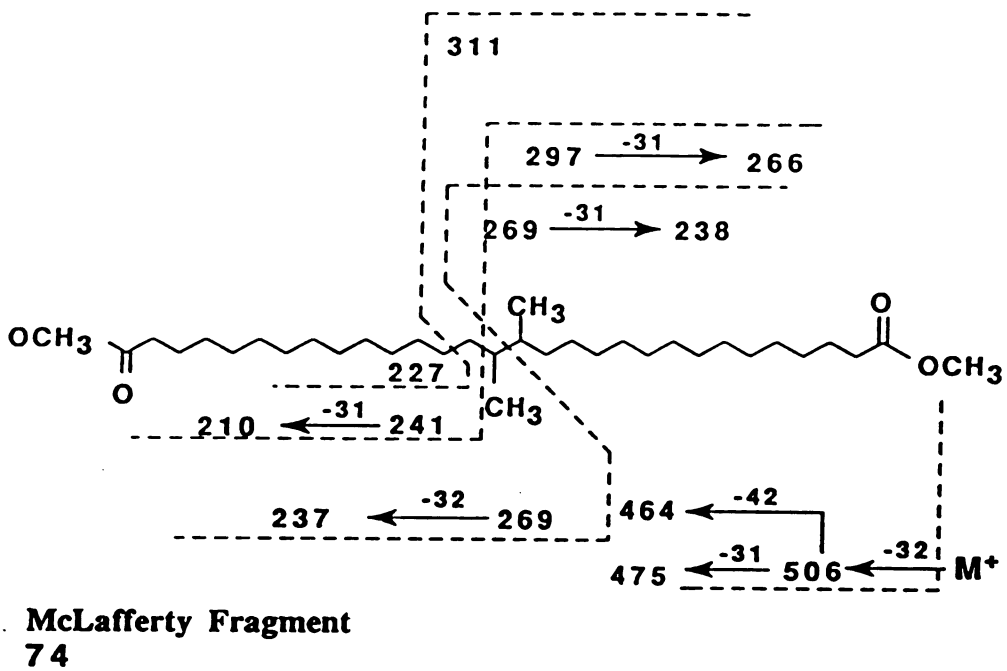

Figure 4. Electron impact mass spectral fragmentation pattern of -α,ω-15,16-dimethyltricotanedioate dimethyl ester. All numbers indicate the ionic fragments (m/z). 31 mass units indicate the methoxy group (-CH_3O), 32 for methanol (CH_3OH), 42 for ketene(CH_2CO). The ion at m/z 74 is a characteristic McLafferty fragment of aliphatic ester groups.

Table 1. Analysis of 70 ev electron impact mass spectral fragments of α,ω-15,16-dimethyltriacotanedioate dimethyl ester.

Structure of ionic fragment.	mass(m/z)	deuteriated mass(m/z)
$CH_3OCO(CH_2)_{13}CHCH_3CH_3CH(CH_2)_{13}OCOCH_3$	538	544
$CH_3OCO(CH_2)_{13}CHCH_3CH_3CH(CH_2)_{12}CH{=}CO$	506	509
$OC(CH_2)_{13}CHCH_3CH_3CH(CH_2)_{12}CH{=}CO$	475	475
506 - 18 (H_2O)	488	491
$CH_3OCO(CH_2)_{13}CHCH_3CH_3CH(CH_2)_{10}CH{=}CH_2$	464	467
$CH_3OCO(CH_2)_{13}CHCH_3CH_3CH$	311	313
$CH_3OCO(CH_2)_{13}CH(CH_3)CH(CH_3)$	297	300
$CH_3OCO(CH_2)_{13}CHCH_3$	269	272
$CH_3OCO(CH_2)_{13}$	241	244
$CO(CH_2)_{13}CHCH_3$	238	238
$CH_3OC(OH){=}CH_2$	74	77
$CH_3OCO(CH_2)_n$; n=1~13	73 + 14*n	76 + 14*n
$CO{=}CH(CH_2)_n$; n=1~13	55+14*n	55+14*n
CH_3-$(CH2)_n$; n= 3~12	57+14*n	57+14*n
$CH_2{=}CH$-$(CH_2)n$; n=2~11	55+14*n	55+14*n

the deuterated McLafferty fragments (m/z 77). The ions at m/z 272 ($(CD_3OCO-(CH_2)_{13}CH(CH_3))$ and 300 ($CD_3OCO-(CH_2)_{13}CH(CH_3)CH(CH_3)$) corresponded to deuterated m/z 269 ($CH_3OCO-(CH_2)_{15}$) and m/z 297 ($CH_3OCO-(CH_2)_{13}$ CH (CH_3) $CH(CH_3)$) respectively. The ions at m/z 237 and 265 corresponded to loss of tri-deuterated methanol (35 mass units) from the ions at m/z 272 and 300 respectively. Most of the other unusual long chain fatty acid components gave spectra with similar properties indicating that they had structures consistent with α,ω-very long chain dicarboxylic acids. Some of them contained one unsaturated double bond ($C_{34:1}$-α,ω-dimethyldicarboxylic acids) or two unsaturated double bonds ($C_{36:2}$-α,ω-dimethyldicarboxylic acids).

Spectroscopic Analyses of Isolated Dicarboxylic Dimethyl Esters

To definitively prove the general structure of the family of dicarboxylic acids, one of these was isolated by a combination of column chromatography and preparative T.L.C. This component corresponded to α,ω-15,16-dimethyltricotanedioate dimethyl ester.

Proton NMR analysis (Figure 5) also confirmed the presence of branched methyl groups by the presence of a doublet at 0.74 ppm (J = 7.2 Hz) and the methoxy group by the presence of a sharp singlet at 3.65 ppm. Resonances at δ 1.28 (broad singlet) were assigned to methylene groups of a lipid chain. The multiplet at δ 1.58 was assigned to the protons of the β-carbons of the molecule. Resonances at δ 2.28 (triplet) were assigned to the methylene groups α to the carbonyl group ($-CH_2-CO-$). Ester methoxy groups (CH_3O-) were assigned to singlet at δ 3.65. The ^{13}C NMR spectrum (Figure 6) showed the ester carbonyl carbon at δ 174.5, methoxy carbon at δ 51.4 and branched methyl carbons at δ 14.5. Moreover, all these resonances were present as singlets, indicating magnetic equivalence due to molecular symmetry.

The Infrared spectrum (Figure 7) showed strong C-H stretching absorption in the area of 2840-3000 cm^{-1}. The bending vibrations of the C-H bonds in the methylene groups occurred around 1465 cm^{-1} (scissoring) and 1350-1150 cm^{-1} (twisting and

Figure 5. The 300 MHz ^1H NMR spectrum of α,ω-15,16-dimethyltricotanedioate dimethyl ester. Signals at δ 3.65 which were assigned to methyl groups of a methoxycarbonyl function. The peak at δ 1.28 is due to the methylene groups in the saturated hydrocarbon chains. Note also 3 characteristic signals, at δ 2.28 (t, J=13.2Hz) representing the methylene group adjacent to the methoxy carbonyl function, at δ 1.58 due to the protons of the β-carbons of this molecule and at δ 0.74 (d, J=7.2 Hz) corresponding to the protons of a vicinal methyl group. The singlet at δ 7.24 is due to the chloroform. Peaks marked with asterisks are due to contaminants from the silica layer.

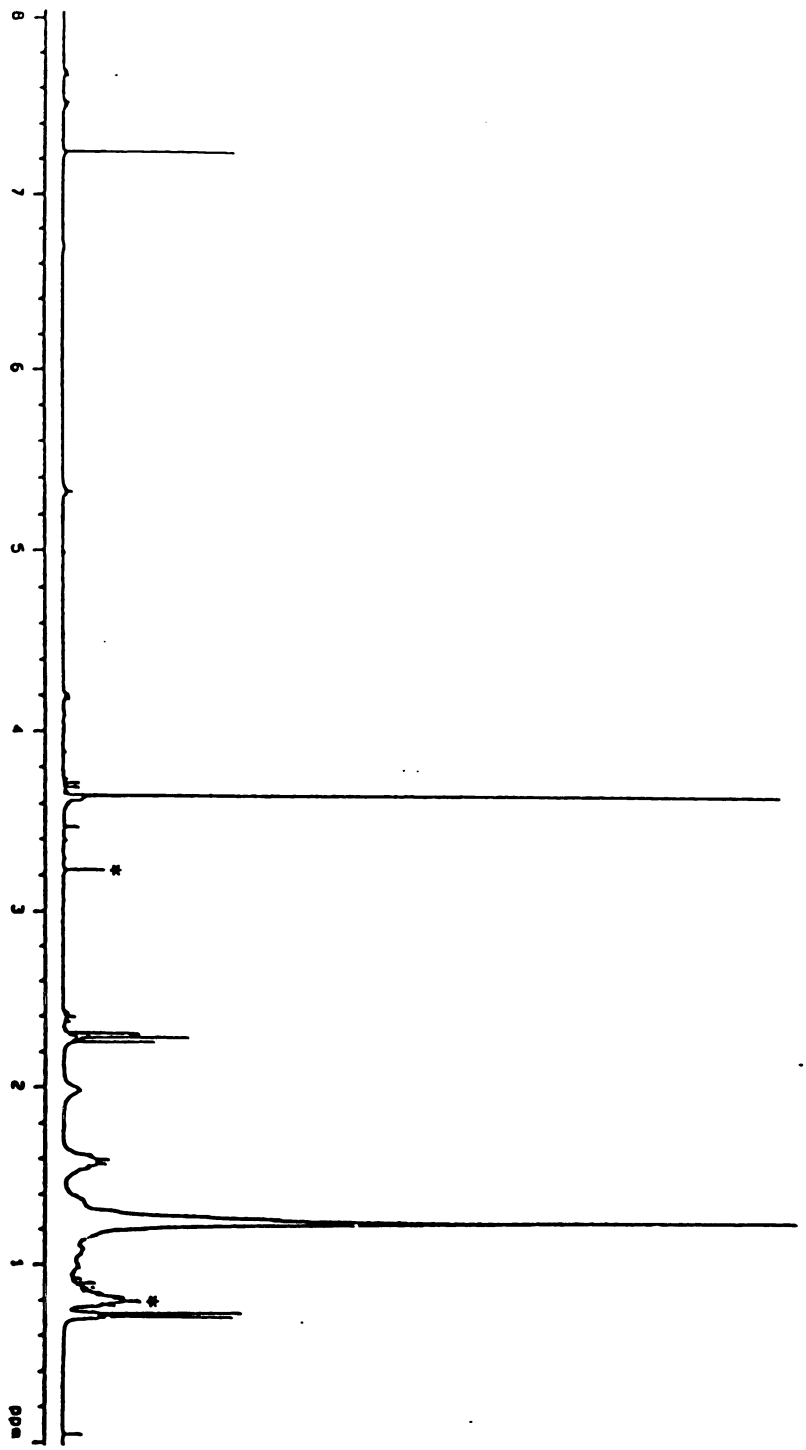

Figure 5

Figure 6. The 125 MHz ^{13}C-NMR spectrum of α,ω-15,16-dimethyltricotanedioate dimethyl ester. The presence of a methyl ester and branching methyl group are confirmed by signals at δ 51.4 and 14.5 respectively. The signal at δ 174.5 was assigned to the carbonyl carbon of the ester group.

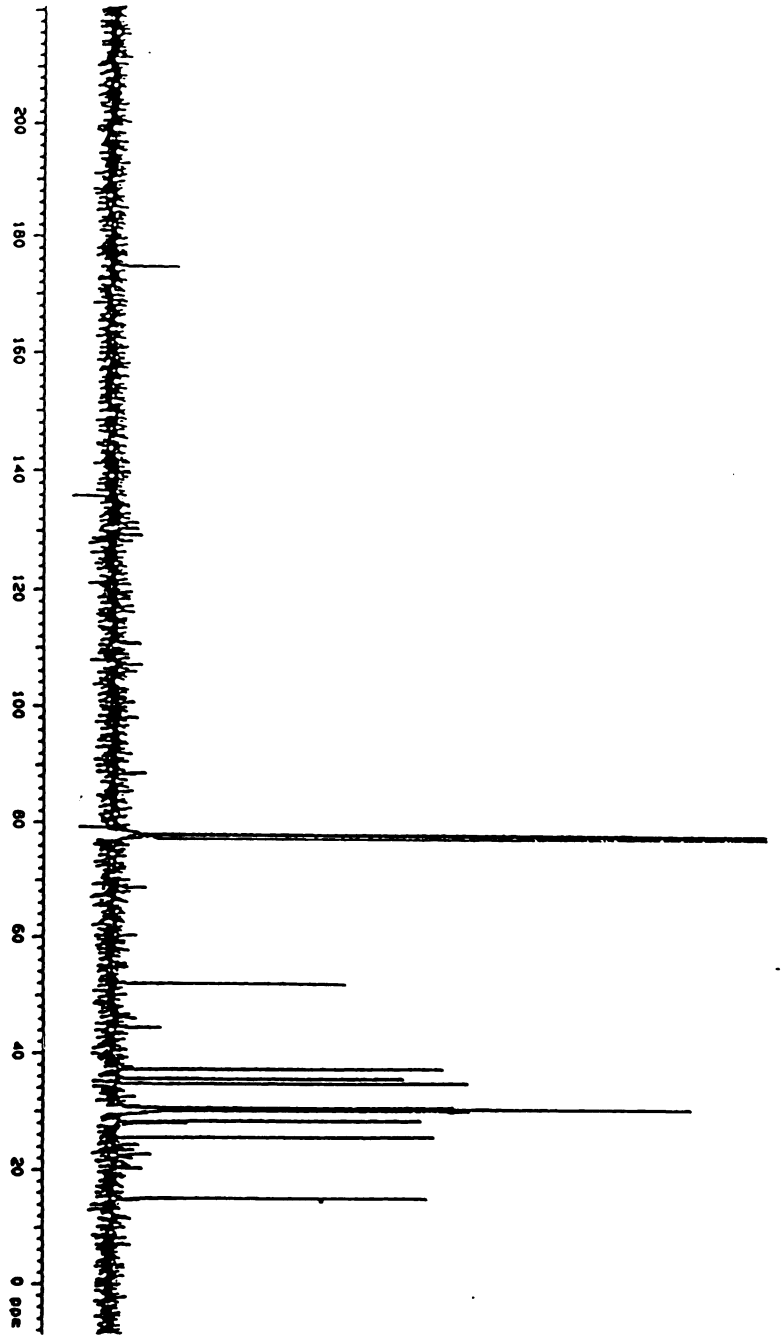

Figure 6

Figure 7. The Fourier transform infrared spectrum of α,ω-15,16-dimethyl-tricotane dioate dimethyl ester. It shows strong C-H stretching in the area of 2840-3000 cm^{-1}. The bending vibrations of the C-H bonds in the methylene group occurred around 1465 cm^{-1} (scissoring) and 1350-1150 cm^{-1} (twisting and wagging). The characteristic C=O absorption band of the aliphatic ester group appeared at 1735 cm^{-1}. There was no evidence of unsaturation or of oxygen combined in hydroxy or simple ether linkages.

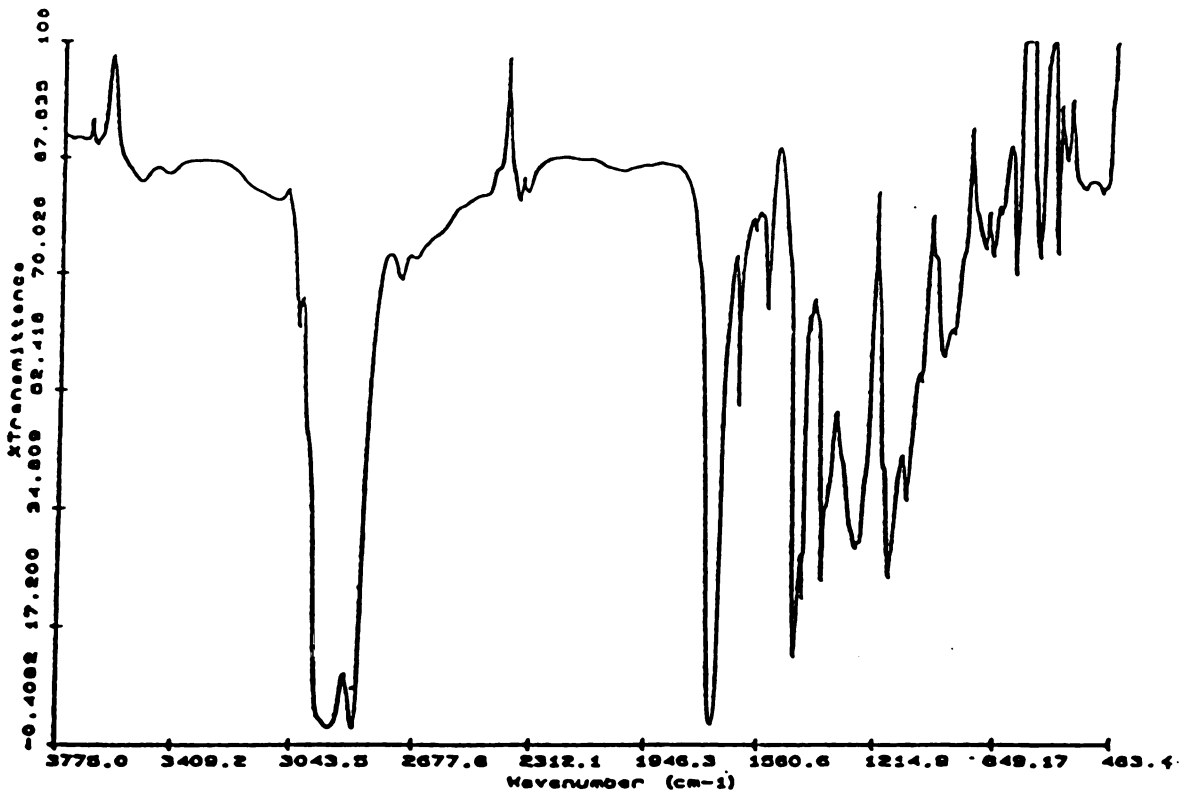
%Transmittance
100
87.035
70.026
52.416
34.805
17.800
-0.4082
3778.0
3409.2
3043.5
2677.8
2312.1
1946.3
1580.6
1214.9
849.17
483.4
Wavenumber (cm-1)

Figure 7

wagging). The characteristic C=O absorption band of the aliphatic ester group appeared at 1735 cm^{-1}. It also showed the stretching of the carbon-oxygen bond of the alkoxy group (O=C-O-R) in the area of 1175-1250 cm^{-1}.

With all these spectroscopic data, the structure of this component was confirmed as -α,ω-15,16-dimethyltricotanedioate dimethyl ester.

Induction of Dicarboxylic Acids in Response to Various Forms of Environmental Stress

The alteration in metabolic end product formation occurring as a function of pH includes cessation in acid production at low pH and an increase in ethanol formation. Either event may cause the organism to alter cellular components to adapt to these changes. The cell may synthesize these unusual very long chain α,ω-dicarboxylic fatty acids in response to the presence of acids during growth at pH 3.0, in order to prevent translocation of protons across the cytoplasmic membrane by the protonated form of the acid and dissipation of the proton motive force. In other bacteria the undissociated forms of these acids are able to permeate through the cytoplasmic membrane and accumulate inside the cell at large ΔpH values and decrease the internal pH (19).

The presence of solvents would increase fluidity of the membrane and could trigger production of longer chain fatty acids to increase membrane integrity. As growth of *S. ventriculi* at low pH is inhibited in the presence of elevated levels of metabolic acids, but not solvent, experiments were conducted at neutral pH in the presence of high levels of solvents to determine if any changes occurred in the lipid composition of the cell. *S. ventriculi* grew at pH 7.0 in solvent concentrations as high as 0.6 M methanol, 0.5 M ethanol, 0.3 M propanol and 0.10 M butanol. To examine the effect of solvents on the fatty acid composition of *S. ventriculi* at neutral pH, the organism was grown in the presence of 0.25 M ethanol or 0.05 M butanol (concentrations at which growth was unaffected), and the fatty acid composition determined. If the ethanol levels produced in

the cells of *S. ventriculi* grown at pH 3 can trigger the synthesis of unusual long chain lipid component then this mechanism would be supported by demonstrating that addition of exogenous ethanol to cells grown at pH 7.0 has the same effect on membrane composition as the addition of exogenous acid (i.e., growth at pH 3.0). Cells of *S. ventriculi* grown at pH 7.0 in the presence of ethanol or butanol (Figure 8A and B) contained a similar family of unusual lipid components as those observed in cells grown at pH 3.0. These findings suggest that high levels of ethanol, butanol or protons (organic acids) can trigger the synthesis of the very long chain fatty acids, and that the phenomenon is not specific.

Effect of Alcohol and Thermal Stress on Lipid Composition

There are numerous reports on the adaptations bacteria make in lipid composition when grown in the presence of alcohols (1, 6, 14, 15, 16, 22). Membrane integrity is in many cases the primary site of alcohol, in particular ethanol, damage although alcohol clearly affects the properties of all biological macromolecules to some degree. Ethanol adaptive changes have been divided into two groups; those that strengthen the hydrophobic barrier and those that decrease the lipid sites available for passive leakage (17). The former include the production of longer chain fatty acids and increasing the proportion of nonpolar lipids in the membrane. This mechanism involves the extension of the average chain length by a few carbon chains after the perturbation (18). The other group of adaptive changes include a reduction of the lipid to protein ratio and a reduction of the lipid pitches on the membrane surface sites available for passive leakage (7,15).

Our results indicate a much more dramatic mechanism because the average chain length of the normal fatty acids remain the same after addition of alcohol and an entirely new class of very long chain membrane lipids are synthesized. Since the effect of diverse alcohols on membrane composition seems to be similar in *S. ventriculi*, it became apparent that the synthesis of these unusual lipid components might be a general response to environmental factors which might disrupt the membrane and reduce its fluidity. If the

fluidity of the membrane were the real controlling element for this adaptive response, heat as another external perturbation would be expected to have a similar effect as alcohol or protons. Temperature effects on the composition of the membrane have been thoroughly studied in *E. coli* (16,27,28). The configuration of unsaturated carbons (*cis*- or *trans*) or hydrocarbon chain length of fatty acids are known to be responsible for temperature adaptive changes because configurations and increased chain length can influence the packing density and hence fluidity. The optimum temperature for growth of *S .ventriculi* is 30-37°C(5). Experiments were performed under pH 7.0 controlled conditions to determine the effect of prolonged incubation (4hrs) at 45°C or 55°C on membrane composition. Figure 8C shows the GC profile of membrane lipid components after methanolysis of the membrane lipids of the cells of *S. ventriculi* grown at pH 7 after a temperature shift from 37°C to 55°C. Incubation at elevated temperature resulted in synthesis of the long chain fatty acids even though the organism became nonviable. Cells of *S. ventriculi* were viable after a shift in temperature to 45°C, and synthesis of the α,ω-dicarboxylic very long chain acids occurred at this temperature. For the reversibility of the synthesis of these unusual membrane components, the temperature was shifted to 45°C from 37°C at the mid-log phase of growing cells of *S. ventriculi* at neutral pH. A small amount ranging from close to zero and rarely exceeding 7% of long chain lipids were always found in cells of *S. ventriculi* grown at neutral pH, and probably represents the basal level of these lipids. After shifting the temperature to 45°C, the amounts of long chain lipid components dramatically increased and returning the temperature to 37°C reduced their proportions. In order to demonstrate that decrease in very long chain fatty acids was due to the decrease in temperature, rather than turnover or dilution before the temperature was returned to 37°C, part of the culture was removed and the incubation at 45°C continued. The temperature of the remainder of the culture was brought down to 37°C and after 90 min the very long chain dicarboxylic acid content in the 45°C culture

Figure 8. Gas chromatographic analyses of lipid components extracted from cells of *S. ventriculi* grown at pH 7.0 in the presence of various forms of environmental stress. (A) 0.25 M ethanol, (B) 0.05 M butanol, (C) elevated temperature (55°C), 1. $C_{14:0}$ - carboxylic methyl ester, 2. $C_{17:1}$ - fatty aldehyde, 3. $C_{16:0}$ - carboxylic acid methyl ester, 4. unknown, 5. $C_{18:1}$ - carboxylic acid methyl ester, 6. $C_{18:0}$ - carboxylic acid methyl ester, 7. $C_{32:0}$ - α,ω - dicarboxylic dimethyl ester (α,ω-15,16-dimethyl tricotanedioate dimethyl ester), 8. $C_{34:1}$ - α,ω - dicarboxylic dimethyl ester , 9. $C_{36:2}$ - α,ω - dicarboxylic dimethyl ester .

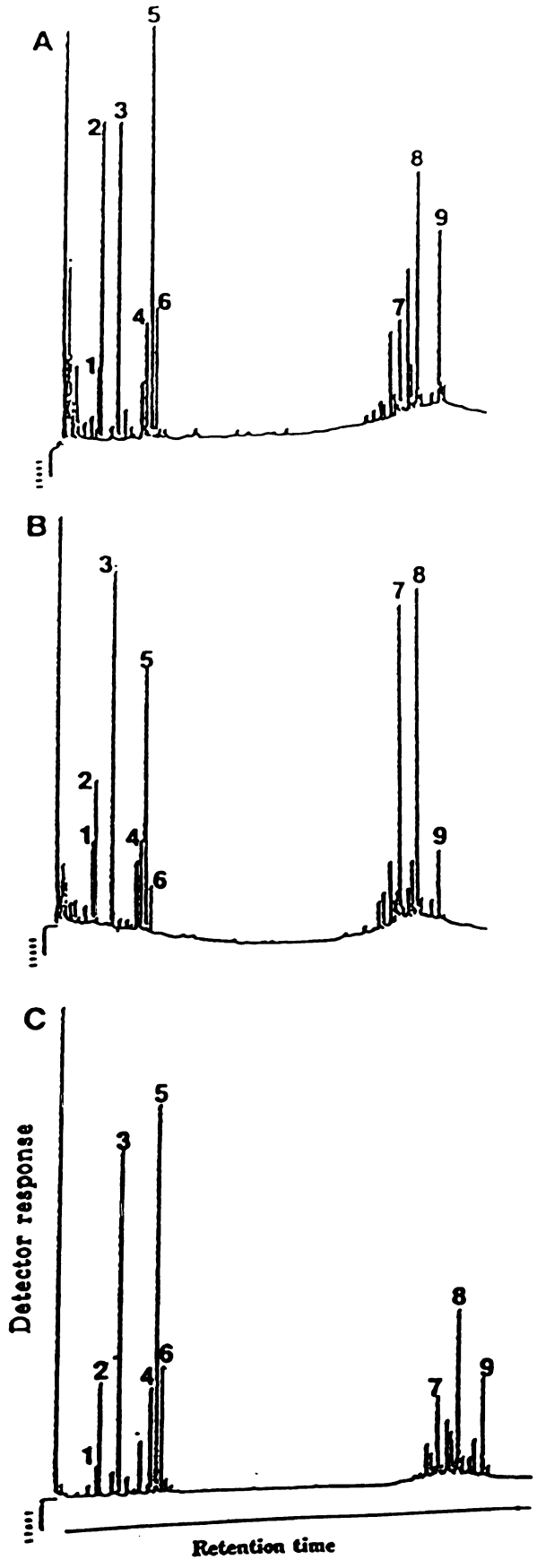

Figure 8

was much higher than the culture at 37°C (data not shown) demonstrating that synthesis of which fatty acids was reversible and dependent on temperature.

E.coli compensate for an increase in growth temperature or the presence of ethanol by increasing the relative abundance of saturated fatty acids (14, 26, 37). The same changes are also observed when *Clostridium acetobutylicum* is grown in the presence of alcohol (1, 22). Our finding suggest that the ratio of saturated to unsaturated fatty acids is not decreased by increasing temperature or solvent but rather that *S. ventriculi* overcomes the increase in membrane fluidity by increasing the ratio of the very long chain fatty acids to regular length fatty acids (Table 2). Such a response has also been observed in *C. acetobutylicum* with increasing growth temperature (1, 22), but the increase in chain length is not as dramatic as that observed in *S. ventriculi*, whereby the chain length almost doubles. In *Zymomonas mobilis* longer chain fatty acids appear to be beneficial for the high ethanol tolerance exhibited by the organism (6). In *Z. mobilis* the mechanism by which ethanol tolerance is achieved appears to be a concerted shift in the relative amounts of phospholipids, hopanoids and proteins in the cell envelope. The large ethanol-dependent shifts in the hopanoid content suggest a major function of these sterol-like substances for membrane stabilization (34).

There have been a few other reports of bacteria producing unusually long chain fatty acids. *Lactobacillus heterohiochii* is a spoilage organism of Japanese wine, growing in concentrations of alcohol greater than 20%, possessing short chain fatty acids and considerable amounts of saturated and mono-unsaturated fatty acids ranging in length from C_{20} to C_{30} (40, 41). Sulfate-reducing bacteria, *Desulfotomaculum sp.* and three strains of *D. ruminis* contained α-hydroxy and α,ω-dicarboxylic acids with more than 20 carbons, and in addition very long chain fatty acids up to C_{34}, were identified (33). A *Butyrivibrio* spp. (strain S2) occurring in the rumen has an absolute requirement for fatty acid, and a new series of long chain dicarboxylic acids (C_{20-36}) were found to be major components of the lipids (10,11,20). Another unusual C_{30} fatty acid is present in *Clostridium*

Table 2. Effect of environmentsl stress on chain length and the degree of saturation of the fatty acids in *Sarcina ventriculi.*

Fatty acids(%)[a]	pH 7.0 (37°C)	pH 7.0 + (0.25 M Ethanol, 37°C)	pH 7.0 + (0.05 M Butanol, 37°C)	pH 7.0 (45°C)	pH 7.0 (55°C)	pH 3.0 (37°C)
Saturated	32.7	24.6	24.6	29.7	29.4	35.7
Unsaturated	67.3	75.4	75.4	70.3	70.6	64.3
Regular (< C20)	> 93	55.2	55.2	58.2	62.0	48.9
Very long chain (> C28)	< 7	44.8	44.8	41.8	38.0	51.1
Ratio of U/S[b]	2.06	3.06	3.06	2.37	2.40	1.80
Ratio of V/R[c]	0.08	0.81	0.81	0.72	0.61	1.05

[a] Relative amounts of unsaturated, saturated, regular (lesss than 20 carbon atoms) or very long chain (more than 28 carbons) fatty acids were determined by the calculation of integrated peak areas on GC analysis at each condition.

[b] Unsaturated fatty acid/Saturated fatty acid.

[c] Very long chain fatty acid/Regular fatty acid

thermohydrosulfuricum and *Cl. thermosulfurogenes*, and this dicarboxylic acid accounts for about 10 and 23% respectively of the total apolar chains of these organisms (21). Fatty acids such as 27-hydroxyoctacosanoic acid bipolar long chain fatty acids are thought to be key membrane components for controlling the fluidity of bacterial membranes in other systems where oxygen diffusion has to be regulated or where the organism might have to survive intracellularly within eucaryotic organisms (2,12,13).

Recently, homeoviscous adaptations in the archaebacterum, *Methanococcus jannashcii*, have been reported in which changes in the proportions of diether, macrocyclic ether and tetraether lipids of the membrane were found at different temperatures (36). The relative amounts of tetraether lipid (C_{40}) increased with increasing temperature relative to the level of diether lipid (C_{20}). This indicates that the transmembrane lipid components function to modulate the reduced viscosity due to increased temperature thus, maintaining the optimum fluidity.

Increased temperature, solvents, or proton levels disrupt membrane order and lead to increased molecular motion, affecting the viscosity of the membrane. This may trigger the synthesis of the very long hydrophobic lipid components which would reduce the increased viscosity. There are several classical mechanisms which are known to be activated in response to these changes. The first is the heat shock gene phenomenon (23) whereby proteins are synthesized in response to various forms of stress including heat (31), ethanol (32, 38, 42), puromycin (8), anaerobiosis (35) and pH (7). It is not clear to what extent the phenomenon we see in *S. ventriculi* is related to heat shock or stress proteins.

Our results suggest that there is a common membrane response to various environmental stresses in *S. ventriculi*. This response involves the synthesis of a new family of very long α,ω-dicarboxylic acids which may control membrane fluidity. From the structural data the two polar groups on the dicarboxylic groups are present at either end, which suggests that this unusual lipid component probably spans the membrane, a position

which would be more energetically favorable.

CONCLUSIONS

Changes in the composition of membrane lipids in a strictly anaerobic, facultative acidophilic eubacterium, *Sarcina ventriculi* were studied in response to various forms of environmental stress. Changes in lipid composition and structure occurred in response to changes in environmental pH. At neutral pH, the predominant membrane fatty acids ranged in chain length from C_{14} to C_{18}. However, when cells were grown at pH 3.0, a family of unique very long chain fatty acids containing 32 to 36 carbon atoms was synthesized and accounted for 50 % of the total membrane fatty acids. These acids were identified as very long chain α,ω-dicarboxylic acids ranging in length from 28 to 36 carbons by electron impact mass spectrometry of methyl and (perdeuterio) methyl ester derivatives. These methyl esters all bore a vicinal dimethyl group toward the center of the chain. The assignment of the structures was confirmed by isolating one of the very long chain unusual fatty acids as the ester form after methanolysis and performing further analyses including ^{1}H and ^{13}C NMR (Nuclear Magnetic Resonance) spectroscopy and Fourier Transform infrared spectroscopy. Coupling this information with the data from Gas Chromatography/Mass Spectrometry (GC/MS) analysis, the exact structure was confirmed as α,ω-15,16-dimethyltricotanedioate dimethyl ester.

Addition of alcohols, either metabolic (0.25 M ethanol) or nonmetabolic (0.05 M butanol) to cells grown at pH 7.0, or thermal stress (growth temperature at pH 7.0 was raised from 37°C to 45°C or 55°C) also resulted in the synthesis of these very long chain fatty acids. Synthesis of these very long chain α,ω-dicarboxylic acids was reversed by reducing the temperature back to 37°C. *S. ventriculi* is also unusual in that the membrane components are not the usual phospholipid components but appear to be predominantly glycolipids.

REFERENCES

1. Baer, S. H., H. P. Blaschek, and T. L. Smith. (1987) *Appl. Environ. Microbiol.* **53**, 2854-2861
2. Bhat, U.R., Mayer, H., Yokota, A., Hollingsworth, R. I., and Carlson, R. W. (1991) *J. Bacteriol.* **173** , 2155-2159
3. Canale-Parola, E. (1970) *Bacteriol. Rev.*, **34**, 82-97
4. Canale-Parola, E. (1986) Genus *Sarcina Goodsir* 1842, 434^{AL}, p. 1100-1103. In P. H. A. Sneath, N. S. Mair, M. E. Shaarpe and J. G. Holt (ed.), Bergey's manual of systematic bacteriology, vol. 2. The Williams & Wilkins Co., Baltimore
5. Carey, V. C., and L. O. Ingram. (1983) *J. Bacteriol.* **154**, 1291-1300
6. Dombek, K. M., and L. O. Ingram. (1984) *J. Bacteriol.* **157**, 233-239
7. Foster, J. W., and H. K. Hall. (1990) *J. Bacteriol.* **172**, 771-778
8. Goff, S. A., and A. L. Goldberg. (1985) *Cell* **41**, 587-595
9. Goodwin, S., and J. G. Zeikus. (1987) *J. Bacteriol.* **169**, 2150-2157
10. Hazlewood, G. P., N. G. Clarke, and R. M. C. Dawson. (1980) *Biochem. J.* **191**, 555-569
11. Hazelwood, G. P., and R. M. C. Dawson. (1979) *J. Gen. Microbiol.* **112**, 15-27
12. Hollingsworth, R. I., and Carlson, R. W. (1989) *J. Biol. Chem.* **264**, 9300-9303
13. Hollingsworth, R. I., and Lill-Elghanian, D. A. (1989) *J. Biol. Chem.* **264**, 14039-14042
14. Ingram, L. O. (1976) *J. Bacteriol.* **125**, 670-648
15. Ingram, L. O. (1977) *Can. J. Microbiol.* **23**, 779-789
16. Ingram, L. O. (1982) *J. Bacteriol.* **149**, 166-172
17. Ingram, L. O. (1990) *Crit. Rev. Biotechnol.* **9**, 305-319
18. Ingram, L. O., and N. S. Vreeland. (1980) *J. Bacteriol.* **144**, 481-488

19. Kell., D. B., M. W. Peck, G. Rodger, and J. G. Morris. (1981) *Biochem. Biophys. Res. Comm.* **99**, 81-88

20. Klein, R. A., P. G. Hazlewood, P. Kemp, and R. M. C. Dawson. (1979) *Biochem. J.* **183**, 691-700

21. Langworthy, T. A., and J. L. Pond. (1986) Membranes and lipids of thermophiles, p. 107-135. *In* T. D. Brock (ed.), Thermophiles, General, Molecular, and Applied Microbiology. Wiley & Sons, New York.

22. LePage, C., F. Fayolle, M. Hermann, and J.-P. Vandecasteele. (1987) *J. Gen. Microbiol.* **133**, 103-110

23. Lindquist, S. (1986) *Ann. Rev. Biochem.* **55**, 1151-1191

24. Lowe, S. E., H. S. Pankratz, and J. G. Zeikus. (1989) *J. Bacteriol.* **171**, 3775-3781.

25. Lowe, S. E., and J. G. Zeikus. (1991) *Arch. Microbiol.* **155**, 325-329

26. Marr, A. G., and J. L. Ingraham. (1962) *J. Bacteriol.* **84**, 1260-1267

27. deMendoza, D., and J. E. Cronan, Jr. (1983) *Trends Biochem. Sci.* **8**, 49-52

28. deMendoza, D., A. K. Ulrich, and J. E. Cronan, Jr. (1983) *J. Biol. Chem.* **258**, 2098-2101

29. Morris, J. L. (1962) *Chem. & Ind.* 1238-1240

30. Holme, J. D. and Peck, H. (1983) Analytical Chemistry pp 436-467 Longman, Inc. New York

31. Neidhardt, F. C., R. A. VanBogelen, and V. Vaughn. (1984) *Ann. Rev. Genet.* **18**, 295-329

32. Plesset, J., C. Palm, and C. S. McLaughlin. (1982) *Biophys. Res. Commun.* **108**, 1340-1345

33. Reznak, T., M. Yu. Sokolov, and I. Viden. (1990) *FEMS Microbiol. Ecol.* **73**, 231-238

34. Schmidt, A., S. Bringer-Meyer, K. Porolla, and H. Sahm. (1986) *Appl. Microbiol.*

Biotechnol. **25**, 32-36

35. Spector, M. P., Z. Aliabadi, T. Gonzalez., and J. W. Foster. (1986) *J. Bacteriol.* **173**, 3907-3910.

36. Sprott, G. D., M. Meloche, and J. C. Richards. (1991) *J. Bacteriol.* **173**, 3907- 3910

37. Sullivan, K. H., Hegeman, G. D. and Cordes, E. H. (1979) *J. Bacteriol.* **138**, 133-138

38. Terracciano, J. S., E. Rapaport, and E. R. Kashket. (1988) *Appl. Environ. Microbiol.* **54**, 1989-1995

39. Tilak, K. V. B. R. (1970) *Sci. Cult.* **36**, 399-400

40. Uchida, K. (1974a) *Biochim. Biophys. Acta* **348**, 86-93

41. Uchida, K. (1974b) *Biochim.Biophys. Acta* **369**, 146-155

42. VanBogelen, R. A., P. M. Kelley, and F. C. Neidhardt. (1987) *J. Bacteriol.* **169**, 26-32

CHAPTER III

CHEMICAL PROOF FOR THE FORMATION OF VERY LONG α,ω-BIFUNCTIONAL ALKYLSPECIES IN THE MEMBRANE OF *SARCINA VENTRICULI* BY TAIL-TO-TAIL COUPLING OF EXISTING ALKYL CHAINS FROM OPPOSITE SIDES OF THE BILAYER

INTRODUCTION

The membrane is a universal structural feature which is responsible for signal and energy transduction, compartmentalization of biological processes and maintenance of the structural integrity of the cell in all living systems, from microorganisms through plants and animals. Membranes play a central role in critical events such as DNA replication, cell division, protein synthesis, electron transfer and photosynthesis. Despite this, due largely to the preeminence of molecular genetics approaches, most of the current research on cellular adaptation to environmental stress focuses on proteins and nucleic acids and not on lipids which are the primary membrane components.

There is the growing concept that proteins are the structural entities which control membrane fluidity at elevated temperatures rather than lipids and that changes in external temperature is sensed directly by proteins with no stated involvement of lipids (2, 3, 4). Protein changes are easier to demonstrate and understand genetically. Lipid changes are, in contrast, much more difficult to demonstrate, more difficult to understand and close to impossible to trace back to a specific gene or genes. Probably because of a combination of these factors, the roles of lipids in ensuring cell survival during stress is often underestimated and very poorly understood.

Proteins are thought to be the universal entities which structurally preserve cell function and integrity. This model is that proteins sense environmental changes and cause the synthesis of new proteins which then alter membrane lipid structure (5, 6). A simpler, more desirable system would be one in which changes in membrane dynamics are transmitted through the lipids to trigger a constitutive, fluidity-regulated, dynamic adaptation system. This system would act on the membrane lipids to return the membrane to its original fluidity or dynamic state (at which the adaptation system is inactive). This would constitute the ultimate in adaptation systems since the entire transcription/translation machinery would not have to be set in motion. It is therefore, independent of the very

cellular events (the viability of which are in question during stress) which it is trying to preserve. In the case of bacteria, a likely course would be for the organism to adopt a membrane structure which is typical of bacteria whose normal habitat is similar to the new environmental conditions. In the case of substantial temperature increases from normal ambient temperatures, the new membrane structure might resemble that found in thermophilic eubacteria (7, 8, 9) or archaebacteria (10, 11) in some important ways. Bacteria with a very dynamic range of environmental tolerance are especially suited as model systems for studying these adaptation phenomena since the chemistry of the membrane can be studied as a function of the perturbed state and mutants which are tolerant to the new conditions do not have to be obtained.

Sarcina ventriculi is a gram positive, strict anaerobic eubacterium which can adapt to environmental pH values between 3 and 9 (12, 13, 14). The organism synthesizes very long chain α,ω-dicarboxylic acids in response to lowering pH, the addition of organic solvents or raising the temperature (1). The gas chromatography profile of the methanolysate of the total cell mass after these perturbations (Figure 1) showed two separate domains of fatty acid chain lengths. An early eluting one due to regular chain length fatty acyl components and a later one due to components with lengths twice that of the regular fatty acyl components. This latter domain contained the methyl ester derivatives of the α,ω-dicarboxylic acids. The unusual chain length distribution and the large variety of very long chain dicarboxylic species formed in the membrane of *S. ventriculi* during the response to various environmental perturbations suggest the possibility of an unusual, new mechanism for their formation. The typical 2-carbon addition process involving the acetyl Co-A cannot be used to explain the structures(α,ω-bifunctional) and chain length distribution of the very long chain components of the membrane of this species. Here, we report chemical evidence for the mechanism of formation of very long chain bifunctional alkyl species by tail-to-tail addition of hydrocarbon chain from opposite sides of the bilayer. This would constitute an entirely new, very sophisticated mechanism for

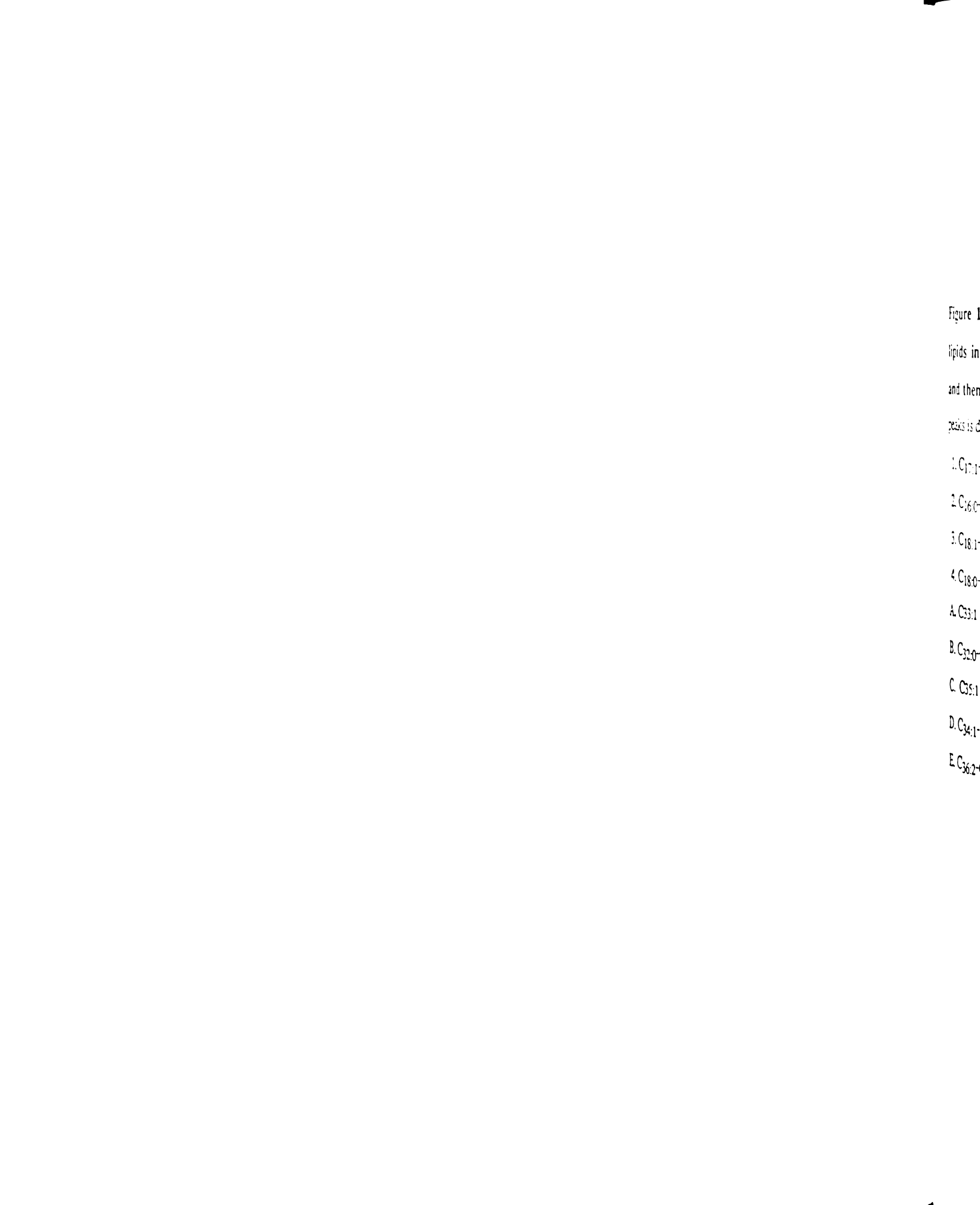

Figure 1

lipids in

and then

peaks is c

1. $C_{17:1}$-

2. $C_{16:0}$-

3. $C_{18:1}$-

4. $C_{18:0}$-

A. $C_{33:1}$

B. $C_{32:0}$-

C. $C_{35:1}$

D. $C_{34:1}$-

E. $C_{36:2}$-

Figure 1. Gas Chromatographic analyses of the total methanolysate of the lipids in the membrane of *Sarcina ventriculi* cells grown at pH 7.0 at 37°C and then shift to 45°C at late log phase for 3hrs. The later eluting cluster of peaks is due to very long chain α,ω-bifunctional fatty acids. The major components are :

1. $C_{17:1}$-fatty aldehyde ($HCO(CH_2)_9CH=CH(CH_2)_4CH_3$)
2. $C_{16:0}$-carboxylic acid methyl ester ($CH_3OCO(CH_2)_{14}CH_3$)
3. $C_{18:1}$-carboxylic acid methyl ester ($CH_3OCO(CH_2)_9CH=CH\ (CH_2)_5CH_3$)
4. $C_{18:0}$-carboxylic acid methyl ester ($CH_3OCO(CH_2)_{16}CH_3$)

A. C33:1 ω-formylmethyl ester

B. $C_{32:0}$-α,ω-dicarboxylic acid dimethyl ester

C. C35:1 ω-formylmethyl ester

D. $C_{34:1}$-α,ω-dicarboxylic acid dimethyl ester

E. $C_{36:2}$-α,ω-dicarboxylic acid dimethyl ester

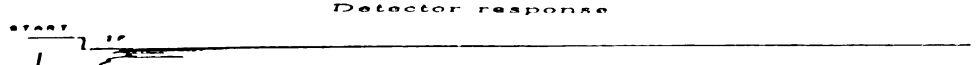
Detector response

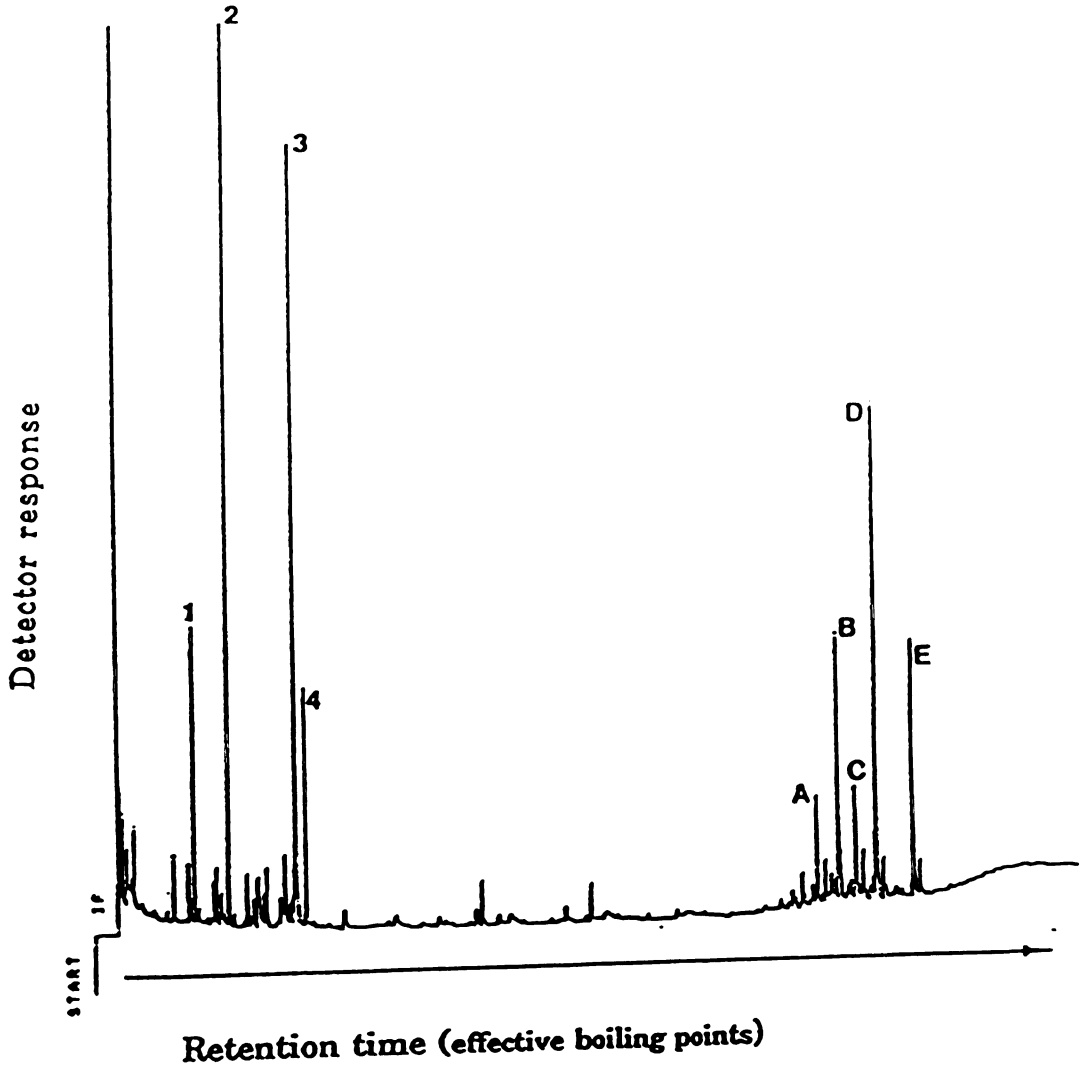
Detector response
1
2
3
4
A
B
C
D
E
START
Retention time (effective boiling points)

Figure 1

membrane adaptation. The conclusions about the mechanism are drawn from the satisfaction of certain structural and stereochemical features of the new bifunctional lipids imposed by the nature of the mechanism.

It is clear from the structure of the fatty acid methyl ester (15,16-dimethyltriacotane-1,30-dicarboxylic acid dimethyl ester) described in our earlier study (1) that the combination of the regular fatty acyl chains to form the new bifunctional species could involve coupling between the ω-1 positions of the chains of two hexadecanoyl (C_{16}) species leading to the vicinal dimethyl group. Hence coupling between two $C_{16:0}$ acyl species should yield a 15,16-dimethyl C_{30} bifunctional molecule. A C_{30} dimethyl bifunctional molecule can also be obtained by the similar coupling of a C_{18} and a C_{14} fatty acid. However, the vicinal methyl groups will be located at the 13 and 14 positions. These two isomeric acids can be distinguished by mass spectrometry since fragmentation between the two methyl groups is dominant. The only unsaturated, regular fatty acid in *S. ventriculi* membranes is *cis*-vaccenic acid (a C_{18} acid). In this molecule, the double bond occurs at the 11 position. If the ω-1 carbon coupling theory is correct, the very long, bifunctional unsaturated alkyl species should have a *cis* double bond at the 11 position and a methyl group at the 17 position relative to the closest carbonyl carbon. In instances when the two acyl species are identical, combination at the ω-1 positions by this mechanism should yield an asymmetric bifunctional species provided that the two hydrogen atoms which are lost in the coupling are removed from the same side of the intermediate, partially bonded species (Figure 2). Another consequence of this proposed mechanism is that it should be possible to detect ω-formyl long chain acids among the very long chain bifunctional species formed during the membrane adaptation process. These would be formed by coupling of the acyl chains of phospholipid fatty ester groups with the alkenyl chains of plasmalogens. Plasmalogens are known to be present since fatty aldehydes were detected among the regular chain length components of the methanolysate (Figure 1) in comparatively minor proportions. It should therefore be possible to rationalize the detailed structural features of

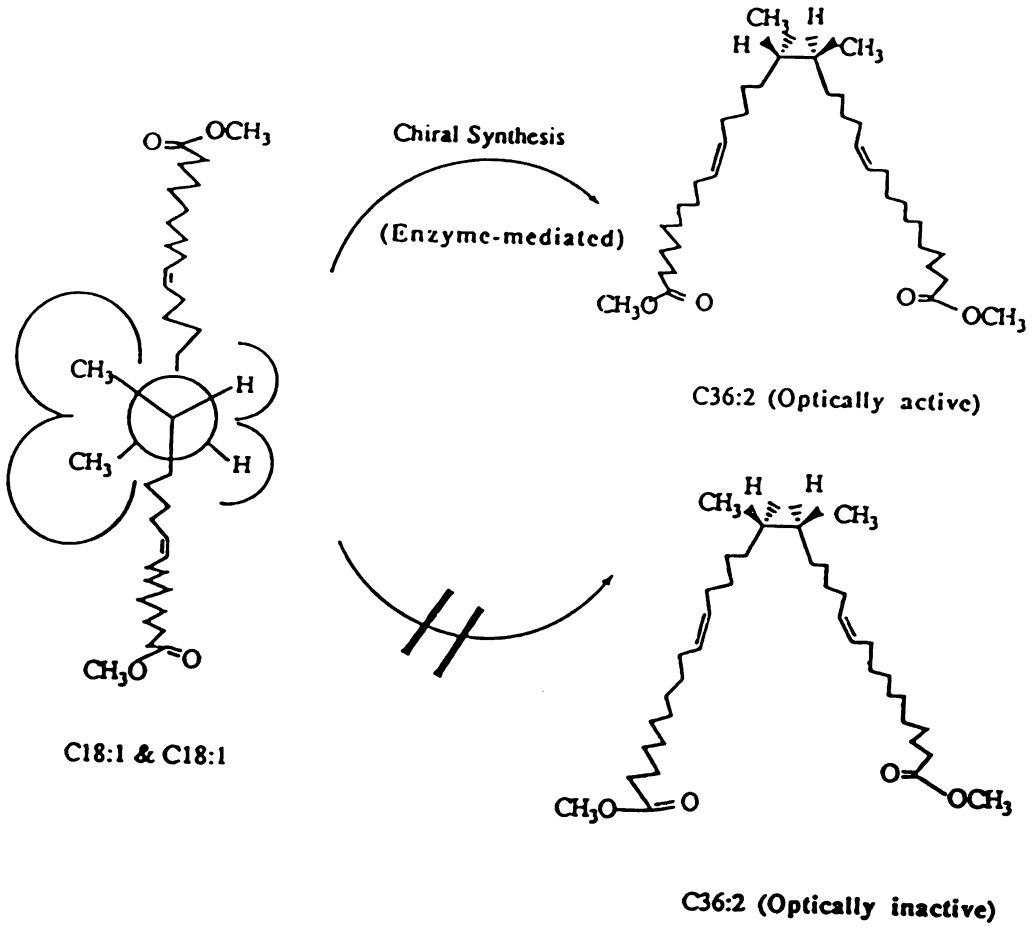

Figure 2. Rationalization of the stereochemistry of the products formed by tail-to-tail coupling of alkyl chains from opposite sides of the bilayer.

any of the bifunctional lipid species by considering the structural features of the regular chain length species. Satisfaction of these requirements should constitute proof of the transmembrane coupling mechanism. In this work we describe the isolation and characterization of a variety of fatty acids from *S. ventriculi* cultured under conditions which promote the synthesis of bifunctional, very long chain fatty acids. This allowed the definitive chemical proof of the transmembrane lipid coupling mechanism.

MATERIALS AND METHODS

Organism and Culture Conditions

S. ventriculi JK was cultivated as described previously (1). For growth under pH control, 4 liter Kimax jars (Baxter Scientific Products, Romulus, Mich.) containing 3 liters of medium were used. The jars were equipped with a pH probe, and the culture mixed by placing the jars on a magnetic stirrer. The organism was grown at pH 3.0. The cells were harvested at midexponential phase, washed twice with distilled water and stored at -70°C for further analysis.

Membrane Preparations

Cells were disrupted by passage through a French Pressure cell (American Instruments Co., Inc., Silver Spring, Md.) at 20,000 lb/in^2. The disrupted cells were centrifuged at 20,000 x g to remove unbroken cells, and the supernatant was centrifuged at 110,000 x g to sediment the membranes, which were washed twice with distilled water.

Total Fatty Acids Analysis

Fatty acid analyses were performed on whole cells or isolated membrane fractions by treatment with methanolic HCl using either of two procedures. Procedure (a) was employed for whole cells and procedure (b) for isolated membranes. (a) cells (1-5 mg) suspended with 0.3 ml chloroform and 1.5 ml 5% methanolic HCl solution, were sealed in a teflon-lined screw-capped vial, and heated in a water bath or oven at 72°C for 24 hours. Chloroform (3 ml) was added every 8 hours followed by mild sonication for 5 minutes. After concentration to dryness under nitrogen gas, samples were partitioned between water and chloroform and the aqueous layer washed several times with chloroform or hexane. The combined solutions were filtered through glass wool. (b) 3 ml of chloroform was

added to 1 ml of membrane suspension followed by 15 ml 5% methanolic-HCl solution. The flask was sealed and heated in an oven at 72°C for 12 hours. Three (3) ml of chloroform was added every 6 hours followed by mild sonication for 5 minutes. The mixture was then concentrated on the rotary evaporator to dryness and extracted with chloroform. The combined organic fraction was redissolved in 1 ml of hexane. The fatty acid methyl esters prepared by either procedure (a) or (b) were subjected to Gas Chromatography (GC) analysis on a 25 M J&W Scientific DB1 capillary column using helium as the carrier gas and a temperature program of 150°C initial temperature, 0.00 min hold time and 3.0 deg/min rate, to a temperature of 200°C. A second ramp of 4.0 deg/min was then immediately started until the final temperature of 300°C was obtained. This temperature was held for 30 min. The relative proportion of lipid components were calculated from the integrated peak areas. The fatty acid identification and molecular weight were determined using GC/MS analysis using a Jeol JMS-AX505H spectrometer interfaced with a Hewlett-Packard 5890A Gas Chromatograph.

Isolation of the α,ω-Dicarboxylic Acid Dimethyl Esters

The total lipids (100 mg) extracted from the cells as described above were methanolysed with 5 % (w/v) HCl in methanol (5 ml) for 12 h at 72°C. Chloroform (1 ml) was added every 4 hours followed by mild sonication for 5 minutes. The mixture was then concentrated on the rotary evaporator to dryness and extracted with chloroform. The combined organic fraction was redissolved in 1 ml of hexane. This fraction was applied to a silica flash chromatography column and eluted with chloroform/hexane (1:1, by vol). Fractions were assayed by Gas Chromatography. Fractions containing very long chain fatty acid methyl esters were concentrated and rechromatographed on 5% $AgNO_3$ impregnated-preparative thin layer silica chromatography plates which were eluted with petroleum ether/ diethyl ether /acetone (10:1:0.5, by vol). Spots were made visible either by spraying with 50% ethanolic-sulfuric acid and heating at 250°C to char the organic

components, or by spraying with a 0.1% solution of 2',7,-dichlorofluorescein in aqueous ethanol (1:1) and viewing under ultraviolet light. Bands were scraped from the plate into a column fitted with a sintered disc and the material was eluted from the silca gel with methanol and chloroform. Each fraction was concentrated by evaporation and redissolved in choloroform for further analysis. Purity of each fraction was assayed by GC/MS.

Isotope Labeling

Isotope labeling was used to aid in deducing the structures of esterified lipid components using GC/MS. Methyl esters of fatty acids obtained by acid methanolysis were further treated with 5% deuterated methanolic-HCl for 6 hours at 72°C. Deuterated methyl esters of fatty acids were extracted and analyzed as described above.

^{1}H NMR and ^{13}C NMR Spectroscopy

Proton NMR spectra were recorded at 500 MHz on solutions in $CDCl_3$. Fourier transform ^{13}C NMR spectra were recorded at 125 MHz on solutions in $CDCl_3$. Chemical shifts are quoted relative to the chloroform resonances taken at 7.24 ppm for proton and 77 ppm for ^{13}C measurements, respectively.

Fourier Transform Infrared Spectroscopy

Spectra were obtained with a Nicolet model 710 FT-IR spectrometer on a 10% (w/v) solution of dicarboxylic acid dimethyl ester in chloroform.

Optical Rotation Analysis (Polarimetry)

Optical polarimeter (Perkin Almer) was used for measuring the optical activity with the mercury (Hg) light at various wavelengths (578 nm, 546 nm and 436 nm). Measurements were performed on 20mg samples dissolved in 1 ml chloroform solution.

Reductive Ozonolysis (15)

For ozonolysis of unsaturated lipids, a solution of 50 mg sample in 2 ml methylene chloride was cooled to -70 ^{o}C. Ozone was passed through the solution at a rate of 60 mg/hr from a ozone generator while maintaining the temperature at -70^{o}C. The extent of the reaction was checked every 10 min. by TLC. Ozonides were decomposed to aldehydes by reductive cleavage using Lindlar catalyst. These shorter chain aldehydes then were isolated by preparative TLC or flash column chromatography (16). The products were further analyzed by GC and GC/MS.

RESULTS AND DISCUSSION

GC Analyses of Fatty Acids of *S.ventriculi*

Sarcina ventriculi were grown at 37°C, pH 7.0, and then shift to 45°C at late log phase for 3hrs. GC analyses of fatty acid methyl esters extracted from cells are shown in Figure 1. The peaks from 1 to 4 are due to typical membrane fatty acyl components ranging from 14 to 18 carbons. Major regular fatty acids are hexadecanoic acid (peak 2, $C_{16:0}$) and *cis*-vaccenic acid (peak 3, $C_{18:1(11)}$). The peaks from A to E, however, correspond to very long bifunctional fatty acids components containing from 32 to 36 carbon atoms.

Mass Spectrometric Analyses of Very Long Bifunctional Fatty Acids

The mass spectrum of peak B indicated that it was the previously described (1) α,ω-diacid **1**. The electron impact mass spectrum of Peak D (Figure 3A) contained major ions at m/z 564, 532 and 501.

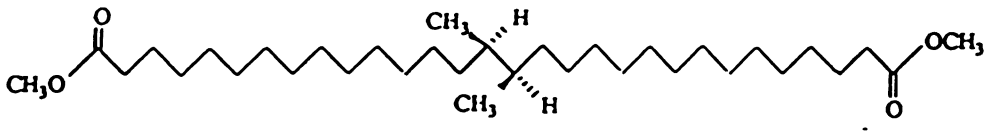

1

α,ω-(15,16-dimethyl)-triacotanedioate dimethyl ester

These corresponded to the molecular ion of a C34-α,ω-dicarboxylic dimethyl ester (M^+) with the sequential losses of methanol (CH_3OH) and a methoxy (CH_3O) group, respectively. The ions at m/z 514 was assigned to the structure obtained by sequential losses of methanol (CH_3OH) and water (H_2O) from the parent ion. The mass spectrum also contained a series of ions, the general structure of which corresponded to CH_2=CH-

Figure 3. Electron impact mass spectrums of peak D. (A) Note the major ions at m/z 564, 532 and 510. These corresponded to molecular ion (M^+) with the sequential losses of methanol and methoxy respectively. The cluster of ions at m/z 263, 296 and 324 are due to the vicinal methyl groups. (B) The electron impact mass spectrum of deuterium labeled molecule obtained by deuteration with D-4 methanolic HCl solution. The presence of two carboxyl groups was confirmed by the shift of 6 units of the M^+ ion. Other predicted mass increases due to deuterium were easily observed.

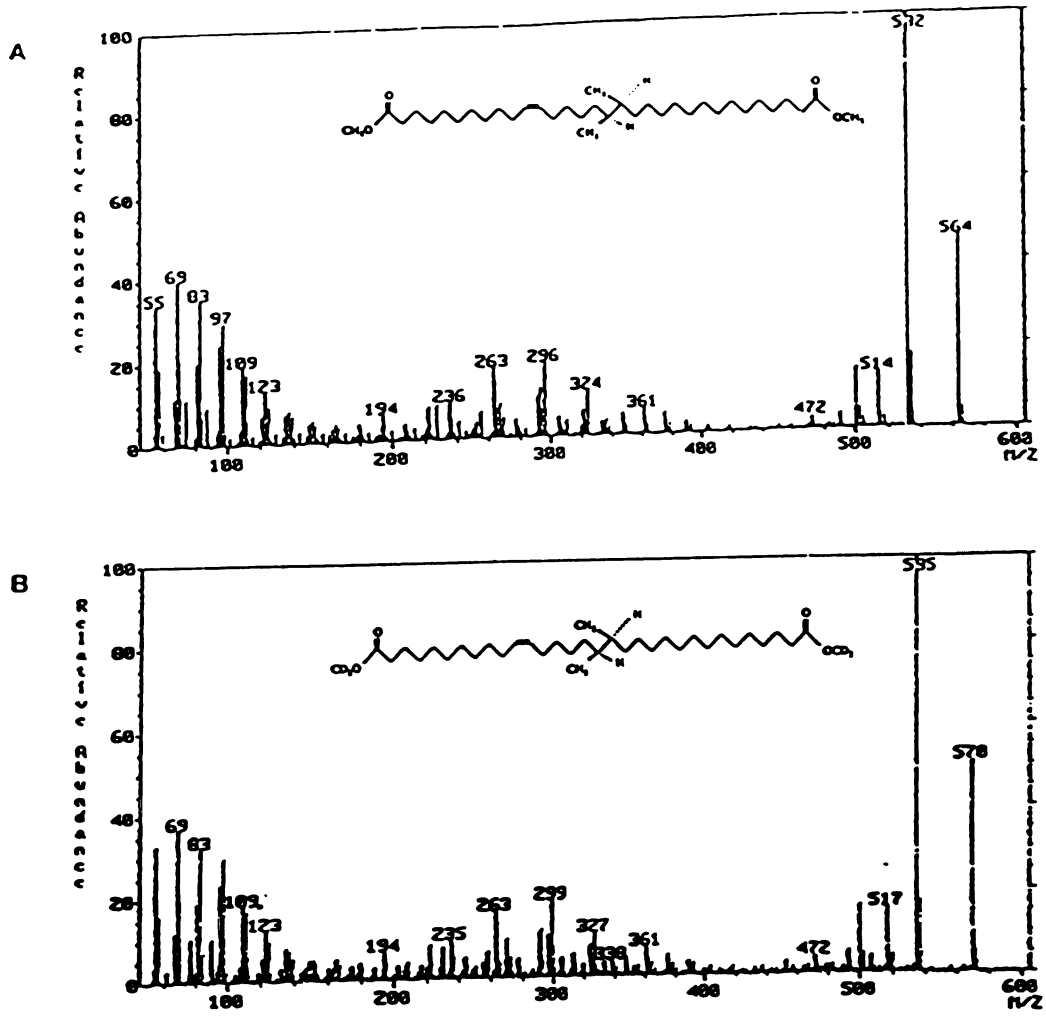
A
B
100
80
60
40
20
0
100
200
300
400
500
600
M/Z
55
69
83
97
109
123
194
236
263
296
324
361
472
514
564
512
595
578
517

Figure 3

$(CH_2)_n$ (n=2,3,4..), characteristic of an alkene. It also contained a series of ions, the general structure of which corresponded to $CH_3OCO\text{-}(CH_2)_n$, beginning at m/z 73 (n=1), as well as the characteristic McLafferty fragment at m/z 74 ($CH_3OCOH{=}CH_2$) of a saturated methyl ester. This series of ions beginning at m/z 73 continued up to and included two prominent ions at m/z 263 and 296 suggesting the presence and location of vicinal methyl groups. Scission between these methyl groups explained the primary fragments at m/z 269 and 295. The general structure of the molecule was consistent with the coupling between hexadecanoic and *cis*-11-octadecanoic acid at their ω-1 positions to give structure 2.

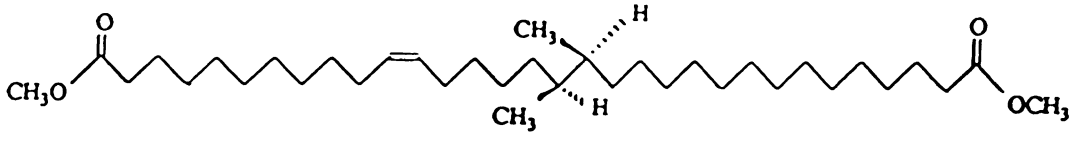

2

α,ω-(17,18-dimethyl)-*cis*-11-dotriacotaenedioate dimethyl ester

The ion at m/z 263 corresponded to the loss of methanol (CH_3OH) from the m/z 295 fragment. The ion at m/z 296 is due to a rearrangement resulting in elimination of a hydrogen atom from m/z 297 fragment or capture of a hydrogen atom by the m/z 295 fragment. The ion at m/z 237 represented the losses of methanol (CH_3OH) from the m/z 269. The fragments are tabulated and assigned in Table 1. Figure 3B shows the electron impact mass spectrum of the deuterium labeled molecule obtained by methanolysis with D-4 methanol/HCl solution to produce the trideutero methyl ester. The most striking change was the upward shift of the molecular ion by 6 mass units which confirmed the presence of two methoxy groups. The losses due to trideutero methanol (CD_3OH) and the sequential loss of a trideutero methoxy group (CD_3O) from the molecular ion (m/z 570) give ions at m/z 535 and 501. The deuterium labeled McLafferty fragment (m/z 77) was also observed. Ions at m/z 272 and 299 corresponding to m/z 269 and m/z 296 in the unlabeled

Table 1. Analyses of 70ev electron impact mass spectral fragments of proposed structure 2.

Structure of ionic fragments	mass(m/z)	deuteriated mass(m/z)
$CH_3OCO(CH_2)_9CH=CH(CH_2)_4CHCH_3CH_3CH(CH_2)_{13}OCOCH_3$	564	570
$CH_3OCO(CH_2)_9CH=CH(CH_2)_4CHCH_3CH_3CH(CH_2)_{12}CH=CO$	532	535
$OC(CH_2)_9CH=CH(CH_2)_4CHCH_3CH_3CH(CH_2)_{12}CH=CO$	501	501
532 - 18 (H_2O)	514	517
$CH_3OCO(CH_2)_9CH=CH(CH_2)_4CHCH_3CH_3CH(CH_2)_{10}CH=CH2$	490	493
$CH_3OCO(CH_2)_9CH=CH(CH_2)_4CHCH_3CH_3CH$ - 1(H)	324	327
$CH_3OCO(CH_2)_9CH=CH(CH_2)_4CHCH_3$	297	300
297 - 1 (H)	296	299
$CH_3OCO(CH_2)_{13}CHCH_3$	269	272
$OC(CH_2)_9CH=CH(CH_2)_4CHCH_3$	266	266
$CO=CH(CH_2)_{12}CHCH_3$	237	237
$CH_3OC(OH)=CH_2$	74	77
$CH_3OCO(CH_2)_n$; n=1-13	73 + 14*n	76 + 14*n
$CO=CH(CH_2)_n$: n=1-13	55+14*n	55+14*n
$CH_3-(CH2)_n$: n= 3-12	57+14*n	57+14*n
$CH_2=CH-(CH_2)n$: n=2-11	55+14*n	55+14*n

ester were also observed. The ion at m/z 263 corresponded to the loss of trideuterated methanol (CD_3OH) from the ions at m/z 298. Other major fragments are listed in Table 1. Although the mass spectra indicated the exact positions of vicinal methyl groups and the presence of one degree of unsaturation in the molecule, the location of the double bond could not be deduced and was proven by chemical degradation. The mass spectral fragmentation is illustrated in Figure 4.

Figure 5A shows the electron impact mass spectrum of peak E. This spectrum contained major ions at m/z 590, 558 and 527. These corresponded to the molecular ion of a bis-unsaturated C36-α,ω-dicarboxylic dimethyl ester (M^+) with the sequential losses of methanol (CH_3OH) and a methoxy (CH_3O) group, respectively. This was consistent with coupling of two *cis*-11-octadecanoic acid chains to form structure 3.

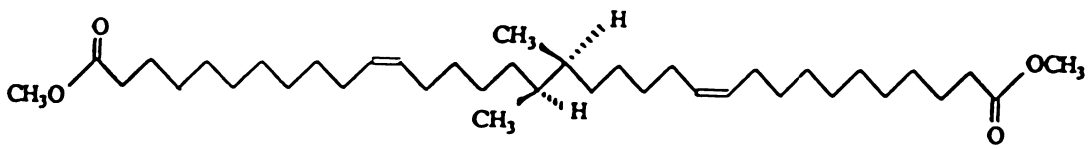

3

α,ω-(17,18-dimethyl)-*cis*-11,23-hentriacotadienedioate dimethyl ester

The prominent ion cluster at m/z 293 indicated fragmentation between the vicinal dimethyl groups in the acyl chain followed by the elimination of hydrogen to produce two identical stabilized, bis-unsaturated acyl chain fragments. The 28 mass unit difference between the primary 293 and 321 chain cleavage fragments also indicated the presence and location of vicinal dimethyl groups.

Figure 5B shows the electron impact mass spectrum of the deuterium labeled peak E molecule obtained by methanolysis with D-4 methanol/HCl solution to produce the trideuterated methyl ester. A 6 mass unit increase in the molecular ion (consistent with two methyl ester functions) was observed as well as the sequential losses of trideutero methanol

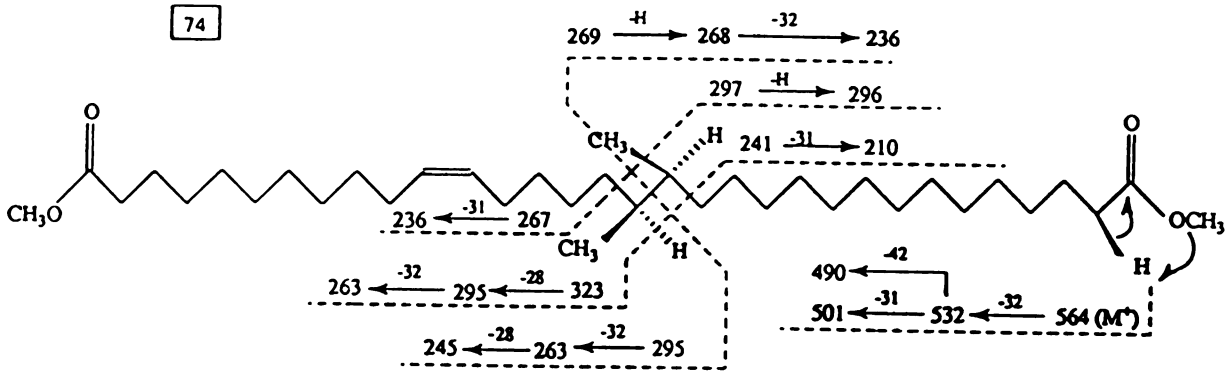

Figure 4. Electron impact mass spectral fragmentation pattern of peak D (assigned structure 2). All numbers indicate mass fragments. 42 Mass units indicate ketene (CH_2CO), 32 indicate methanol (CH_3OH), 31 a methoxy (CH_3O) group and 28 for ethylene ($CH_2=CH_2$). The ion at m/z 74 is the characteristic McLafferty fragment of an aliphatic methyl ester group.

Figure 5. The electron impact mass spectrum of peak E (assigned structure 3). (A) Major ions appear at m/z 564, 532 and 510. These correspond to the molecular ion (M^+) with the sequential losses of methanol and a methoxy group respectively. The cluster of ions at m/z 265, 293 and 321 confirm the presence and location of the vicinal methyl groups. (B) The electron impact mass spectrum of deuterium labeled peak E obtained by deuteration with D-4 methanolic HCl solution. The presence of two carboxyl groups was confirmed by isotope labeling. Mass increases due to deuterium were easily observed. The most striking change is the increase of the molecular ion by 6 mass units.

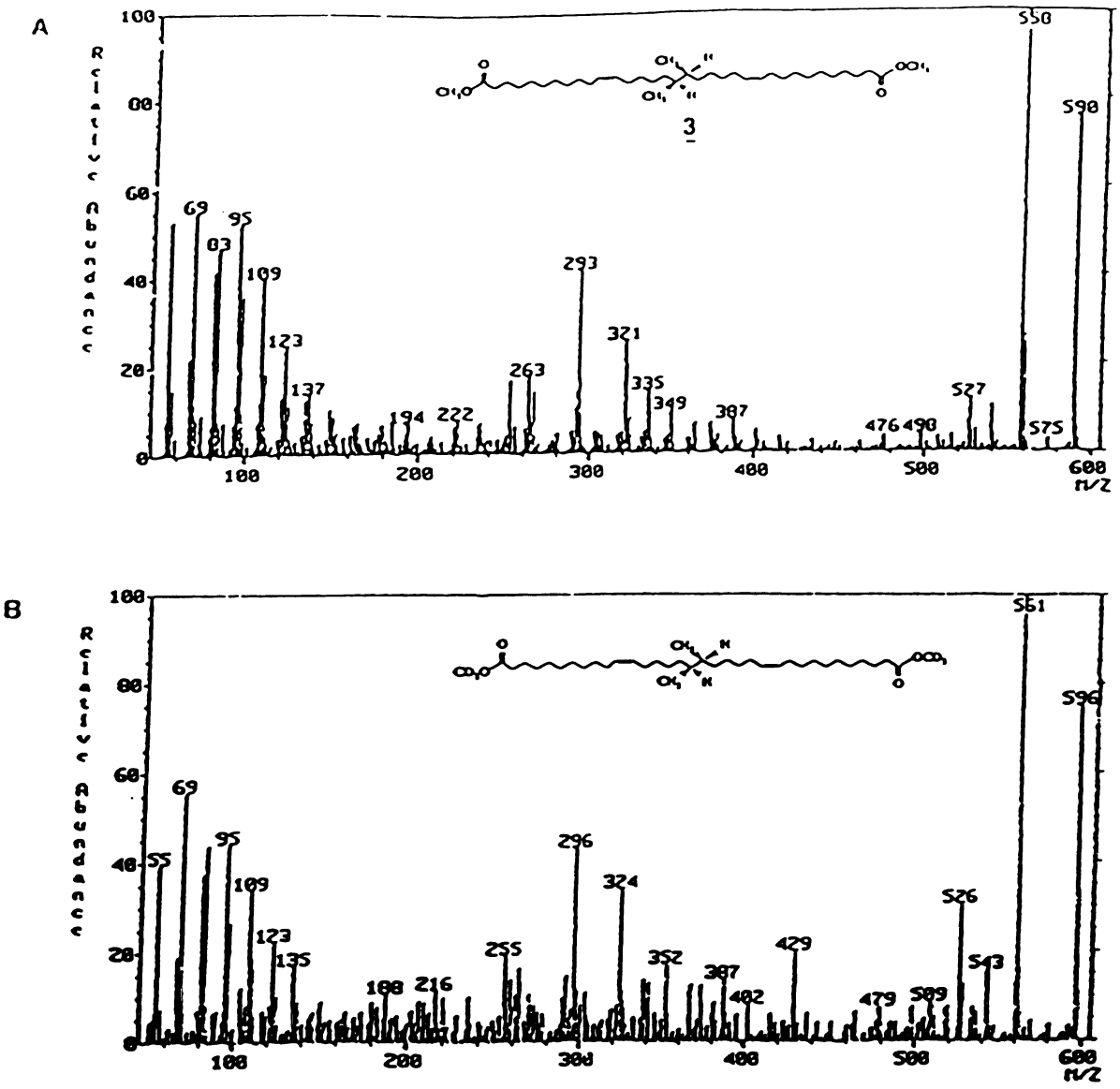
A
100
80
60
40
20
0
100
200
300
400
500
600
m/z
69
95
83
109
123
137
194
222
263
293
321
335
349
387
476
490
527
550
575
590
3
B
100
80
60
40
20
0
100
200
300
400
500
600
m/z
55
69
95
109
123
135
180
216
255
296
324
352
387
402
429
479
509
526
543
561
596

Figure 5

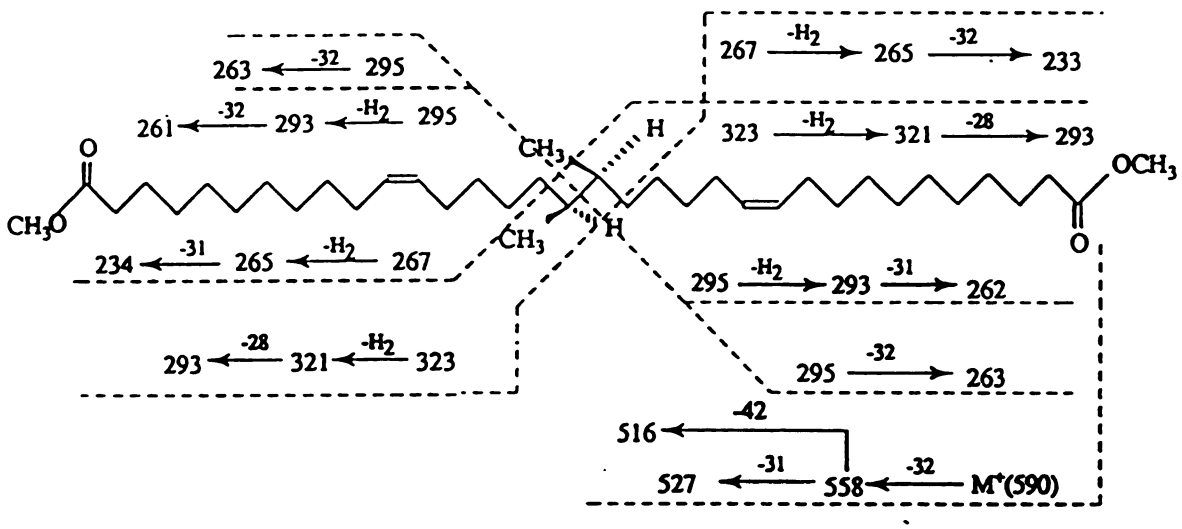

Figure 6. Electron impact mass spectral fragmentation pattern of peak E (assigned structure 3). All numbers indicate mass fragments (m/z). 42 mass units indicate ketene (CH_2CO), 32 indicate methanol (CH_3OH), 31 a methoxy (CH_3O) group and 28 for ethylene ($CH_2=CH_2$).

(CD_3OH) and a trideutero methoxy group (CD_3O). Figure 6 shows the mass spectral fragmentation pattern of peak E.

NMR and FTIR Analyses of Isolated Dicarboxylic Dimethyl Esters

Proton NMR (Nuclear Magnetic Resonance) analysis of peaks D and E (Figure 7 and 8, respectively) confirmed the presence of the double bond and vicinal methyl groups deduced from GC/MS data. In the spectrum of peak D (Figure 7), the methyl groups resulted in a 6H doublet at δ 0.74 (J=7.20 Hz). A triplet at δ 5.32 (J=6.92 Hz) in both spectra was assigned to the vinyl protons. In the case of peak D, this triplet integrated for two protons. However, in the case of peak E it integrated for four protons. Resonances at δ 1.27 were assigned to the methylene groups of the lipid chain. The multiplet at δ 1.58 was assigned to the methylene protons β to the carbonyl group. Resonances at δ 2.28 (t, J=7.69 Hz) were assigned to the methylene groups α to the carbonyl function. A 6H singlet at δ 3.65 was assigned to ester methoxy group resonances . The 4H multiplets at δ 2.00 was assigned to the protons of the methylene groups α to the vinyl carbons. The ^{13}C NMR spectrum of peak D (Figure 9) contained resonances ascribed to the ester carbonyl carbons at δ 174.5, methoxy carbon at δ 51.4 and branched methyl carbons at δ 14.5. The vinylic carbons appeared at δ 131.5. In the ^{13}C NMR spectrum of peak E (Figure 10), an increase in intensity of the signal at δ 130.8 (vinylic carbons) was observed. This spectrum only contained 19 signals confirming the proposed symmetry of the molecule. Information on the configuration of the double bonds as well as other information confirming the specific chemical functional groups was obtained by Fourier Transform Infrared Spectroscopy. The infrared spectrum of peak D (Figure 11) showed a strong aliphatic C-H asymmetric stretching absorption at 2928 cm^{-1} and symmetric stretching at 2856 cm^{-1}. The characteristic alkene stretching (=C-H) was observed at 3020 cm^{-1}. A band due to the bending vibration of aliphatic C-H bonds in the methylene groups appeared at 1464 cm^{-1} (scissoring) and one due to the twisting and wagging

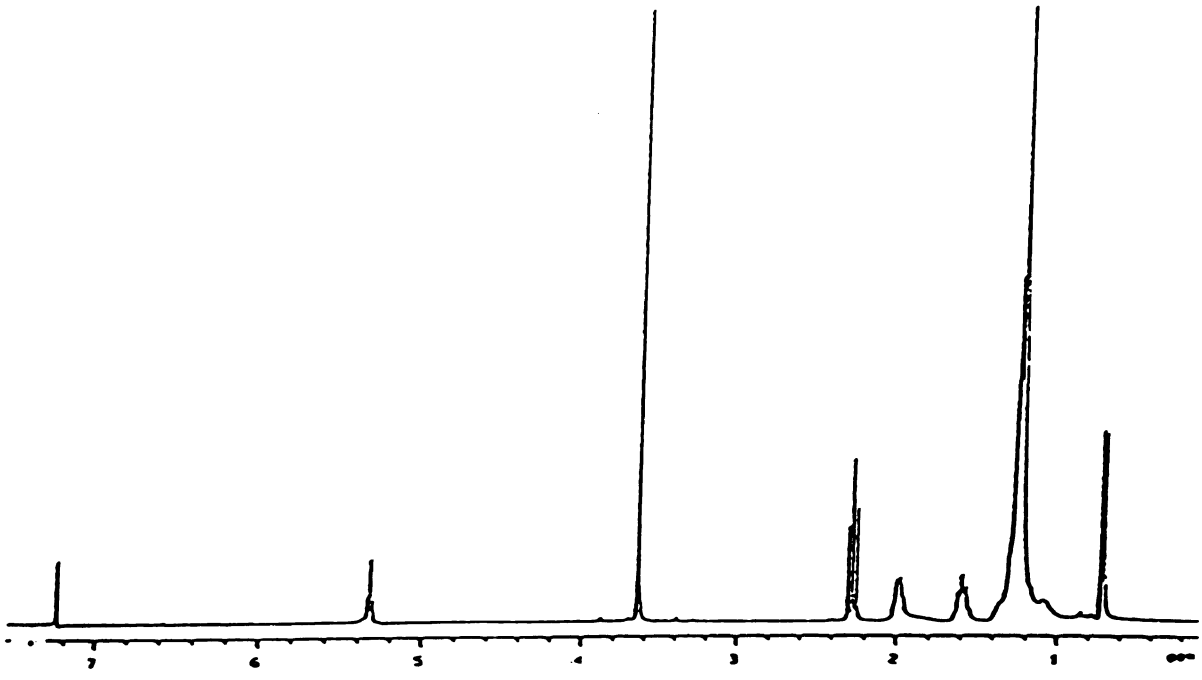

Figure 7. The ^{1}H NMR spectrum of proposed structure 2 (peak D). The signal at δ 5.32 (t, J=6.92Hz) represented a methine proton on an unsaturated carbon atom. The mutiplet at δ 2.00 was assigned to the protons of methylene groups adjacent to the unsaturated carbons. The peak at δ 1.27 is due to the methylene groups of the hydrocarbon chains. The signal at δ 3.65 is due to the methyl group of the methoxycarbonyl functions. The multiplet at δ 1.58 arises from the protons on the carbons β to the carbonyl function. The doublet at δ 0.74 (J=7.20Hz) is due to the protons of the vicinal methyl groups. The signal at δ 7.24 is due to chloroform.

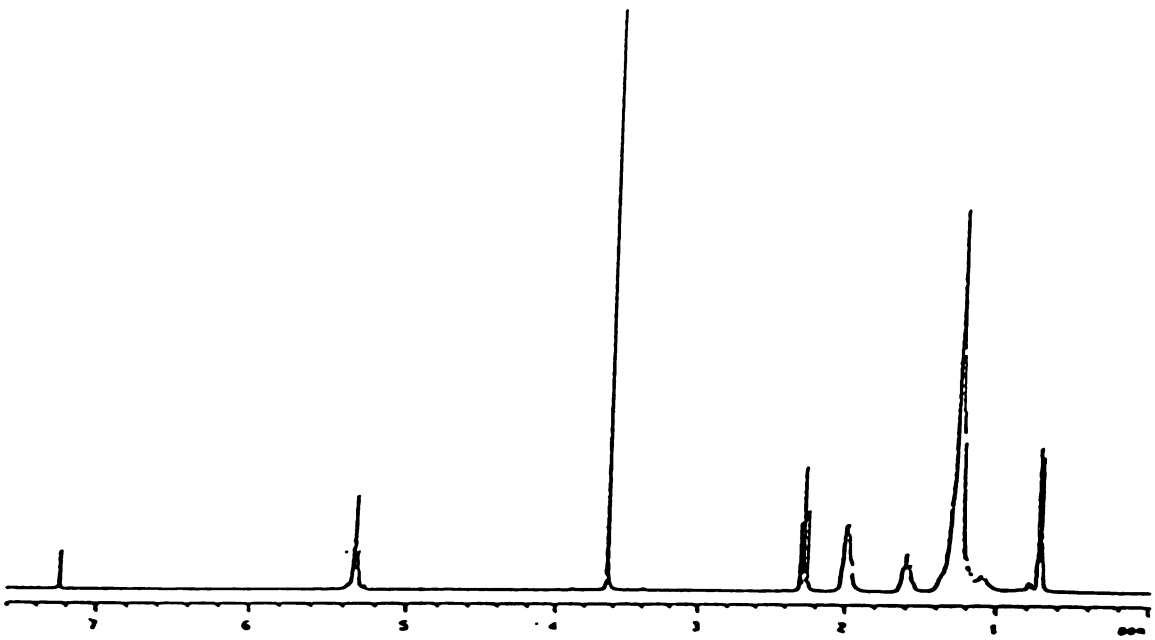

Figure 8. The ^1H NMR spectrum of proposed structure 3. The signal at δ 5.32 (t, J=6.83Hz) is due to a methine proton on an unsaturated carbon atom. The mutiplet at δ 2.00 is assigned to the protons of the methylene groups adjacent of the unsaturated carbons. The intense peak at δ 1.27 is due to the methylene groups of the hydrocarbon chains. The signal at δ 3.65 result from methyl group of the methoxycarbonyl functions. The multiplet at δ 1.58 for the protons of the carbons β to the methylcarbonyl function. The doublet at δ 0.70 (J=7.58Hz) arise from the protons of the vicinal methyl group.

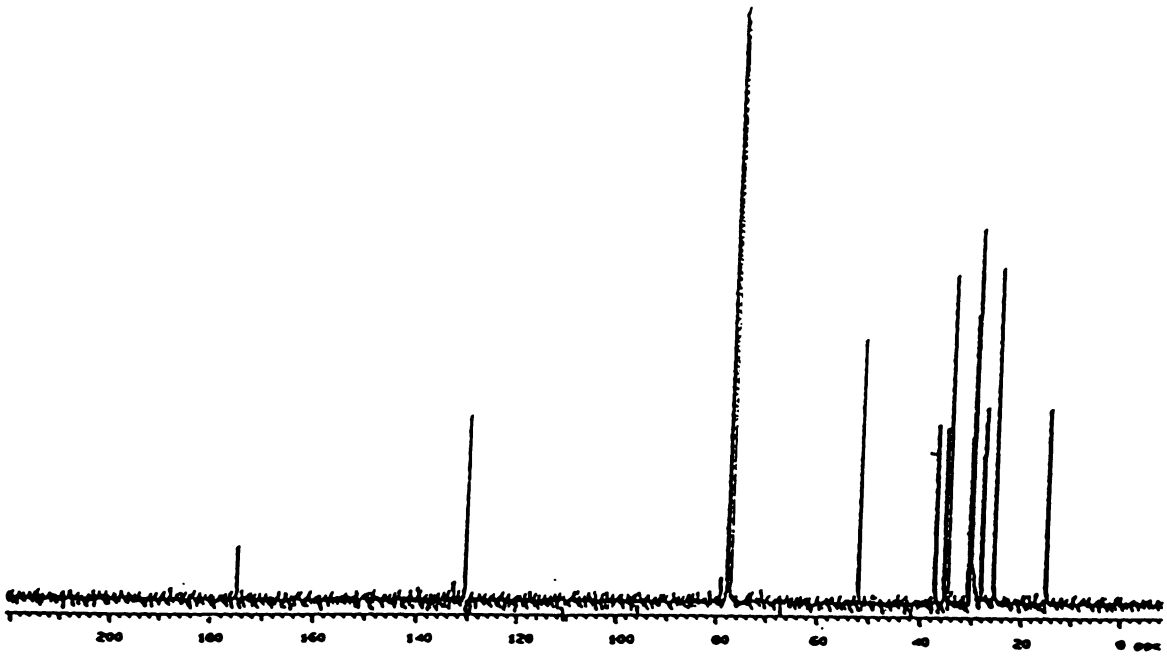

Figure 9. The ^{13}C NMR spectrum of proposed structure 2. Signals at δ 131.5 correspond to olefinic carbons. Signals at δ 174.5 and at δ 51.4 confirmed the presence of methyl ester group. The vicinal methyl group gives rise to the signal at δ 14.5.

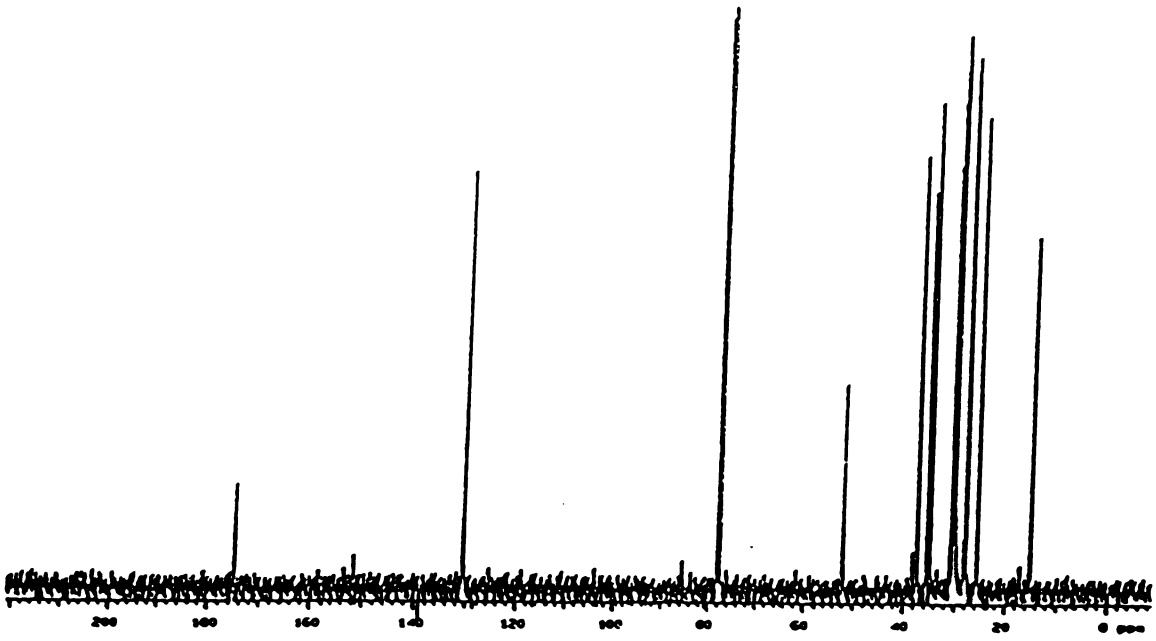

Figure 10. The ^{13}C NMR spectrum of proposed structure 3. Signals at δ 130.8 correspond to olefinic carbons. Signals at δ 174.8 and at δ 51.5 confirmed the presence of methyl ester group. The vicinal methyl group gives rise to the signal at δ 14.8.

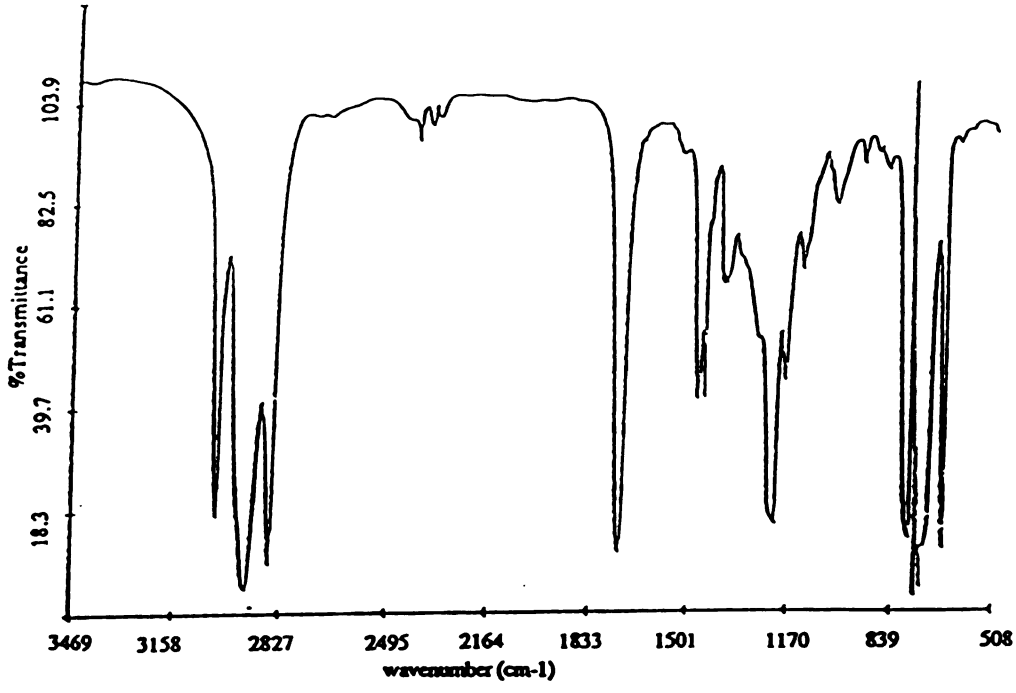

Figure 11. The Fourier Transform Infrared spectrum of proposed structure 2. The characteristic olefinic C-H stretching vibration appeared 3020 cm^{-1} and the out of plane *cis* C=C-H bending vibration at 667 cm^{-1} . Typical C=O stretching vibration at 1732 cm^{-1} for the carbonyl group is also present.

deformation at 1315 cm^{-1}. The characteristic C=O absorption bond of the aliphatic ester group appeared at 1732 cm^{-1} and the ester alkoxy stretch at 1213 cm^{-1}. The stereochemistry (*cis*- or *trans*-) of the unsaturated carbons was determined by the clear presence of a strong peak at 667 cm^{-1} due to the C=C-H bending deformation for *cis*-alkenes (17). The IR spectrum of peak E also indicated a *cis*- configuration for the two unsaturated double bonds in the molecule. Note that the configuration of the double bonds of the regular length $C_{18:1\ (11)}$ acyl chains was *cis* from *cis* vaccenic acid (11-octadecenoic acid). With regard to the mechanism of the formation of peak D or E, one of the most important questions was the location of the unsaturation in the acyl chain. The regular length monofunctional unsaturated acid contained the double bond at the 11 position of its carbon chain. The determination of the exact position of unsaturation of the bifunctional acyl chain was therefore very important since if it were located at any position other than the 11 position (with respect to the closest end) our model would be invalidated.

Reductive Ozonolysis and Mass Spectrometry

The exact locations of the unsaturation in **2** and **3** were confirmed by ozonolysis followed by reduction of the ozonide with zinc/acetic acid. This led to several fragments which were assigned structures **4**, **5** and **6** (Figure 12) based on their mass spectra and were consistent with the proposed locations of the double bonds. As expected, structure **2** produced two fragments on ozonolysis in contrast to three fragments (two of which were identical) for structure **3**. The mass spectrum of **4** (Figure 13A) contained major ions at m/z 186, 183, 171, 74 and 87. These corresponded to the ions of M (m/z 214) - 28 (CH_2=CH_2), M - 31 (CH_3O), M - 43 (CH_2=CH=O) and the typical McLafferty fragment (m/z 74) of an aliphatic methyl ester. The ion at m/z 139 was assigned to the sequential losses of CH_2=CH-O and a methoxy group from the molecular ion. Figure 13B shows the EI mass spectrum of the deuterium labeled molecule with structure **4** obtained by

Figure 12. Fragments expected for the reductive ozonolysis of structure 2 (A) and 3 (B). Each product was analyzed by GC/MS with and without isotope labeling.

A

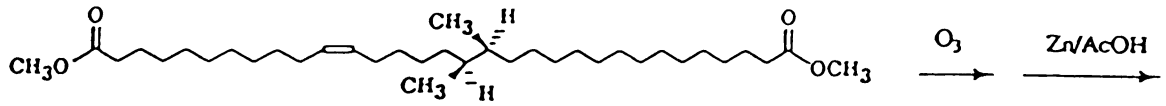

2 (M.W 564)

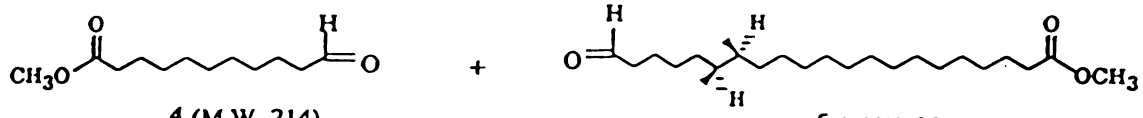

4 (M.W. 214) 5 (M.W. 382)

B

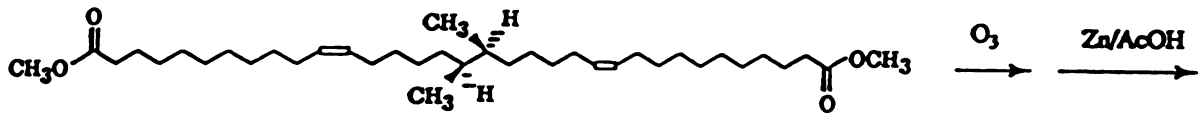

3

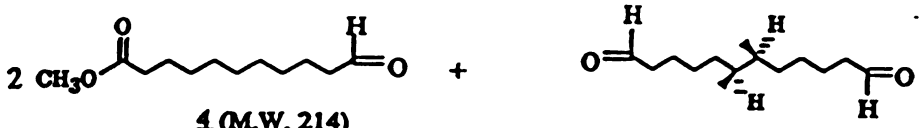

4 (M.W. 214) 6 (M.W. 226)

Figure 12

Figure 13. The electron impact mass spectrum of 4. (A) Note the major ions at 186, 183, 171 and 74. These correspond to loss of ethylene (CH_2=CH_2) from the molecular ion (M^+=214), loss of methoxy group from M^+, loss of CH_2=CH-O from M^+ and the typical McLafferty fragment (at m/z 74). The ion at m/z 139 was assigned to the sequential losses of CH_2=CH-O and a methoxy group from the molecular ion. (B) The electron impact mass spectrum of deuterium labeled 4 obtained by deuteration with D-4 methanolic HCl solution. Note the expected mass increases because of deuterium.

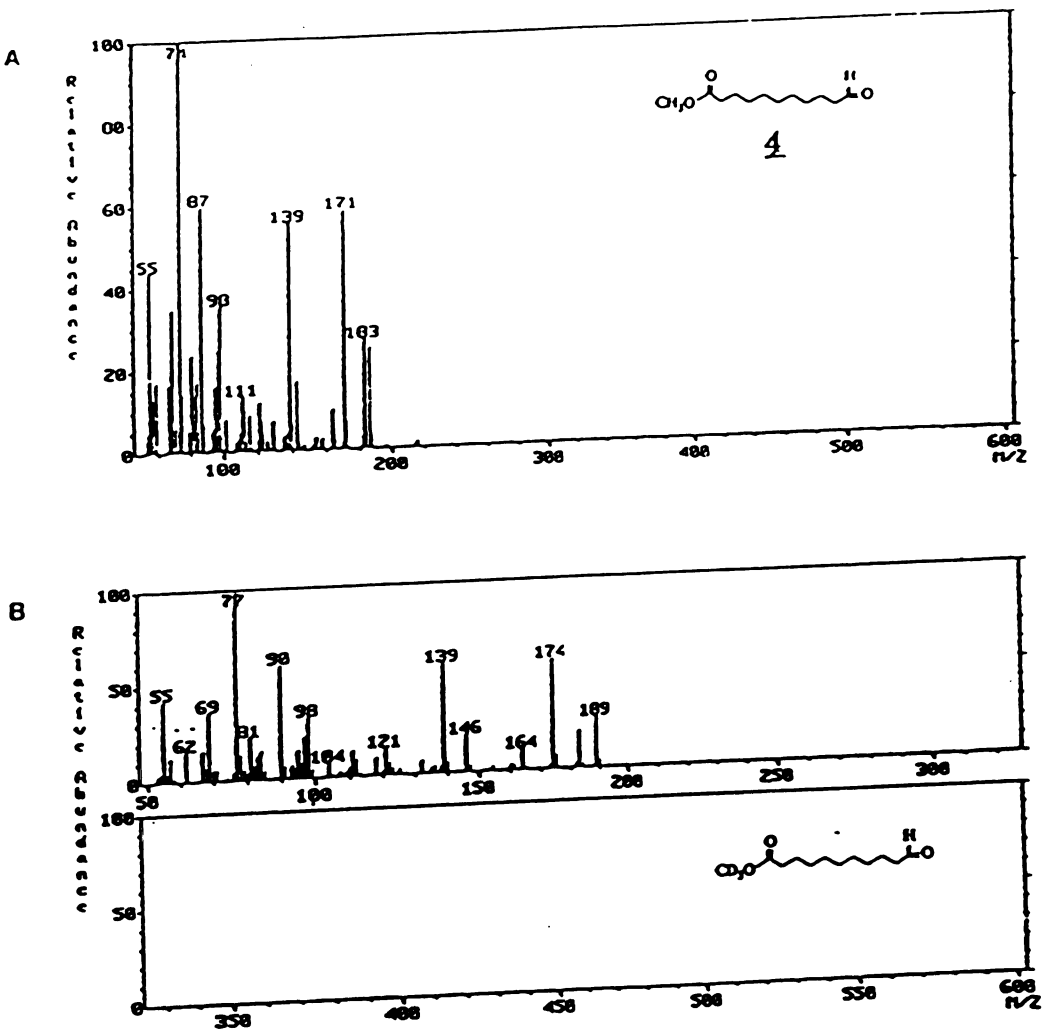
A
100
80
60
40
20
0
71
87
55
99
111
139
171
183
100
200
300
400
500
600
m/z
4
B
100
50
0
77
99
55
69
81
98
62
121
139
146
164
174
189
50
100
150
200
250
300
350
400
450
500
550
600
m/z

Figure 13

performing the methanolysis with D-4 methanol/HCl solution. The expected mass increases due to the deuterium were easily observed.

The EI mass spectrum of **5** (Figure 14A) contained major ions at m/z 382, 364, 357 and 350. These were attributed to the molecular ion (M^+) and the losses of water (H_2O), ethene and methanol respectively. It also contained the typical ion series of the general structure ($CH_3OCO-(CH_2)_n$), beginning at m/z 73, for a saturated methyl ester. There were three prominent ions at m/z 237, 269 and 297 (296 is due to the loss of one hydrogen from m/z 297). The intense clusters of ions 28 mass units apart centered at m/z 269 And 297 indicated the presence of a vicinal dimethyl group. The ion at m/z 237 represented the loss of methanol (CH_3OH) from the ion at m/z 269. Figure 14B shows that the EI mass spectrum of the deuterium labeled molecule with structure **5**. The expected increases in mass units due to isotope labeling were easily observed. Figure 15 shows the electron impact mass spectrum of the dialdehyde (**6**). It contained major ions at m/z 208, 182 and 95. These were assigned to M^+-18(H_2O), M-44(CH_2=CH-OH) and m/z 113-18(H_2O). The ion at m/z 113 was designated to the product formed by the fragmentation between the two methyl branches. There was no difference in the EI mass spectrum before and after the deuterium labeling, thus indicating the absence of a methyl ester function. The dimethyl acetal which should have been formed would have been hydrolysed back to the aldehyde during work up.

These reductive ozonolysis studies provided structures consistent for peaks D and E. They also provided conclusive proof for the proposed coupling mechanism since the exact positions of unsaturation of the bifunctional acyl chains and the position of the vicinal methyl groups were completely consistent with ω-1 coupling of two monocarboxylic acid acyl chains, one of which was *cis*-vaccenic acid. The combined spectroscopic and chemical methods confirmed the proposed structures corresponding to peaks D and E as α,ω-(17,18-dimethyl)-*cis*-11-dotriacotaenedioate dimethyl ester (**2**) and α,ω-(17,18-dimethyl)-*cis*-11-23-hentriacotadienedioate dimethyl ester (**3**), respectively. Compounds

Figure 14. The electron impact mass spectrum of 5. (A) Note the major ions at 382, 364, 339 and 269. These can be attributed to M^+, M-18 (H_2O), M-28 ($CH_2=CH_2$), M-43($CH_2=CH-O$) and M-113 ($HCO(CH_2)_5$ CH (CH_3)). (B) The electron impact mass spectrum of deuterium labeled 5 obtained by deuteration with D-4 methanolic HCl solution. Mass increases because of deuterium are easily observed.

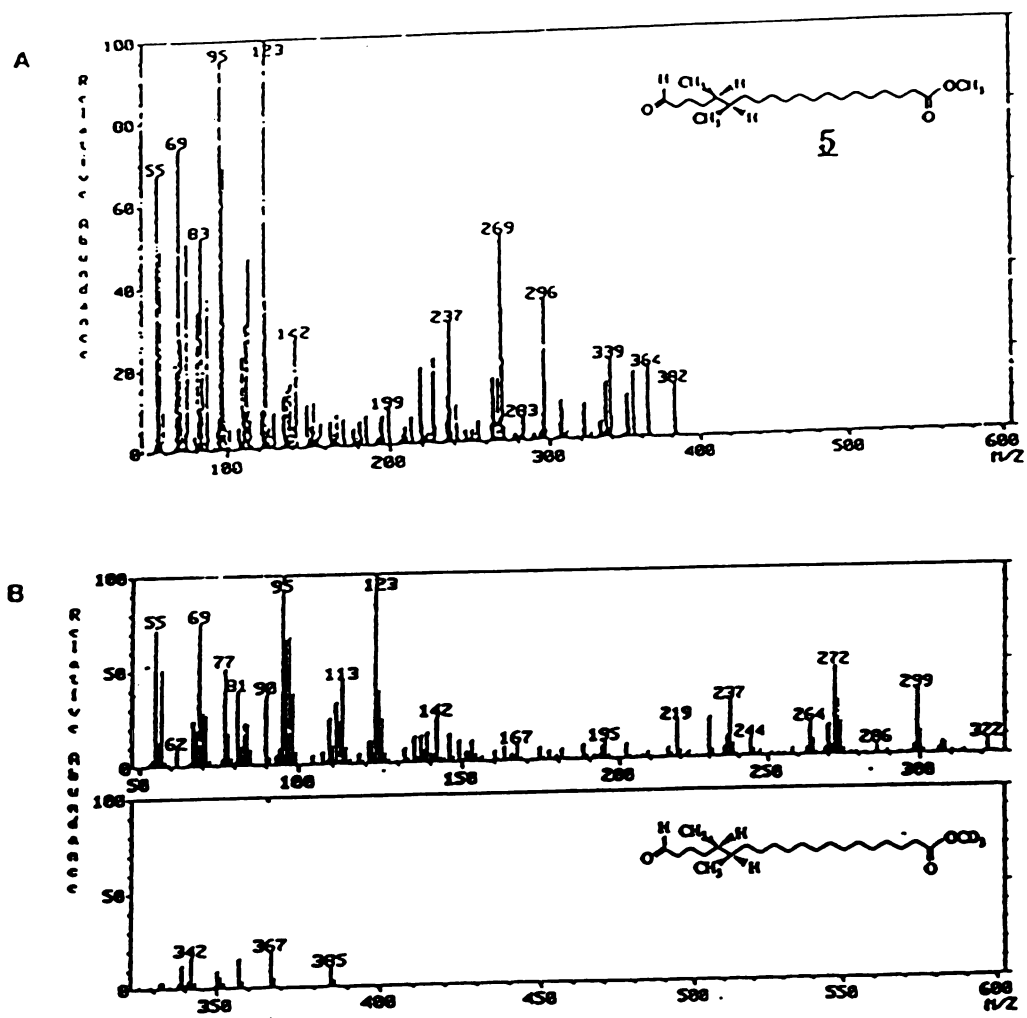

Figure 14

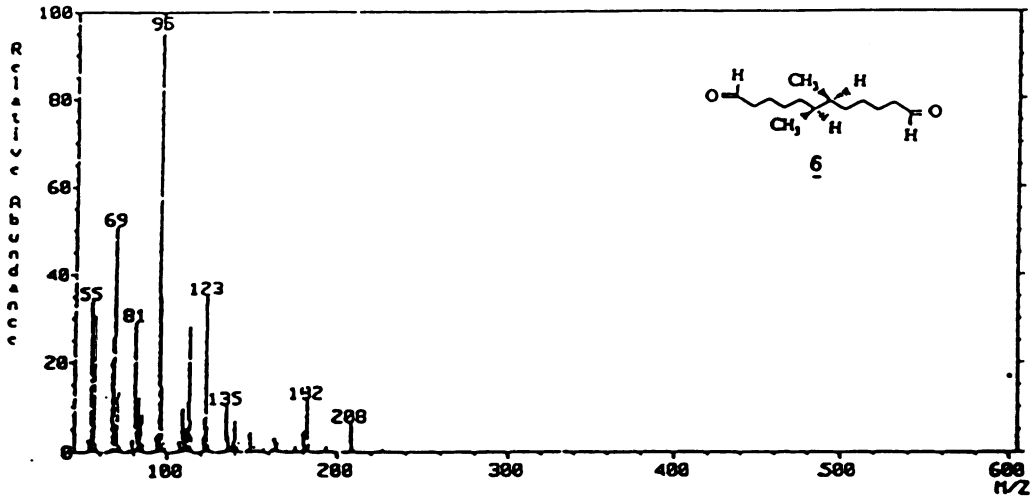

Figure 15. The electron impact mass spectrum of 6. Note the major ions at m/z 208, 182 and 95. The molecular ion peak (M^+) was not observed but $M^+ - 18$ (H_2O) give rise to the ion at m/z 208. The strong peak at m/z 95 corresponds to the loss of water from the fragmentation products obtained from cleavage between the two methyl branches.

1, **2** and **3** all displayed an optical rotations (Table 2). This precluded the possibility of any of these bifunctional acyl chain species being racemates or meso-compounds.

Molecular Mechanism for the Formation of Very Long Chain Dicarboxylic Acids

The presence of very long bifunctional lipids in the membrane of S. ventriculi could have arisen by coupling the tails of fatty acids of membrane lipids from the same side of the bilayer. This, incidently, was ruled out by freeze-fracture studies which demonstrated that the leaflets could not be separated and that the very long chain fatty acids were transmembrane (data not shown). Several pieces of information showed unequivocally that the formation of these very long fatty acids occurred by the chemical linkage at the ω-1 positions of the tails of fatty acids from opposite halves of the bilayer. The structures and gross relative proportions of individual very long chain fatty acids were closely correlated with the structures and the relative proportions of normal chain fatty acids in the same isolates. Since $C_{16:0}$ and *cis*-$C_{18:1(11)}$ fatty acids were the major regular chain species, the predominant very long chain fatty acid species were combinations of $C_{16:0}$ plus $C_{16:0}$, $C_{16:0}$ plus *cis*-$C_{18:1(11)}$ and *cis*-$C_{18:1(11)}$ plus *cis*-$C_{18:1(11)}$. In this case the $C_{18:1}$ species was *cis*-11-octadecenoic acid (*cis*-vaccenic acid) thus explaining the positions of the double bonds of the unsaturated α,ω-dicarboxylic acids. When an odd-numbered carbon alcohol was added to the growth medium, the regular chain fatty acids were all of odd carbon number (mostly $C_{17:0}$, *cis*-$C_{17:1}$ and $C_{15:0}$). This is consistent with propanol being converted to propionyl CoA which was used to initiate fatty acid synthesis with a C-3 unit leading to odd-numbered fatty acids. However, in this case, the new very long fatty acids were all of even chain length and predominantly saturated C-30 (strictly speaking dimethyl C-28), monounsaturated C-32 (dimethyl C-30) and di-unsaturated C-34 (dimethyl C-32) dicarboxylic acids. Further proof of the ω-1 coupling mechanism was obtained by the structural comparison of the two different C-32 (or vicinal methyl branched C-30) α,ω-

species / Hg light (nm)	1	2	3
$[\alpha]_{578}$	0.51	5.44	5.76
$[\alpha]_{546}$	0.89	6.30	6.46
$[\alpha]_{436}$	5.49	11.39	11.49

Table 2. Optical rotation analyses of peak B, D and E. It indicates that all of bifunctional molecules are chiral.

Figure 16. Mass spectral fragments of $C_{32:0}$ α,ω-dicarboxylic very long chain acyl species (9) in the case of propanol (0.15M) induction. The location of the vicinal methyl groups was determined by GC/MS analyses. Figure 17A shows the EI mass spectrum. Figure 16B shows the EI mass spectrum of deuterium labeled 9. The ions at m/z 258 and 286 corresponded to the trideutrated $C_{15:0}$ fatty acid methyl ester and trideuterated $C_{17:0}$ fatty acid methyl ester.

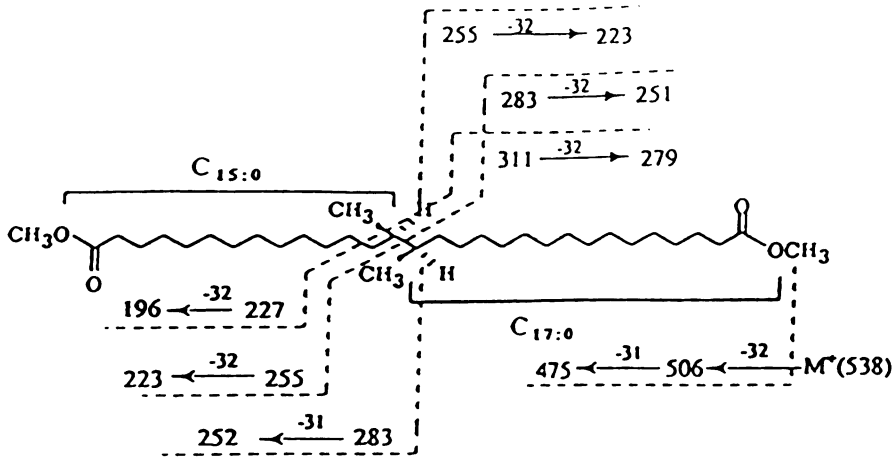

9

α,ω-(14,15-dimethyl)-triacotanedioate dimethyl ester

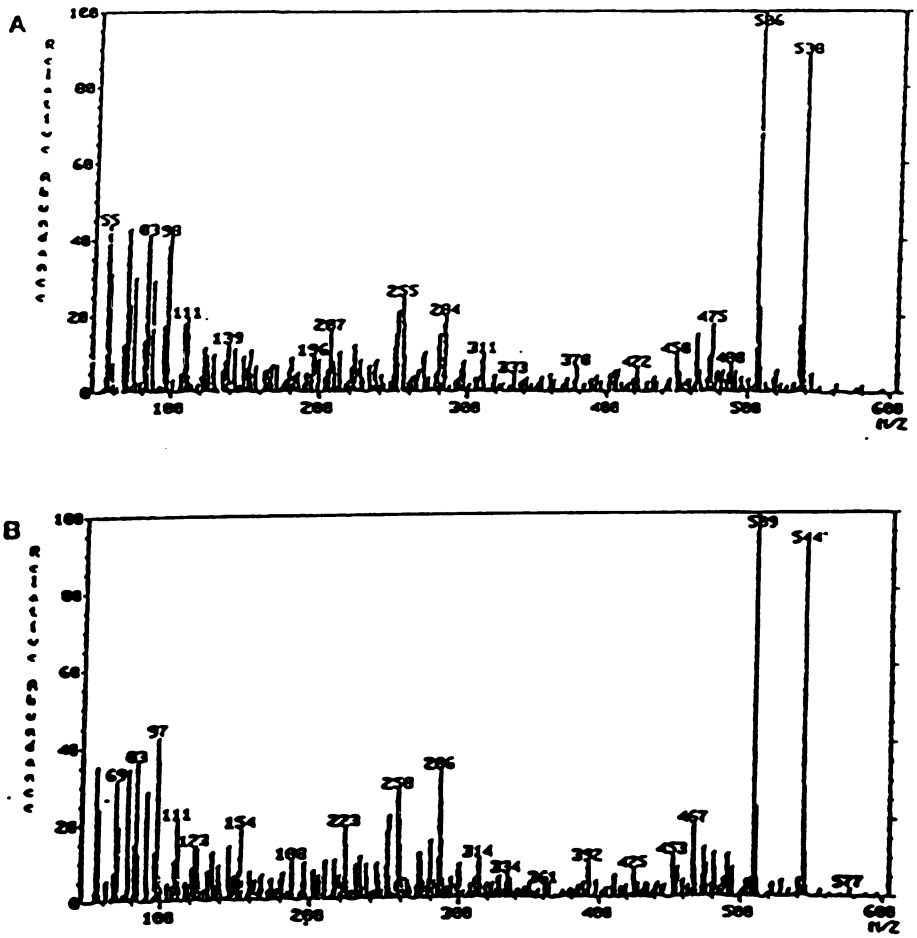

Figure 16

dicarboxylic fatty acid esters obtained from the two different induction conditions: propanol induction and temperature induction. They are both vicinal methyl-branched C-30 α,ω-dicarboxylic acids. However, careful analyses of the mass spectra clearly indicated that the one formed on propanol induction (Figure 16) bore the vicinal methyl group in a position consistent with the combination of $C_{15:0}$ plus $C_{17:0}$ to give structure 9. The mass spectrum contained major ions at m/z 538, 506 and 475. These corresponded to the molecular ions and sequential losses of methanol (CH_3OH) and a methoxy (CH_3O) group, respectively. Important fragments giving information on the position of the vicinal methyl groups appeared at m/z 255 and 283. These prominent peaks corresponded to the fragmentation products formed by cleavage between the two methyl branches. In contrast, the mass spectrum of the acid with the symmetrically placed vicinal methyl group (consistent with a combination of $C_{16:0}$ plus $C_{16:0}$) obtained from acidic or high temperature culture conditions showed the predominent alkyl chain cleavage ion m/z 269 (1). Another proof of the proposed mechanism came from the isolation of a very long bifunctional species formed by the combination of a fatty acid and a fatty aldehyde. Using GC/MS (Figure 17A), it was possible to demonstrate the presence of normal chain fatty aldehydes such as 7 indicating the presence of plasmalogens. Corresponding ω-formylmethyl esters with structures such as 8 (structure 7 plus $C_{16:0}$) were identified (Figure 17B) by mass spectrometry.

The optical rotations of the dicarboxylic acids clearly showed them to be chiral. This is consistent with a transition state which gives rise to the stereochemistry having two centers of asymmetry. In an enzymatic process leading to coupling of the alkyl chains by the proposed mechanism, the methyl groups would be expected to be directed away from the face of the enzyme and would therefore appear on the same side of the Neuman projection (Figure 2). A possible mechanism would be abstraction of a hydrogen radical from each of the two opposing fatty acids from the same side followed by coupling of the radical species. The secondary radical is more stable than a primary radical hence coupling

Figure 17. The electron impact mass spectrums of 7. (A) Note the major ions at m/z 252, 224 and 55+14n (n=1, 2 ..). These corresponded to molecular ion (M^+), M^+ - 28 (CO) and a long chain alkene series respectively. (B) The electron impact mass spectrums of 8 contained major ions at m/z 520, 492 and 460. These corresponded to molecular ion (M^+) with the sequential losses of carbon monoxide (CO) and methanol (CH_3OH) respectively.

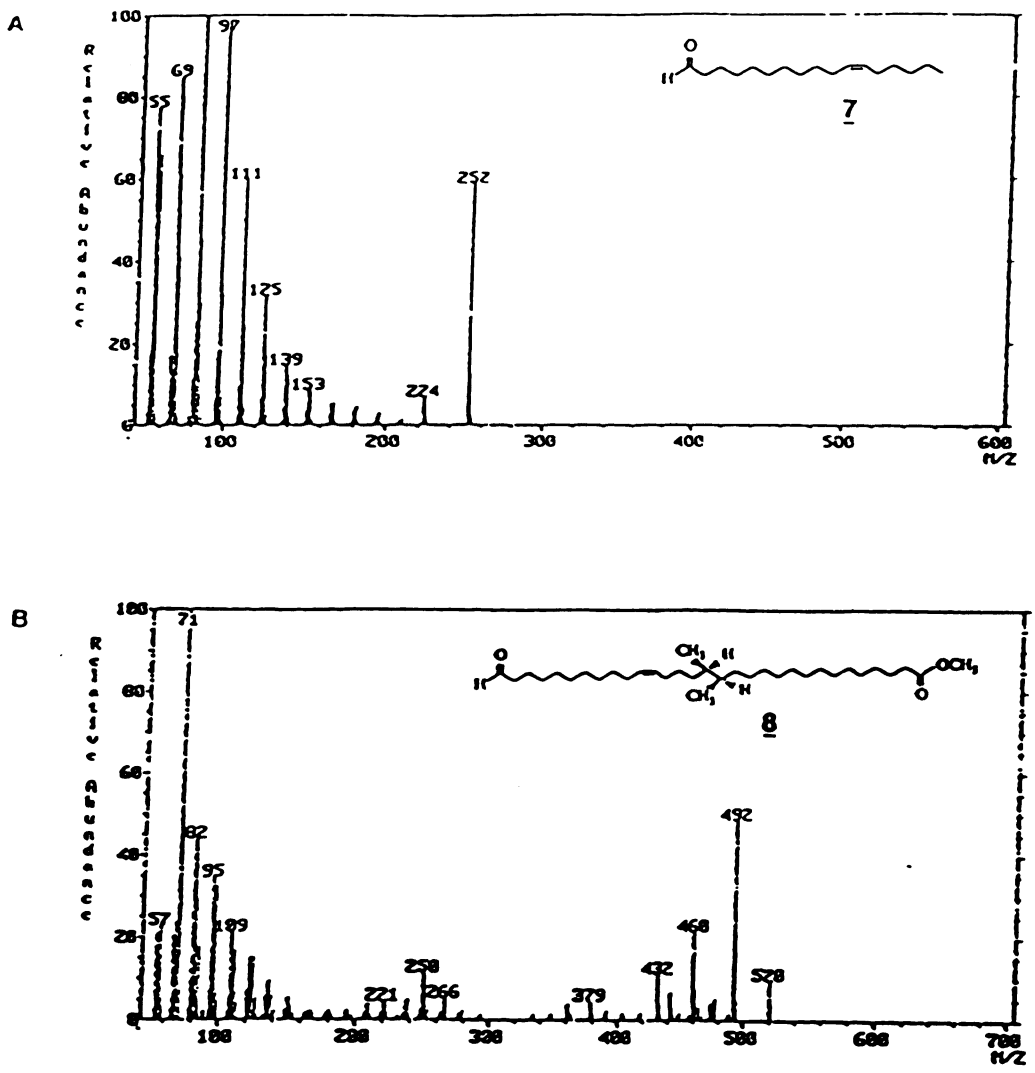
A
100
80
60
40
20
0
55
69
97
111
125
139
153
224
252
100
200
300
400
500
600
m/z
7
B
100
80
60
40
20
0
57
71
82
95
109
221
258
266
379
432
460
492
528
100
200
300
400
500
600
700
m/z
8

Figure 17

at the ω-1 instead of ω-positions. The resulting molecule would have the (*R*, *R*) or (*S*, *S*) stereochemistry and would be chiral even if the two chains are identical as is the case in structures **1** and **3**. If coupling of two identical chains occurs on the same side of the bilayer by the same mechanism, the resulting product would be *meso* and have the (*R*, *S*) or (*S*, *R*) stereochemistry.

The General Significance of the Coupling Mechanism

The unusual mechanism has very important implications for adaptive processes in bacteria. The tail of the fatty acids of a lipid can be expected to have the highest freedom of motion in the entire molecule since the other end is firmly attached to the head group. It is, therefore, desirable for the organisms to develop methods or mechanisms to restrict this motion especially under conditions (such as increased temperature or the presence of organic solvents) which will tend to increase it. One very important aspect of the adaptive response that we describe here is that it accomplishes this motional restriction by the most direct mechanism one could imagine: the direct coupling of fatty acid tails across the bilayer in a random, indiscriminate fashion. Another striking aspect of this adaptive response is that it utilizes pre-existing fatty acids rather than initiating the complete biosynthesis of the new species in a *de novo* fashion. This makes the response much more effective since the element of speed (which is of the utmost importance for survival) is ensured.

CONCLUSIONS

Uncoupling the maintenance system and survival mechanisms of biological membranes from events which depend on them for their proper execution is a key step in adaptation. Such a system was studied in a strictly anaerobic, facultative acidophilic eubacterium *Sarcina ventriculi.* In a previous study, we demonstrated that this organism is capable of adjusting to alterations in environmental conditions such as increase in temperature, lowering of pH or addition of exogenous organic solvents by the synthesis of unusual fatty acids (1). These fatty acids were a family of α,ω-dicarboxylic acids ranging from 28 to 36 carbons long. One of these fatty acids, 15,16-dimethyltriacotane-1,30-dicarboxylic acid was isolated as its dimethyl ester and characterized in that study. The chain lengths and relative abundance of very long dicarboxylic acids found in *S. ventriculi* suggest they may be formed after the perturbation by combinations of existing regular monofunctional fatty acids and not *de novo* by direct 2-carbon addition of acetyl Co-A. One possible explanation is that these new, very long chain, bifunctional species are formed by combination of existing lipid species by tail-to-tail coupling of the acyl chains across opposite sides of the bilayer. Definite chemical proof for this mechanism was obtained by analyzing the structures and stereochemistry of the very long bifunctional species in the light of the structures of the regular monofunctional species. The exact structures of fatty acid components were determined by various spectroscopic and chemical methods including GC (Gas Chromatography), GC/MS (Gas Chromatography/Mass Spectrometry), ^{1}H NMR and ^{13}C NMR (Nuclear Magnetic Resonance) spectroscopy, FTIR (Fourier Transform Infrared) spectroscopy, polarimetry and reductive ozonolysis. These analyses were performed on the methylester derivatives which were isolated after acid-catalyzed methanolysis by a variety of chromatographic techniques. The proposed mechanism was supported by precise structural and stereochemical information such as the position of substitution of the acyl chain by methyl groups, position and configuration of

double bonds, analysis of chirality and by the identification of predicted ω-formyl acids among the bifunctional fatty acid species. This mechanism allows the rationalization of the structures and identities of the various bifunctional, very long alkyl species elaborated by *S. ventriculi* in response to environmental stress.

REFERENCES

1. Jung, S., Lowe E.S., Hollingsworth I. R., and Zeikus, J. G. (1993) *J. Biol. Chem.* **268**, 2828-2835
2. Lindquist, S. (1986) *Ann. Rev. Biochem.* **55**, 1151-1191
3. Plesset, J., Palm, C., and McLaughlin, C.S. (1982) *Biochem, Biophys. Res. Commun.* **108**, 1340-1345
4. VanBogelen, R. A., Kelley, P. M., and Neidhardt, F. C. (1987) *J. Bacteriol.* **169**, 26-32
5. deMendoza, D., and Cronan, J. E. Jr. (1983) *Trends Biochem. Sci.* **8**, 49-52
6. deMendoza, D., Ulrich, A. K., and Cronan J. E. Jr. (1983) *J. Biol. Chem.* **258**, 2098-2101
7. Silvius, J. R., and McElhaney, R. N. (1979) *Chem. Phys. Lipids* **24**, 287-296
8. Silvius, J. R., and McElhaney, R. N. (1980) *Chem. Phys. Lipids* **26**, 67-77
9. Kannenberg, E., Blume, A., McElhaney, R. N. and Poralla, K. (1983) *Biochim. Biophys. Acta* **733**, 111-116
10. Langworthy, T. A. (1982) *Curr. Top. Membr. Transp.* **17**, 45-77
11. Langworthy, T. A. (1977) *Biochim. Biophys. Acta* **487**, 37-50
12. Lowe, S. E., Pankratz, H. S., and Zeikus, J. G. (1989) *J. bacteriol.* **171**, 3775-3781
13. Lowe, S. E., and Zeikus, J. G. (1991) *Arch. Microbiol.* **155**, 325-329
14. Tilak, K. V. B. R. (1970) *Sci. Cult* **36**, 399-400
15. Knowles, W.S., and Thompson, Q. E. (1960) *J. Org. Chem.* **25**, 1031-1033
16. Still, W.C., Kahn, M., and Mitra, A. (1978) *J. Org. Chem.* **43**, 2923-2927
17. Shreve, O. D., and Heether, M. R., (1950) *Analytical Chemistry* **22**, 1261-1264

CHAPTER IV

A MATHEMATICAL MODEL EXPLAINING THE MOLECULAR WEIGHTS AND DISTRIBUTION OF VERY LONG CHAIN DICARBOXYLIC ACIDS FORMED DURING THE ADAPTIVE RESPONSE OF *SARCINA VENTRICULI*

INTRODUCTION

The membrane is one of the most critical structures in all biological systems. In bacteria, it is the central structure across which the electric potential gradient which drives the cellular process is maintained. Bacteria therefore must develop very sophisticated mechanisms for repair, maintenance and regenerating of this important structures (3, 4, 5, 6, 7, 8).

In a recent study (1, 2), we described an adaptive mechanism in a strict anaerobic, facultative acidophilic eubacteria, *Sarcina ventriculi* in which a family of very long chain fatty acid species is synthesized in response to environmental stress (Figure 1). The size and the distribution of these fatty acid species (Figure 1) indicates that a very sophisticated mechanism which does not require *de novo* fatty acid synthesis must be at work. The molecular weights and distributions of these unusual bifunctional species could not be explained by simple 2-carbon additions of acetyl-CoA.

One possible mechanism for the synthesis of these unusual species is the chemical coupling of lipid acyl chains across opposite sides of the bilayer leaflet by an enzymatic activity which is located at the interface between the leaflets. This activity would then select the ends of two fatty acid chains (independently of head group) one from either leaflet and chemically couple them to form new lipids containing α,ω-dicarboxylic transmembrane fatty acyl species. If there is no asymmetry in the distribution of the fatty acyl species between the two leaflets, it should be possible to prove or disprove this theory by a mathematical model. Here we propose a model where the regular length fatty acid chains are treated as units which are selected for combination to form transmembrane acyl species by a coupling entity.

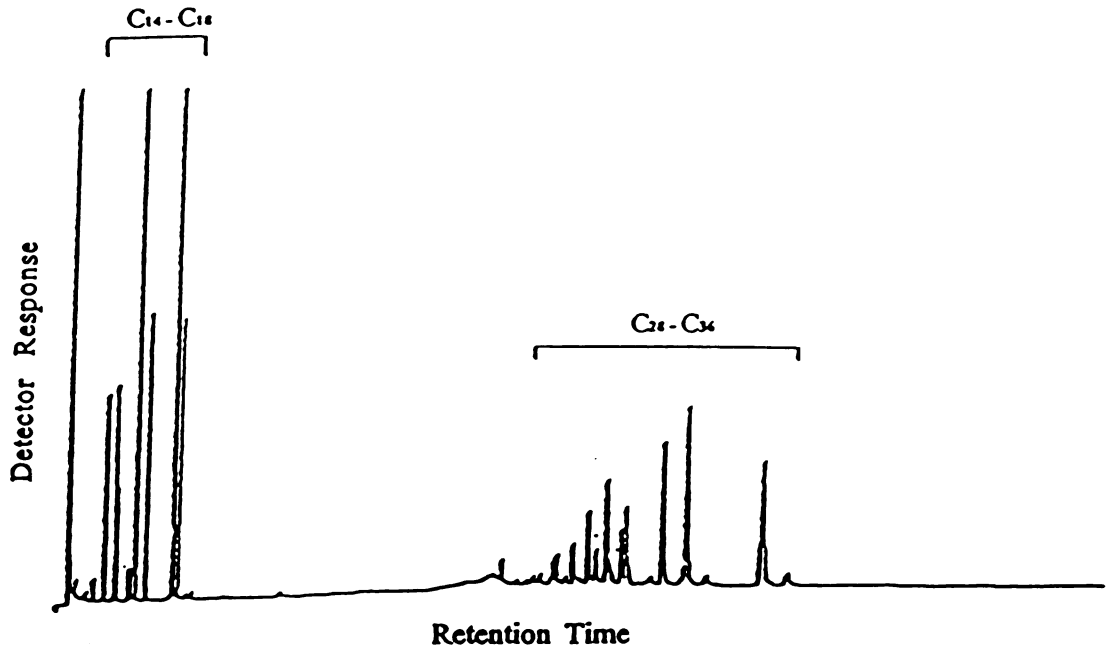

Figure 1. Gas chromatographic profile of methyl ester derivatives of total fatty acids of *Sarcina ventriculi* at pH 3.0 and 37°C. The family of peaks labeled C_{28} - C_{36} dicarboxylic acids are not synthesized at pH 7.0 at 37°C in the absence of exogenous organic solvents.

MODELS AND PROBABILITY CALCULATIONS

Model Construction

The random coupling model is shown in Figure 2. It shows an enzymatic activity randomly selecting and coupling acyl chains from lipid species on opposite sides of the membrane bilayer to form transmembrane lipid species. The randomness is ensured by the rapid rotation (about the lipid long-axis) and lateral diffusion of the lipid species. Acyl chain (Fatty acids) in each leaflet is represented by F_i and the other F_j (i or j=1, 2, 3..n where n = total number of fatty acids species).

Definition of Parameters for Model

$F_1, F_2, ...F_i, F_j, ...F_n$:= Fatty acid species (total number of species is equal to n)

$N_1, N_2, ...N_i, N_j, ...N_n$:= Number of each fatty acid (ex. F_i for N_i)

F_{ij} := Transmembrane fatty acid synthesized by the ordered coupling of the fatty acid F_i and F_j

$P(F_{ij})$:= The probability of the formation of the transmembrane fatty acid F_{ij}

$F_i:F_j$:= Transmembrane fatty acid made by the two fatty acids F_i and F_j (F_{ij} or F_{ji})

$P(F_i:F_j)$:= The probability of the formation of the transmembrane fatty acid $F_i:F_j$

$P(F_i:F_j)$ [%] := The relative percentage of $P(F_i:F_j)$

Calculation of $P(F_{ij})$

$$P(F_{11}) = ({}_{N_1}C_1 * {}_{N_1}C_1) / ({}_{\Sigma N_i}C_1 * {}_{\Sigma N_i}C_1) = (N_1 * N_1) / (\Sigma N_i)^2$$

$$P(F_{12}) = ({}_{N_1}C_1 * {}_{N_2}C_1) / ({}_{\Sigma N_i}C_1 * {}_{\Sigma N_i}C_1) = (N_1 * N_2) / (\Sigma N_i)^2$$

- - - - - - -

$$P(F_{ij}) = ({}_{N_i}C_1 * {}_{N_j}C_1) / ({}_{\Sigma N_i}C_1 * {}_{\Sigma N_i}C_1) = (N_i * N_j) / (\Sigma N_i)^2$$

Figure 2. Random coupling model for the synthesis of transmembrane fatty acids. (A) Conceptual model showing an enzymatic activity randomly selecting and coupling acyl chains from lipid species on opposite sides of the membrane bilayer to form transmembrane lipid species. The randomness is ensured by the rapid rotation (about the lipid long-axis) and lateral diffusion of the lipid species. (B) Model in which the lipid chains in one leaflet is represented by F_i and the other F_j (i or j=1, 2, 3, ..n where n = total number of fatty acids species). F_i:F_j represents the general transmembrane species formed from the ith acyl chain F_i and jth acyl chain F_j. Let N_i=number of units of the ith fatty acid, N_j=number of units of the jth fatty acid, $P(F_i:F_j)$=probability of forming the transmembrane species F_i:F_j or F_j:F_i then $P(F_i:F_j)= P(F_i)+P(F_j)$ where $P(F_{ij})=P(F_{ji})$; probability of Fi being connected to F_j.

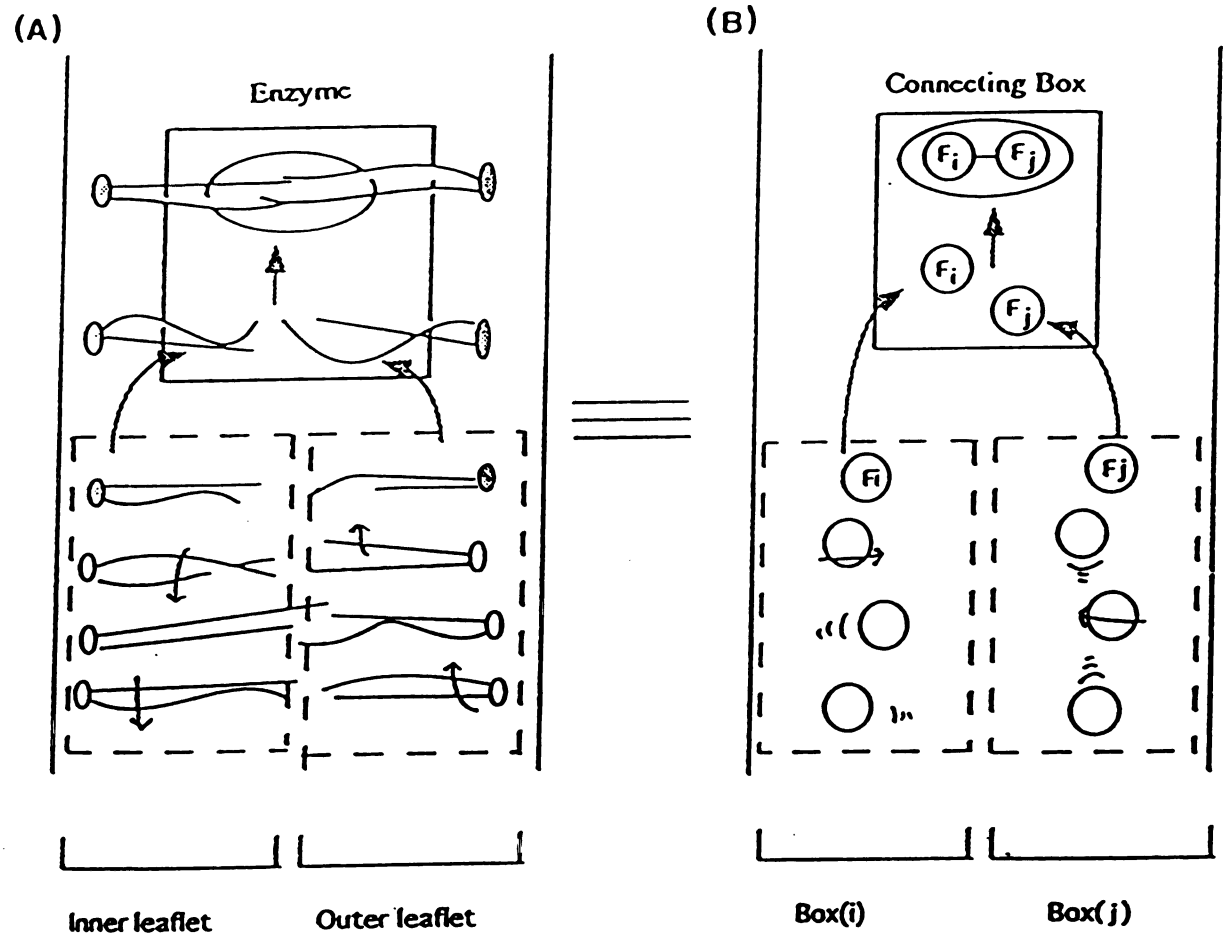
(A)
Enzyme
Inner leaflet
Outer leaflet
(B)
Connecting Box
Box(i)
Box(j)

Figure 2

On the other hand,

$P(F_i{:}F_j) = {}_2P_1 * P(F_{ij}) = 2*P(F_{ij})$

The number (N_i) of each fatty acid species can be expressed in terms of relative ratio to the first fatty acid species (Dividing by N_1)

$N_1 = N_1*f_1,\ N_2 = N_1 * f_2,\ N_3 = N_1 * f_3, \ldots, N_i = N_1 * f_i, N_j = N_1 * f_j, \ldots N_n = N_1 * f_n$

$$\Sigma Ni = N_1 + N_2 + \ldots + N_i + \ldots + N_n$$
$$= N_1*f_1 + N_1 * f_2 + N_1 * f_3 + \ldots + N_1 * f_i + \ldots + N_1 * f_n$$
$$= N_1 * (f_1 + f_2 + f_3 + \ldots + f_i + \ldots + f_n)$$
$$= N_1 * \Sigma f_i$$

Therefore,

$P(F_{ij}) = ({}_{Ni}C_1 * {}_{Nj}C_1) / ({}_{\Sigma Ni}C_1 * {}_{\Sigma Ni}C_1) = (N_i*N_j) / (\Sigma Ni)^2 = (f_i* f_j)/ (\Sigma f_i)^2$

$P(F_i{:}F_j) = {}_2P_1 * P(F_{ij}) = 2*P(F_{ij})=2*(f_i* f_j)/ (\Sigma f_i)^2$

Calculation of $P(F_i{:}F_j)[\%]$

$$P(F_1{:}F_1)\ [\%] := 100* \{P(F_1{:}F_1)\}/\{ (P(F_1{:}F_1) + P(F_1{:}F_2) + .. + P(F_1{:}F_n)) +$$
$$(P(F_2{:}F_2) + P(F_2{:}F_3) + ... + P(F_2{:}F_n)) + (P(F_3{:}F_3) +$$
$$P(F_3{:}F_4) + ... + P(F_3{:}F_n)) + (....) + (P(F_n{:}F_n) \}$$
$$= 100 * \{ (f_1* f_1)/ (\Sigma f_i)^2 \} / \{ (P(F_1{:}F_1) + P(F_1{:}F_2) + .. + P(F_1{:}F_n)) +$$
$$(P(F_2{:}F_2) + P(F_2{:}F_3) + ... + P(F_2{:}F_n)) + (P(F_3{:}F_3) +$$
$$P(F_3{:}F_4) + ... + P(F_3{:}F_n)) + (....) + (P(F_n{:}F_n) \}$$

Here, $P(F_1{:}F_1) + P(F_1{:}F_2) + ... + P(F_1{:}F_n) = f_1*(f_1 + 2* (f_2 + f_3 + ... + f_n)) / (\Sigma f_i)^2$

$P(F_2{:}F_2) + P(F_2{:}F_3) + ... + P(F_2{:}F_n) = f_2*(f_2 + 2* (f_3 + f_4 + ... + f_n)) / (\Sigma f_i)^2$

$P(F_3{:}F_3) + P(F_3{:}F_4) + ... + P(F_3{:}F_n) = f_3*(f_3 + 2* (f_4 + f_5 + ... + f_n)) / (\Sigma f_i)^2$

- - - - -

Therefore,

$$P(F_1:F_1)\ [\%] = 100*\{(f_1*f_1)/(\Sigma f_i)^2\}/\{(\Sigma f_i^2 + 2*\Sigma(f_i*(\Sigma f_j))\}/(\Sigma f_i)^2\}$$

$$= 100*\{(f_1*f_1)/(\Sigma f_i)^2\}/\{\Sigma(f_i^2 + 2*f_i*(\Sigma f_j))\}/(\Sigma f_i)^2\}$$

$$= 100*(f_1*f_1)/\{\Sigma(f_i^2 + 2*f_i*(\Sigma f_j))\}$$

Similarly,

$$P(F_i:F_j)\ [\%]=100*2*(f_i*f_j)/\{\Sigma(f_i^2 + 2*f_i*(\Sigma f_j))\}$$

Here, $\Sigma f_i = \Sigma_{i=1..n} f_i$ $\Sigma(f_i*(\Sigma f_j)) = \Sigma_{i=1..n} (f_i * (\Sigma_{j=i+1..n} f_j))$

RESULTS

Random Coupling Model (RCM)

Figure 2 shows the conceptual model for this mechanism. Acyl chains are selected with a probability based on their molar proportions. The molar proportions are deduced from gas chromatography data. The idea is that the gas chromatography profile of the very long chain fatty acids can be predicted from that of regular-chain fatty acids. The membrane model in Figure 2A in which the enzymatic coupling activity randomly selecting lipid species is replaced by the connecting box in Figure 2B. Box(i) replaces one membrane leaflet and box(j) the other. F_i and F_j are fatty acid chains which are selected to form the new transmembrane fatty acid F_i:F_j. The probability of selecting any given fatty acid species is proportional to the intensity of its peak in the gas chromatogram after correcting for chain length differences by dividing the area of the peak by the molecular weight of the peak to give molar proportions. This is accurate since the flame ionization detector is a mass detector and the detector response for fatty acids of similar chain lengths is the same. The probability, $P(F_i:F_j)$, of forming the transmembrane fatty acid F_i:F_j (or F_j:F_i) is equal to $2*(N_i*N_j)/\{(\Sigma N_i)*(\Sigma N_j)\}$. Here the number of units or moles of ith fatty acid species (N_i) is normalized to the number of units (moles) in the first eluting peak in the gas chromatogram (N_1) and is expressed as the real number (f_i) times the number of units of the 1st fatty acid species (i.e. $N_i=f_i*N_1$, and $f_1=1$). Then $\Sigma Ni=N_1 + N_2 + N_3 + ... = N_1*f_1 + N_1*f_2 + N_1*f_3 + ...= N_1*(f_1 + f_2+..) = N_1* (\Sigma f_i)$. Since the molecular weight identities and relative molar proportions of the regular-chain length fatty acids are known, and if we assume that they are distributed without bias between the leaflets of the bilayer and combine randomly between them, we can then predict the molecular weight of the transmembrane fatty acid species and the relative abundance (%). In other words, $P(F_i:F_j)$ becomes $2*(f_i*f_j)/\{(\Sigma f_i)*(\Sigma f_j)\}$. The initial abundance by gas chromatography

of each regular fatty acid species (g_1, g_2, g_3,... g_n) is converted to f_1, f_2, f_3,...f_n by dividing initial abundance values by that of the first fatty acid species ($f_1=g_1/g_1$, $f_2=g_2/g_1$,...$f_n=g_n/g_1$). Each fatty acid species such as F_i, F_j or F_i:F_j in the case of new transmembrane species, was identified by its molecular weight. These were obtained by Gas Chromatography/Mass Spectrometry and there was no redundancy between weights of regular chain fatty acids. Table 1 shows a combination grid in which all of the pair-wise combinations of normal fatty acid species (F_n) to form transmembrane species (F_i:F_j) are examined and their likelihood (probability) calculated.

Comparison of 'Predicted Data' with 'Observed Data' for Transmembrane Fatty Acids

In Figure 3A the results of Table 1 are presented in a graphical fashion. In Figure 3B the measured distribution and chain lengths (molecular weights) of the new fatty acid species are compared with the theoretically calculated values on a mass axis. There is one instance of redundancy in the molecular weights of transmembrane species; the combination of two 16 carbon fatty acyl group gives a transmembrane species of the same molecular weight as the combination of a 14 carbon and an 18 carbon acyl group. It is very clear that the measured and calculated profiles are practically identical. This proves that the new, very-long chain fatty acids are formed by the random combination of existing fatty acid chains by the tail-to-tail coupling. The assertion that the coupling occurs between fatty acid chains in opposing leaflets and not in the same leaflet is borne out by freeze-fracture electron microscopy which does not show any instances of cleavage between the bilayer leaflets in cells containing these new very-long chain dicarboxylic acids. The result identifies this adaptive process which is characterized by a high degree of speed and efficiency by a hitherto unreported mechanism.

Table 1. Mathematical formula for the prediction of probability for the formation of transmembrane fatty acids. (A) The relative abundance (%) of predicted transmembrane fatty acid species (F_i:F_j) from the initial ratios of the abundance of regular-length fatty acid species (f_1, f_2,..f_n). $P(F_i:F_j)$ (%) = $100*P(F_i:F_j)/ \{(\Sigma P(F_i:F_j)\}$ where $P(F_i:F_j)= \{2*(f_i*f_j)\}/ \{(\Sigma f_i)*(\Sigma f_j)\}$, $\Sigma P(F_i:F_j)= \Sigma(f_i^2 + 2*f_i*(\Sigma f_j))= \Sigma_{i=1..n}(f_i^2 + 2*f_i*(\Sigma_{j=i+1..n} f_j))$ (B) The calculated relative abundance (%) of transmembrane fatty acid species from the experimental initial ratios of the abundance of regular-length fatty acid species. These transmembrane fatty acids were formed on changing the pH of the medium from 7.0 to 3.0. Bolded numbers indicated the molecular weights of regular chain fatty acids (ie. **242**:C_{14} fatty acids, **298**: C_{18} fatty acids). The numbers in parenthesis showed the predicted molecular weights of transmembrane fatty acids.

(A)

$P(F_i:F_j)(\%)$	F_1	..	F_i	..	F_n
F_1	$100 - (f_1 - f_1) / (\Sigma(f_i^2 + 2 \cdot f_i \cdot (\Sigma f_j)))$	..	$100 - 2 \cdot (f_1 - f_i) / (\Sigma(f_i^2 + 2 \cdot f_i \cdot (\Sigma f_j)))$	..	$100 - 2 \cdot (f_1 - f_n) / (\Sigma(f_i^2 + 2 \cdot f_i \cdot (\Sigma f_j)))$
		F_i	$100 - (f_i - f_i) / (\Sigma(f_i^2 + 2 \cdot f_i \cdot (\Sigma f_j)))$	..	$100 - 2 \cdot (f_i - f_n) / (\Sigma(f_i^2 + 2 \cdot f_i \cdot (\Sigma f_j)))$
				F_n	$100 - (f_n - f_n) / (\Sigma(f_i^2 + 2 \cdot f_i \cdot (\Sigma f_j)))$

(B)

P(Fi-Fj)(%)	242	252	255	270	296	298
242	0.02 (*482*)	0.05 (*492*)	0.59 (*495*)	0.71 (*510*)	1.01 (*536*)	0.11 (*538*)
	252	0.04 (*502*)	0.93 (*505*)	1.12 (*520*)	1.59 (*546*)	0.17 (*548*)
		255	5.59 (*508*)	13.48 (*523*)	19.09(*549*)	2.00(*551*)
			270	8.14 (*538*)	23.05(*564*)	2.41 (*566*)
				296	16.32(*590*)	3.42 (*592*)
					298	0.18(*594*)

Table 1

Figure 3. Prediction of the distribution of transmembrane fatty acids based on random coupling model. (A) Calculated distribution of transmembrane fatty acid species from the grid in Table 1. Each value of f_i was determined by analytical gas chromatography. (B) Comparison of the distribution of the observed peaks in gas chromatogram with that of the predicted ones by the random coupling model calculation.

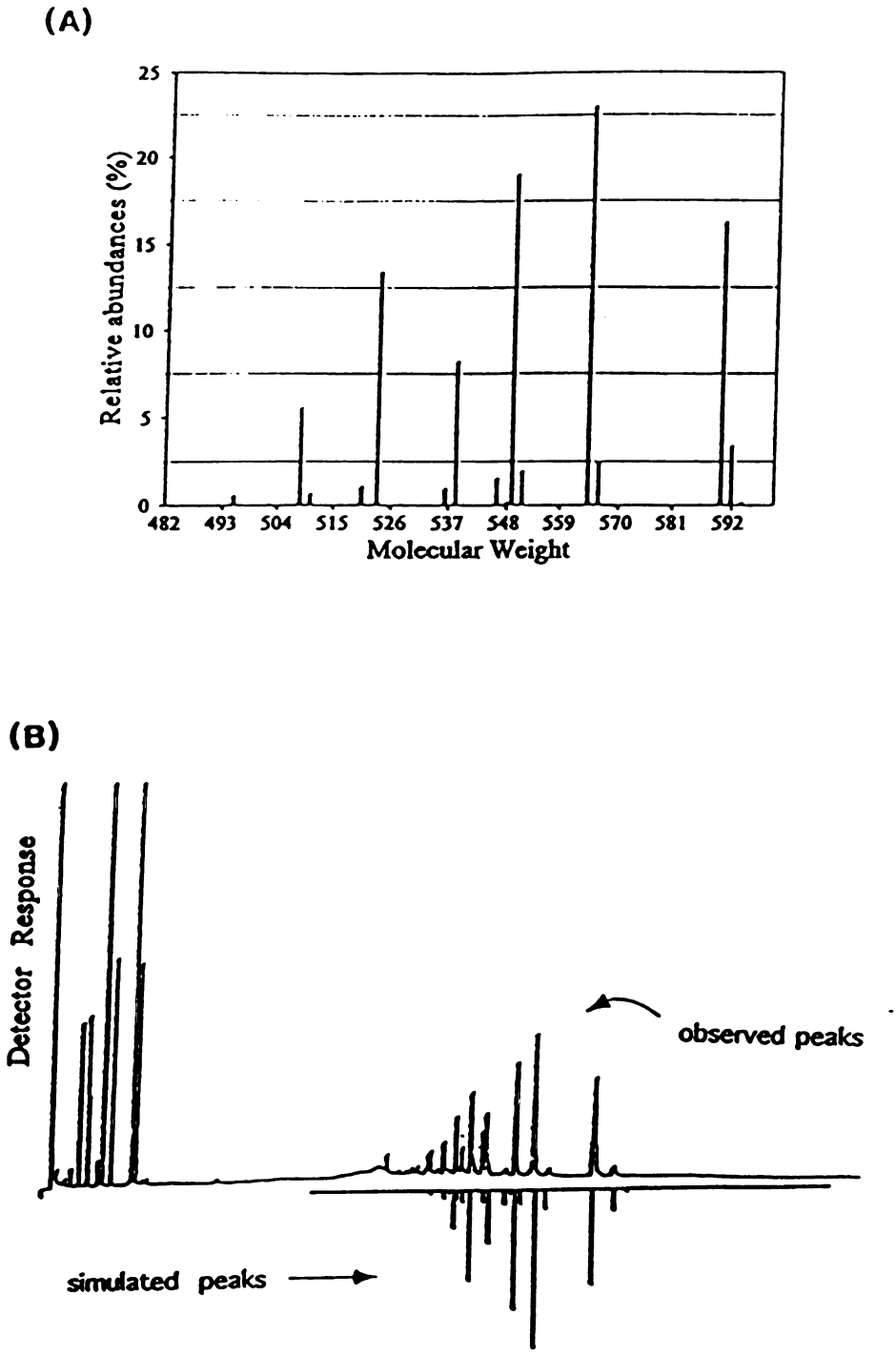
(A)
Relative abundances (%)
25
20
15
10
5
0
482
493
504
515
526
537
548
559
570
581
592
Molecular Weight
(B)
Detector Response
observed peaks
simulated peaks

Figure 3

DISCUSSION

In this work, a random coupling mechanism of establishing the unique distribution and the relative abundance for a new family of transmembrane fatty acid species is introduced. The accurate coincidence with the experimental results provides the conclusive proof for the existence of this new synthetic pathway in *S. ventriculi*. Due to this coupling mechanism, the empty spacing between the C_{14}-C_{18} and C_{28}-C_{36} region in the GC profile in the distribution of fatty acids (Figure 1) can be explained and successfully predicted as well as the structural uniqueness of α,ω-dicarboxylic acid species. The generality of this mechanism in eubacteria is still unexplored.

CONCLUSIONS

A simple mathematical model is presented to explain a recent new discovery of an unusual membrane adaptive response in *Sarcina ventriculi* . In this response, this organism synthesizes very long chain α, ω-dicarboxylic acids ranging from 28 to 36 carbon atoms in length. The distribution of chain lengths of the new fatty acid species is not consistent with *de novo* synthesis but suggests elaboration from the existing regular-chain fatty acids by a coupling process. Here, it is demonstrated, using a mathematical model, that if the molecular weights and relative abundance of regular chain fatty acids are known, then the molecular weights and relative abundance of the new, very long chain dicarboxylic fatty acid species can be predicted using a model based on the random, pairwise combination of regular chain species. This combination takes place across the bilayer leaflet to form transmembrane fatty acids. It is proposed that this coupling phenomenon is regulated by the motional dynamics of the membrane.

REFERENCES

1. Jung, S., Lowe, S. E., Hollingsworth, R.I., & Zeikus, G. J. (1993) *J. Biol. Chem.* **268**, 2828.

2. Jung, S., and Hollingsworth, R.I. (1993) *J. Biol. Chem.* (submitted)

3. Andreoli, T. (1974) *Ann .N.Y. Acad. Sci.* **235**, 448.

4. Cronan, J. *J. Biol. Chem.* (1975) **240**, 7074.

5. Hollingsworth, R & Carlson, R. W. (1989) *J. Biol. Chem.* **264**, 9300.

6. deMendoza, D. & Cronan, J. (1983) *Trends Biochem. Sci.* **8**, 49.

7. Sinensky, M. (1971) *J. Bacteriol.* **106**, 449.

8. Teuber, M & Bader, J. (1976) *J. Arch. Microbiol.* **109**, 51.

CHAPTER V

A NEW FAMILY OF MONOGLUCOSYLGLYCERIDE DIACYL GLYCEROL LIPIDS CONTAINING VERY LONG CHAIN BIFUNCTIONAL ACYL CHAINS IN *SARCINA VENTRICULI*

INTRODUCTION

Membrane lipids are known to play various important roles in the physiological functions of bacteria. These roles include the communication of external information, compartmentalization between the cell and external medium and a matrix for localization and proper functioning of membrane proteins. The membrane serves as a control center (1, 2, 3) for the regulation of the motional dynamics of the membrane proteins. From the standpoint of signal transduction (4, 5), the structural studies of membrane lipids and the induction of the synthesis of unusual structures have their special importance. Recent studies on the adaptive processes in *Sarcina ventriculi* shows that very long chain bifunctional acyl components formed in membranes during stress can function in regulating the membrane dynamics (6, 7). The mode of formation of these unusual lipid species in *S. ventriculi* appears to be by the tail-to-tail condensation of alkyl chains across the two leaflets of the membrane bilayer. Although the structures of the isolated fatty acyl species support this idea, no information on the structures of the intact lipid species is available. The focus of this study, therefore, was to isolate and characterize intact lipid species from the membrane of *S. ventriculi* (11,12). Special emphasis was placed on the isolation and characterization of membrane components which contained the unusual very long chain, bifunctional fatty acyl species. Information on the structures of such lipid components is critical for our understanding of the architecture of the membrane as well as our appreciation for the possible modes of synthesis of these unusual but physiologically important components.

MATERIALS AND METHODS

Culture of Cells

S. ventriculi was cultured at pH 3.0 in liquid medium as described before (6).

Membrane Preparations

Cells were disrupted by passage through a French Pressure cell (American Instruments Co., Inc., Silver Spring, Md.) at 20,000 lb/in^2. The disrupted cells were centrifuged at 20,000 x g to remove unbroken cells, and the supernatant was centrifuged at 110,000 x g to sediment the membranes, which were washed twice with distilled water by suspending and recentrifugation.

Extraction of Lipids

Lipids were extracted from the isolated membrane or whole cells using procedures (a) or (b) respectively. (a) To each 5-10 ml membrane suspension was added 30 vol. of chloroform/methanol (5:1,v/v). The suspension was then mixed to produce a single phase. The mixture was shaken or stirred vigorously at 45°C, with intermittent sonication (for approximately 5 min every 30 min), over a total of 2 hours and then taken to dryness on a rotary evaporator. The residue was partitioned between 10 ml chloroform/methanol (5:1,v/v) and 2.5 ml water. The lower organic phase was taken to dryness and redissolved in 1 ml chloroform/methanol (9:1,v/v). (b) Cells of *S. ventriculi* from 50 liters of culture medium were harvested by centrifugation at 10,000 x g for 10 min. Lipids from approximately 50 g wet weight of cells were extracted at 45°C with 400 ml of a mixture of chloroform/methanol/water (15:3:2, by vol.) for 2 hours, followed by 200 ml of chloroform/methanol (5:1,v/v). Extraction was performed with intermittent sonication over 2 hours or described in procedure (a). After centrifugation at 20,000 x g, the pellet

(cell debris) was extracted again with the same solvent system. After centrifugation, the supernatant was taken to dryness on a rotary evaporator, dissolved in 10 ml of chloroform/methanol (5:1,v/v) and then shaken with 2.5 ml water. The lower phase containing the lipids was taken to dryness and the residue dissolved in 1 ml of chloroform.

Analysis of Lipids

Membrane lipids were separated by 2-dimensional TLC using chloroform/ methanol/ ammonia/ water (3.3:1.0:0.1: 0.05, by vol.) for the first dimension and chloroform /methanol / water (7:1.6:0.2, by vol.) for the second dimension. Analyses were performed on silica-gel plates (Merck). Spots were made visible either by spraying with 50% ethanolic-sulfuric acid and heating at 250^{o}C to char the organic components, or by spraying with a 0.1% solution of 2',7,-dichlorofluorescein in aqueous ethanol (1:1) and viewing under ultraviolet light (8). Standard phospholipids such as phosphatidylcholine (PC), phosphatidylethanolamine (PE), phosphatidylserine (PS) and cardiolipin (CL) and neutral lipids (NL) were used as standards in addition to free fatty acids (FA). Spraying agents (9) for the detection of components included ninhydrin for PE or PS, dragendorff agent for PC, orcinol for glycolipid, and molybdenum blue for phosphate. Each lipid band was scraped from the plate into a column fitted with a sintered disc and the material was eluted from the silca gel with the mixtures of methanol and chloroform. Each fraction was concentrated by evaporation and redissolved in chloroform or a choloroform /methanol (5/1) mixture for further analysis. One of the orcinol-positive lipid bands (A(a), see reference 1) containing the bifunctional acyl chains (by GC/MS analysis) was chosen for further study.

Head Group Analyses

Isolated lipids were hydrolyzed with 2 M TFA (trifluoroacetic acid) at 120^{o}C for 3 hours. The hydrolysate was concentrated to dryness, and then 1 ml of water was added and

the solution concentrated to dryness to remove trace amounts of TFA. The hydrolysate was further analyzed by proton NMR (Nuclear magnetic Resonance) spectroscopy or by conversion to alditol acetates for GC/MS analysis. For GC/MS analysis using alditol acetates, the TFA hydrolysate was extracted with 2 volumes of 1 ml chloroform. The chloroform extracts were discarded and the aqueous layer was concentrated to dryness under nitrogen. The aqueous residue was dissolved in methanol and reduced with sodium borohydride for 1 hr. 3 M HCl was then added to decompose excess borohydride. The solution was repeatedly concentrated to dryness several times from methanol. To the residue was added 0.1 ml pyridine and 0.1 ml acetic anhydride. The solution was briefly sonicated and left at room temperature for 16 hrs. The mixture was concentrated to dryness and then 1 ml chloroform and 1 ml 3M HCl were added to the residue. The chloroform layer was washed once with 1 ml 0.5 M NaCl, dried over anhydrous sodium sulfate, and subjected to GC analysis on a DB225 capillary column with an initial temperature of 200°C, hold time 5.00 min., rate of 2.0 deg/min., final temperature of 230°C, final hold time of 55 min., and total run time of 75 min. Retention times were compared with alditol acetate derivatives of a number of alditol acetate standards. GC/MS analyses were then performed on a JEOL JMA DA5000 mass spectrometer using a DB225 capillary column.

Fatty Acids Analysis

Fatty acid analyses were performed on the isolated lipids by treatment with methanolic HCl using either of two procedures. Three (3) ml of chloroform was added to 1 ml of lipids suspension followed by 15 ml 5% methanolic-HCl solution. The flask was sealed and heated in an oven at 72°C for 12 hours. 3 ml of chloroform was added every 6 hours followed by mild sonication for 5 minutes. The mixture was then concentrated on the rotary evaporator to dryness and extracted with chloroform. The combined organic fraction was redissolved in 1 ml of hexane. The fatty acid methyl esters prepared by above procedure were subjected to Gas Chromatography analysis on a 25 M J&W Scientific DB1

capillary column using helium as the carrier gas and a temperature program of 150°C initial temperature, 0.00 min hold time and 3.0 deg/min rate, to a temperature of 200°C. A second ramp of 4.0 deg/min was then immediately started until the final temperature of 300°C was obtained. This temperature was held for 30 min. The relative proportion of lipid components were calculated from the integrated peak areas. The fatty acid identification and molecular weight were determined using GC/MS analysis using a JEOL JMS-AX505H spectrometer interfaced with a Hewlett-Packard 5890A Gas Chromatograph.

FAB (Fast Atom Bombardment) Mass Spectrometry

FAB-MS was performed on JEOL HX100 (Peabody, MA) double-focusing mass spectrometer (EB configuration) equipped with a high-field magnet operated in the positive ion mode. Ions were produced by bombardment with a beam of Xe atoms (6kv). The accelerating voltage was 10 kv, and the resolution was set at 1000 or 3000 according to the mass range of interest. The samples were dissolved in chloroform solution. Generally , 1 - 1.5µl of sample was mixed with 1µl of NBA (Nitro-Benzyl Alcohol) on the FAB-MS stainless steel probe tip. Calibration was performed using Ultramark (443 or 6121) or $(CsI)_nI^-$ cluster ions, depending on the mass range of interest. A JEOL DA-5000 data system was used for recording the spectra. The spectrum was scanned over 2 min from m/z 0 -3000. Data presented were obtained in a single scan and found to reproducible.

^{1}H NMR Spectroscopy

Proton NMR spectra were recorded at 300 MHz and 500MHz on solutions in $CDCl_3$ or D_2O. Chemical shifts are quoted relative to the solvent resonances taken at 7.24 ppm for chloroform and at 4.65 ppm for water.

Fourier Transform Infrared Spectroscopy

Spectra were obtained with a Nicolet model 710 FT-IR spectrometer on a 10% (w/v) solution of isolated lipids in chloroform.

RESULTS AND DISCUSSION

Structural Characterization of the Isolated Glycolipids

One of the orcinol-positive glycolipid fractions on 2-dimensional TLC was isolated by preparative thin layer chromatography. The total ion chromatogram from the GC/MS analysis of the fatty acid methyl esters obtained from this fraction is shown in Figure 1. The peaks from **a** to **e** are due to typical membrane fatty acyl components ranging from 14 to 18 carbons. The major regular fatty acid methyl esters are hexadecanoic acid methyl ester (peak **c**, $C_{16:0}$), *cis*-vaccenic acid methyl ester (peak **d**, $C_{18:1(11)}$) and stearic acid methyl ester (peak **e**, $C_{18:0}$). The peaks from **f** to **m**, however, correspond to very long bifunctional fatty acyl components containing from 28 to 36 carbon atoms. The major bifunctional acyl species were identified as α,ω-15,16-dimethyltricotanedioic acid dimethyl ester (peak **j**), α,ω-(17,18-dimethyl)-*cis*-11-dotriacotaenedioic acid dimethyl ester (peak **l**) and α,ω-(17,18-dimethyl)-*cis*-11-23-hentriacotadienedioic acid dimethyl ester (peal **m**). A detailed structural characterization of these components has been presented earlier (1, 2). Another unusual, very long chain component (peak **k**) was identified on an ω-formyl methyl ester. Figure 2 shows the EI (electron impact) mass spectrum (70ev) of this molecule. Major ions appeared at m/z 534, 502 and 474. These correspond to the molecular ion (M^+) with the sequential losses of methanol (CH_3OH) and ethylene ($CH_2{=}CH_2$) or carbon monoxide, respectively. The ions at m/z 516 and 484 are due to the loss of water from the ions at m/z 534 and 502 respectively. Primary fragmentation of the alkyl chains between the vicinal methyl groups (Figure 3) give rise to the fragments at m/z 295 and 239. The ions at m/z 264 and 221 correspond to the loss of methoxy group (CH_3O) from the ion at m/z 295 and to the loss of water from the ion at m/z 239, respectively. The characteristic McLafferty fragment of aliphatic methyl ester appears at

Figure 1. Total ion chromatogram of Gas Chromatography/Mass Spectrometry analysis for the esterified fatty acyl components of one of the isolated glycolipids. The later eluting cluster of peaks is due to the membrane spanning α,ω-bifunctional fatty acids.

$C_{16:0}$ fatty aldehyde ($OHC(CH_2)_{14}CH_3$)

$C_{14:0}$ carboxylic acid methyl ester ($OCH_3CO(CH_2)_{12}CH_3$)

$C_{17:0}$ carboxylic acid methyl ester ($OCH_3CO(CH_2)_{15}CH_3$)

$C_{18:1}$ carboxylic acid methyl ester ($OCH_3CO(CH_2)_9CH=CH(CH_2)_5CH_3$)

$C_{18:0}$ carboxylic acid methyl ester ($OCH_3CO(CH_2)_{16}CH_3$)

Unknown

$C_{31:2}$ ω-formylmethyl ester (M.W. = 490)

$C_{33:1}$ ω-formylmethyl ester (M.W. =520)

$C_{30:1}$ α,ω-dicarboxylic dimethyl ester (M.W. = 508)

$C_{32:0}$ α,ω-dicarboxylic dimethyl ester (M.W.= 538)

$C_{34:1}$ ω-formylmethyl ester (M.W.= 534)

$C_{34:1}$ α,ω-dicarboxylic dimethyl ester (M.W.= 564)

$C_{36:2}$ α,ω-dicarboxylic dimethyl ester (M.W = 590)

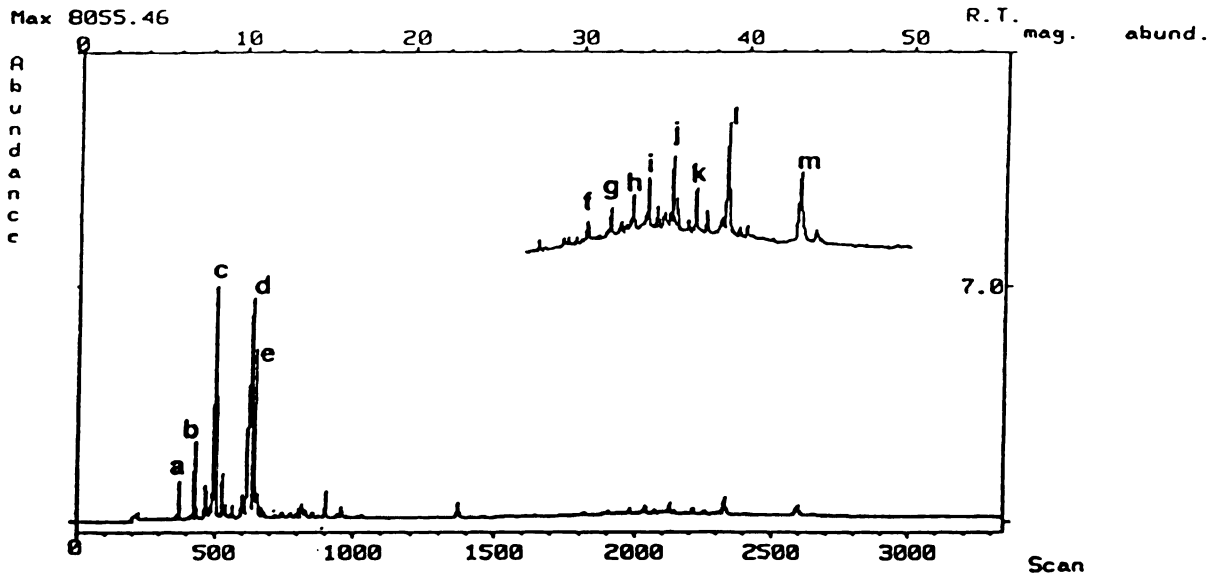
Max 8055.46
R.T.
mag.
abund.
Abundance
0
10
20
30
40
50
a
b
c
d
e
f
g
h
i
j
k
l
m
7.0
0
500
1000
1500
2000
2500
3000
Scan

Figure 1

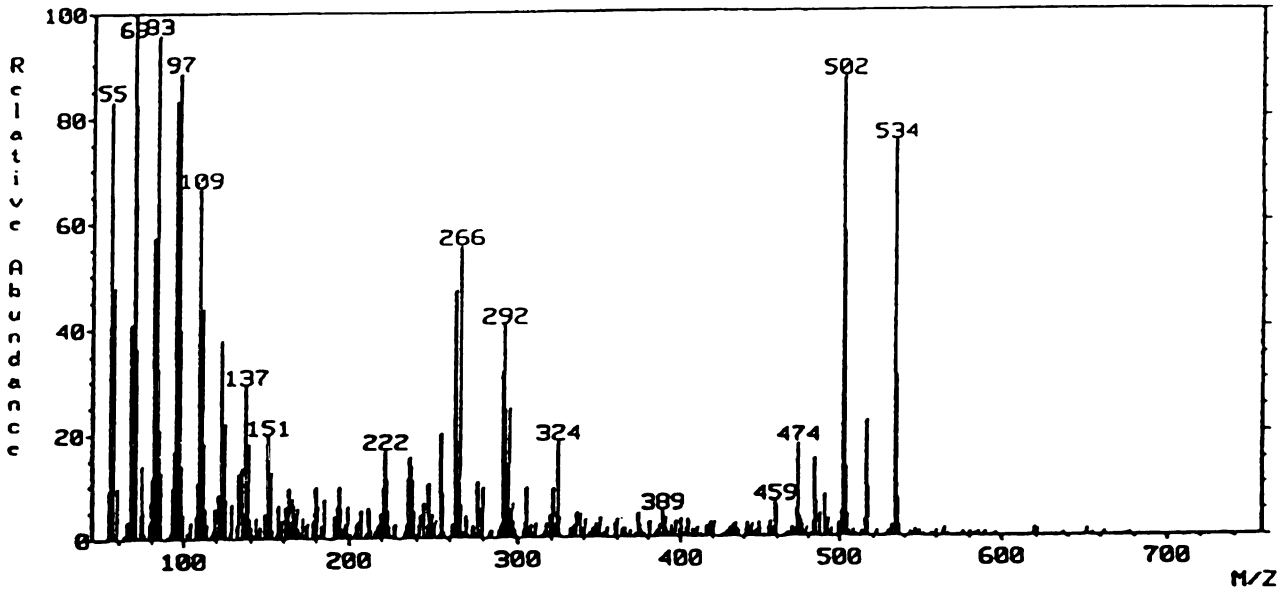

Figure 2. Electron impact mass spectrum of peak k. It contained major ions at m/z 534, 502 and 474. These correspond to the molecular ion (M^+) with the sequential losses of methanol (CH_3OH) and ethylene ($CH_2=CH_2$) or carbon monoxide, respectively.

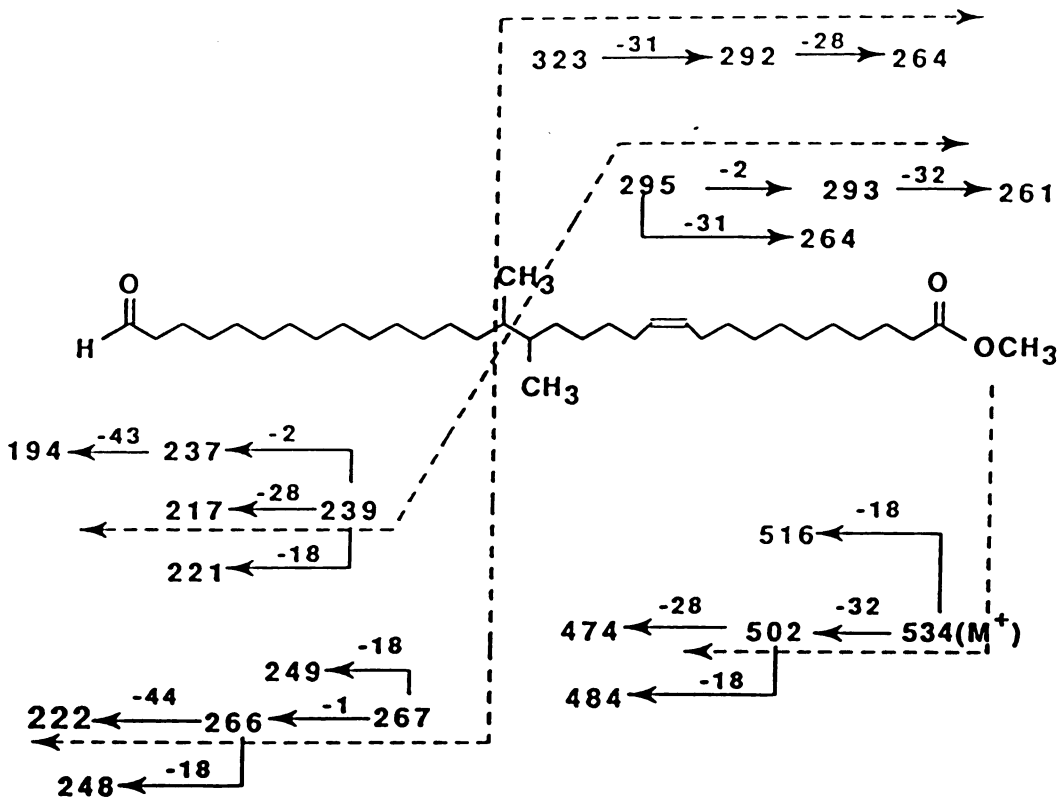

Figure 3. Mass fragmentation pattern of peak k (ω-formyl-(17,18-dimethyl)-*cis*-11-hentriacotanemethyl ester). 1:hydrogen, 2: hydrogen molecule (H_2), 18: water (H_2O), 28: ethylene ($CH_2=CH_2$), 31: methoxy (CH_3O), 32: methanol (CH_3OH), 43: $CH_2=CH-O$, 44: $CH_2=CH-OH$

m/z 74. The other major fragments are shown in Figure 3. The structure of peak **k** was, therefore, determined to be ω-formyl-(17,18-dimethyl)-*cis*-11-hentriacotanemethyl ester (Figure 3). The existence of ω-formylmethyl ester after methanolysis suggested the presence of the vinyl ether (-CH=CH-OC-) functional groups in the parent lipid. This functionality defines the lipid class as a plasmalogen. The molar ratio of the regular length (C_{12}-C_{20}) fatty acids to very long chain bifunctional acyl chains was approximately 2:1. The variety of fatty acid species indicates that, although a single discrete spot is obtained on analysis of this lipid fraction, there is still considerable heterogeneity with respect to alkyl chain length and even type. This heterogeneity is quite normal and an important aspect of membrane structure.

NMR Analyses of Glycolipids

The Proton NMR spectrum of the glycolipid fraction is shown in Figure 4. The intense resonance at δ 1.27 was assigned to the methylene groups of the lipid chain. The multiplet at δ 1.58 were assigned to the methylene protons β to the carbonyl group. The resonances at δ 2.28 (t, J=7.69 Hz) were assigned to the methylene groups α to the carbonyl function. The characteristic 3H-doublet at δ 0.74 (J=7.20 Hz) confirmed the presence of vicinal methyl groups of the ω-1 linked bifunctional acyl chains (6,7). A triplet at δ 5.36 (J=6.92 Hz) was assigned to the vinyl protons of the unsaturated fatty acids. The multiplet at δ 2.00 were assigned to the protons of the methylene groups α to the vinyl carbons. Multiple peaks in the range of δ 3.00 to δ 5.00 strongly indicated the presence of glycerol and carbohydrate functions. This was confirmed by further structural studies.

Head Group Analyses of the Glycolipids

Figure 5 shows the gas chromatographic profile of alditol acetates obtained from the hydrolysate of the lipid fraction by treatment with 2M TFA. There were two major

Figure 4. ^{1}H NMR spectrum of the glycolipids containing bifunctional acyl chains. Signals at 0.74 ppm (d, J=7.20Hz) and 1.27 ppm are characteristic of the methyl and methylene groups of long chain acyl components. Resonance at 2.28 ppm (t, J=7.69Hz) represented methylene groups α to the carbonyl function. The multiplet at 1.58 ppm was assigned to the protons of the β carbons of the molecule. The triplet at δ 5.36 (J=6.92 Hz) was assigned to the vinyl protons. The multiplet at δ 2.00 was assigned to the protons of the methylene groups α to the vinyl carbons. Peaks in the range of δ 3.00 to δ 5.00 strongly indicate the presence of glycerol and carbohydrate functions. The signal at δ 7.24 was assigned to the chloroform.

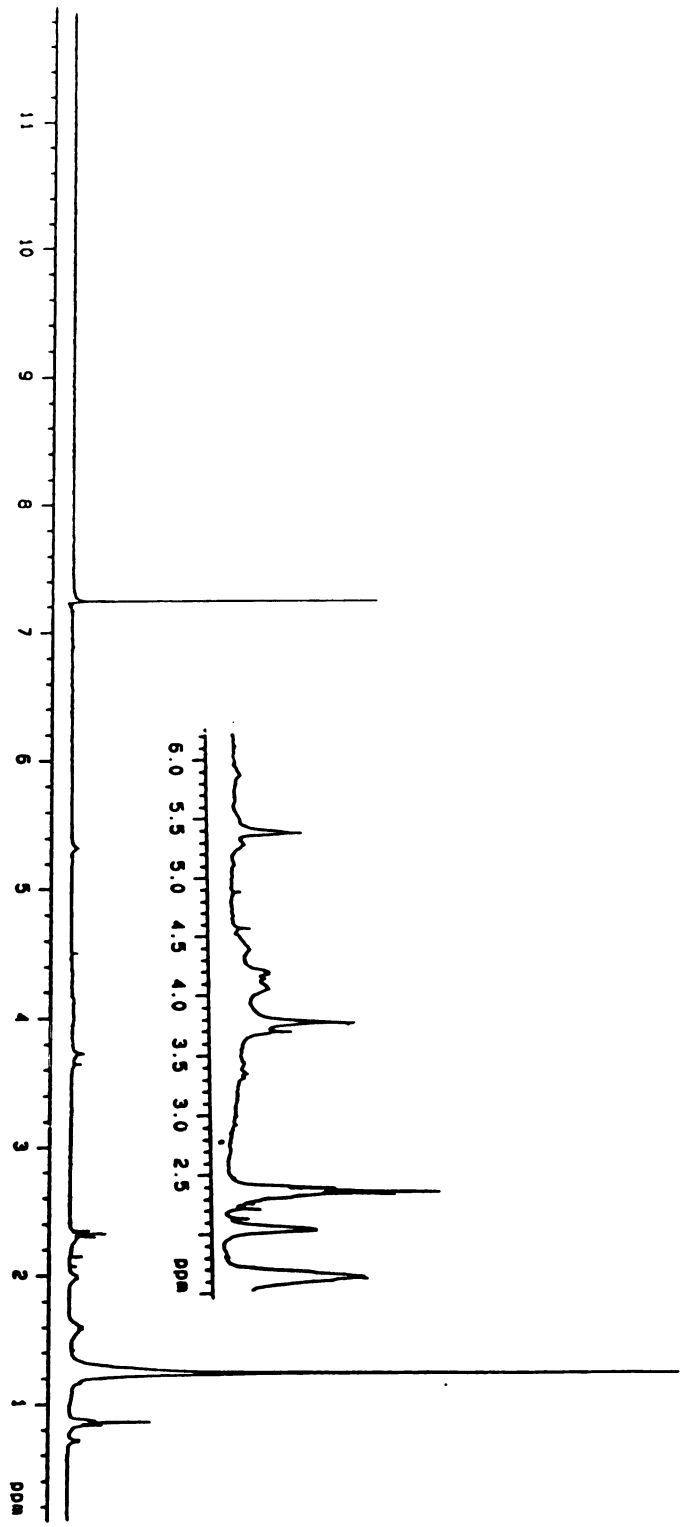

Figure 4

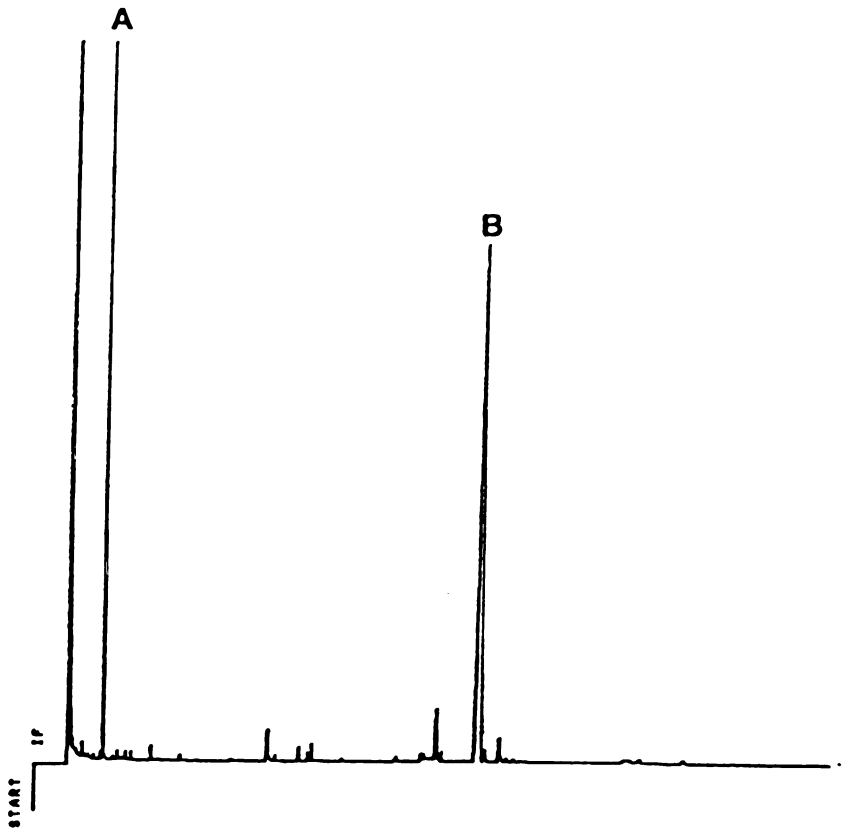

Figure 5. Gas chromatographic profile of the alditol acetates of hydrolysates obtained from the 2 M TFA (Trifluoroacetic acid) hydrolysis of the lipids. A; glycerol triacetates, B; glucitol hexaacetates

components present. Peak **B**(the later peak) had the same retention time of standard glucitol hexaacetate. The presence of this alditol acetate was confirmed by mass spectrometry. The electron impact mass spectrum (70ev) of peak **B** is shown in Figure 6A. Typically, alditol acetate do not give molecular ions, but $(M\text{-}CH_3CO_2)^+$ is found in low abundance by elimination of an acetoxyl group, or by cleavage of the alditol chain, as shown in Figure 6C. In this way, m/z 375 $(M\text{-}CH_3CO_2)^+$ and five other primary fragments are formed from glucitol hexaacetates (Figure 6B). Figure 7 shows the EI mass spectrum of peak **A**. It contains the major ions at m/z 159, 145 and 103. They corresponded to $(M\text{-}\ CH_3CO_2)^+$, $(M\text{-}\ CH_2OCOCH_3)^+$ and the loss of ketene $(-CH_2CO)$ from m/z 145, respectively. The presence of these ions was indicative of the presence of glycerol triacetate. These data indicated that glucose and glycerol are the components of the headgroup. This fact was, further, confirmed by the analyses of the proton NMR spectrum of hydrolysates obtained from TFA hydrolysis (Figure 8). The, α-glucose anomer was confirmed by the characteristic coupling constant of the H-1 proton at δ 4.45 (d, J = 4.00Hz). Characteristic signals of glycerol appeared at δ 3.50 (dd J=4.2 Hz) and δ 3.41 (dd J=4.2 Hz). These data for the glycolipids strongly indicated that they are glucosyl diglycerides that contain the bifunctional acyl chains. Further evidence on the ether linkage between glucose and glycerol was obtained by the Fourier Transform Infrared spectroscopic analysis.

FTIR Analysis of Glucolipids

The Infrared spectrum (Figure 9) showed a strong aliphatic C-H asymmetric stretching absorption at 2918 cm^{-1} and symmetric stretching at 2856 cm^{-1}. The characteristic alkene stretching (=C-H) was observed at 3038 cm^{-1}. Broad -OH stretching band (3600 -3000 cm^{-1}) and hydroxyl stretching vibration at 3411 cm^{-1} were also present. The C-O stretching vibration in the alcohol produced the strong band at 1166 cm^{-1}. A band due to the bending vibration of aliphatic C-H bonds in the methylene groups appeared

Figure 6. Mass spectral analysis of peak B. (A) Electron impact mass spectrum (70ev) of peak B. (B) Ionic fragmentation pattern of the glucitol hexaacetates. Note the presence of ions at m/z 375 $(M\text{-}CH_3CO_2)^+$ and masses corresponding to five other primary fragments. (C) $(M\text{-}CH_3CO_2)^+$ is produced by elimination of an acetoxyl group, or by cleavage of the alditol chain

A

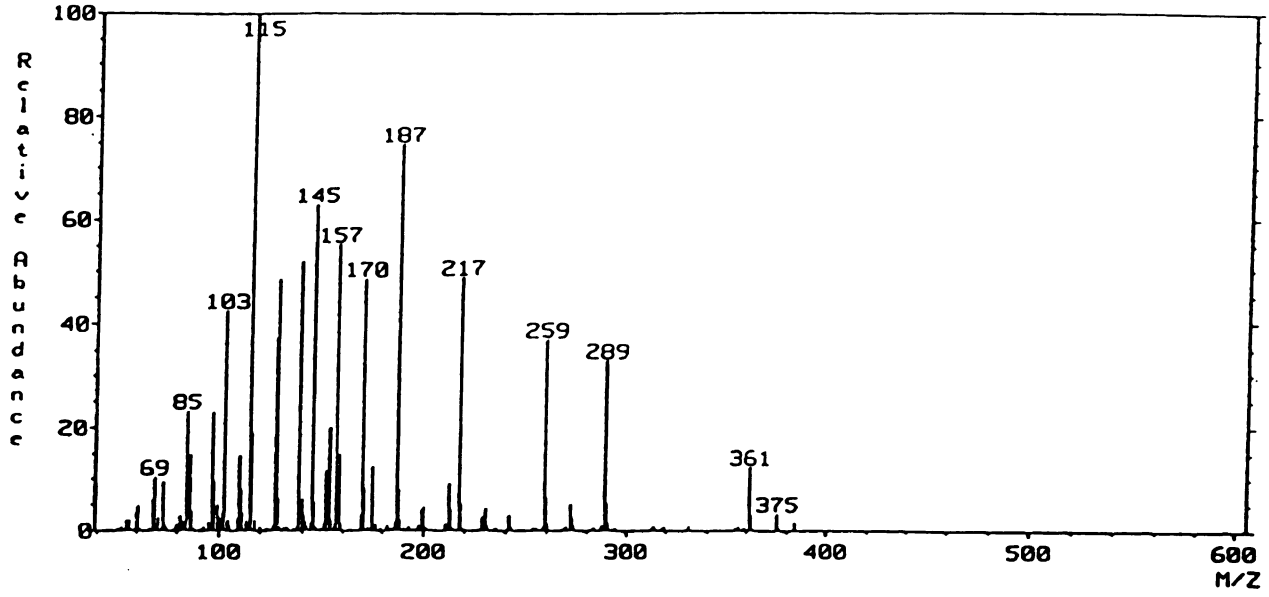

B

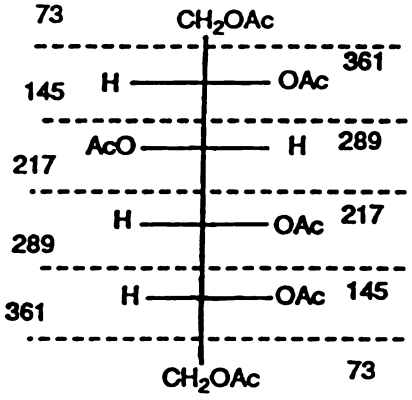

C

*M/Z 375 : (M - CH_3CO_2·)$^+$

Figure 6

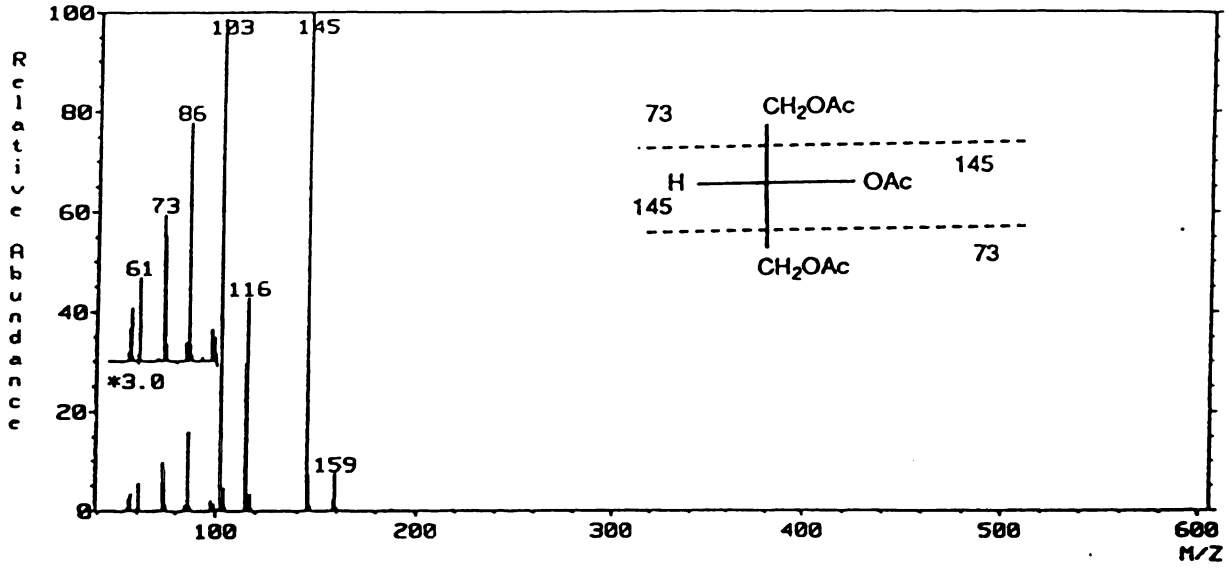

Figure 7. EI mass spectrum of peak A . It contains major ions at m/z 159, 145 and 103. These correspond to the $(M- CH_3CO_2)^+$, $(M- CH_2OCOCH_3)^+$ and loss of ketene ($-CH_2CO$) from m/z 145, respectively.

Figure 8. ^{1}H NMR spectrum of the hydrolysates obtained from the TFA hydrolysis on glycolipids. It shows the anomeric proton of glucose at δ 4.45 (d, J = 4.00Hz). Characteristic signals due to glycerol appear at δ 3.50 (dd J=4.2 Hz) and δ 3.41 (dd J=4.2 Hz). Chemical shifts are quoted relative to the water resonance at 4.65 ppm for proton.

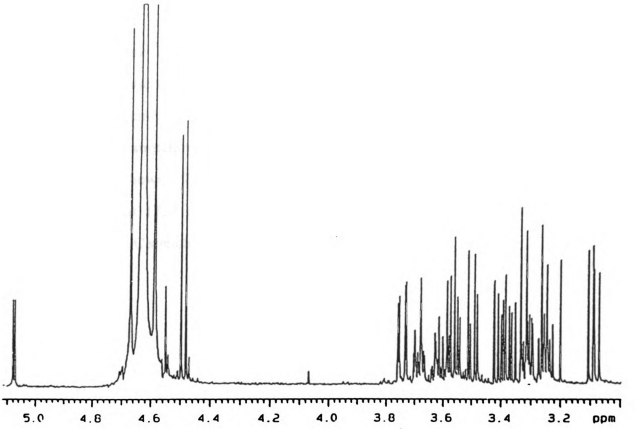

Figure 8

Figure 9. Fourier Transform Infrared spectrum of the glucolipids. Note the presence of aliphatic C-H asymmetric stretching absorption at 2918 $cm^{-1}$and symmetric stretching at 2856 cm^{-1}. The characteristic alkene stretching (=C-H) was observed at 3038 cm^{-1}. Broad -OH stretching band (3600-3000 cm^{-1}) and hydroxyl stretching vibration at 3411 cm^{-1} were shown. The characteristic C=O absorption bond of the aliphatic ester group appeared at 1733 cm^{-1} and the ester alkoxy stretch at 1263 cm^{-1}. The strong asymmetrical C-O-C stretching band appeared at 1099 cm^{-1}.

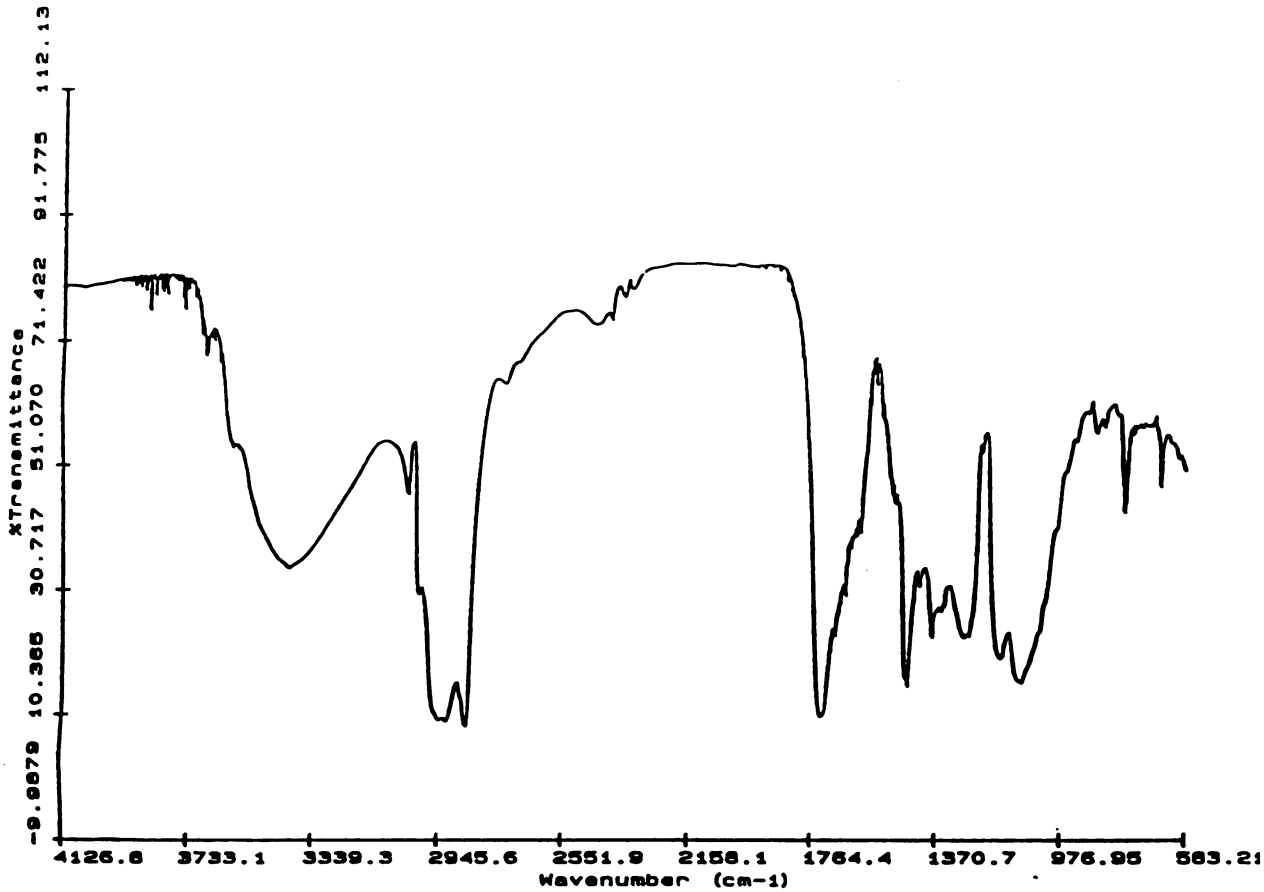
%Transmittance
112.13
91.775
71.422
51.070
30.717
10.365
-9.9879
4126.8
3733.1
3339.3
2945.6
2551.9
2158.1
1764.4
1370.7
976.95
583.21
Wavenumber (cm-1)

Figure 9

at 1465cm^{-1} (scissoring) and one due to the twisting and wagging deformation at 1340 cm^{-1}. The characteristic C=O absorption bond of the aliphatic ester group appeared at 1733 cm^{-1} and the ester alkoxy stretch at 1263 cm^{-1}. The stereochemistry (*cis*- or *trans*-) of the unsaturated carbons was determined by the clear presence of a strong peak at 660 cm^{-1} due to the C=C-H bending deformation for *cis*- alkenes (10). The characteristic response of ethers in the IR is associated with the stretching vibration of the C-O-C system. The strong asymmetrical C-O-C stretching band appeared at 1099 cm^{-1}. The C=C stretching band of vinyl ethers appeared at 1623 cm^{-1} and 1636 cm^{-1} as a doublet because of the presence of the rotational isomers.

FAB(Fast Atom Bombardment) Mass Spectromety Analysis of the Glucolipids

Positive FAB mass spectra of the glucolipids were obtained to determine the range of molecular weight of the lipids and the number of attached glucose groups (Figure 10). Due to the variety of fatty acyl components a cluster of molecular ions ([M+Na+H]$^+$) was observed. The spectra contained two clusters separated by 162 a.m.u. The lower mass cluster was derived from the higher mass cluster by the loss of one glucosyl residue. Figure 11 shows the two clusters at the high mass end of the spectrum. The numbers of the ionic clusters ([M+Na+H]$^+$) indicated various kinds of monoglucosyl lipids. Each ionic cluster numbered in Figure 11 could be predicted from the general structure proposed in Figure 12. This structural formula is based on the compositional data of the lipids, in which the fatty acyl chains and head group components were separately quantitated and analyzed by various spectroscopic methods. There is an approximate 2:1 molar ratio between the regular length acyl chain and membrane spanning bifunctional acyl chains. Based on the fatty acyl components present, the distribution and molecular weights of the peaks in the clusters could be predicted using an unbiased, statistically weighted combination algorithm. Table 1 shows the calculated m/z values of two ionic clusters.

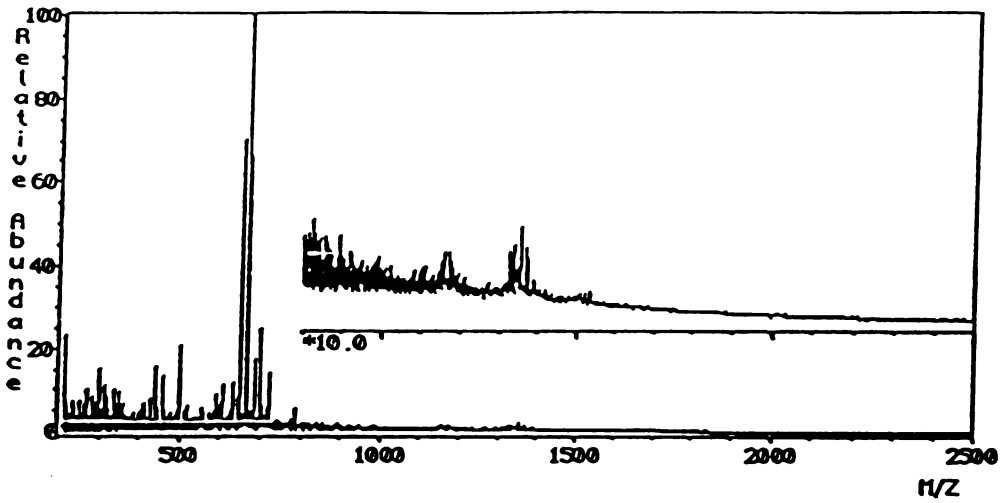

Figure 10. Positive FAB-Mass Spectrum of the glucolipids. Note the cluster of molecular ions $[M+Na]^+$. The other lower mass cluster is due to the loss of one glucose group ($[M+Na - 162]^+$).

Figure 11. Positive FAB-Mass spectrum of two ion clusters ($[M+Na]^+$, $[M+Na - 162]^+$) separated by 162 mass units. It confirmed the presence of one glucose molecule. Each numbered ionic cluster was predicted by the calculated m/z values based on the compositional analyses. Table 1 showed the calculated ionic clusters from the basic frame in Figure 12.

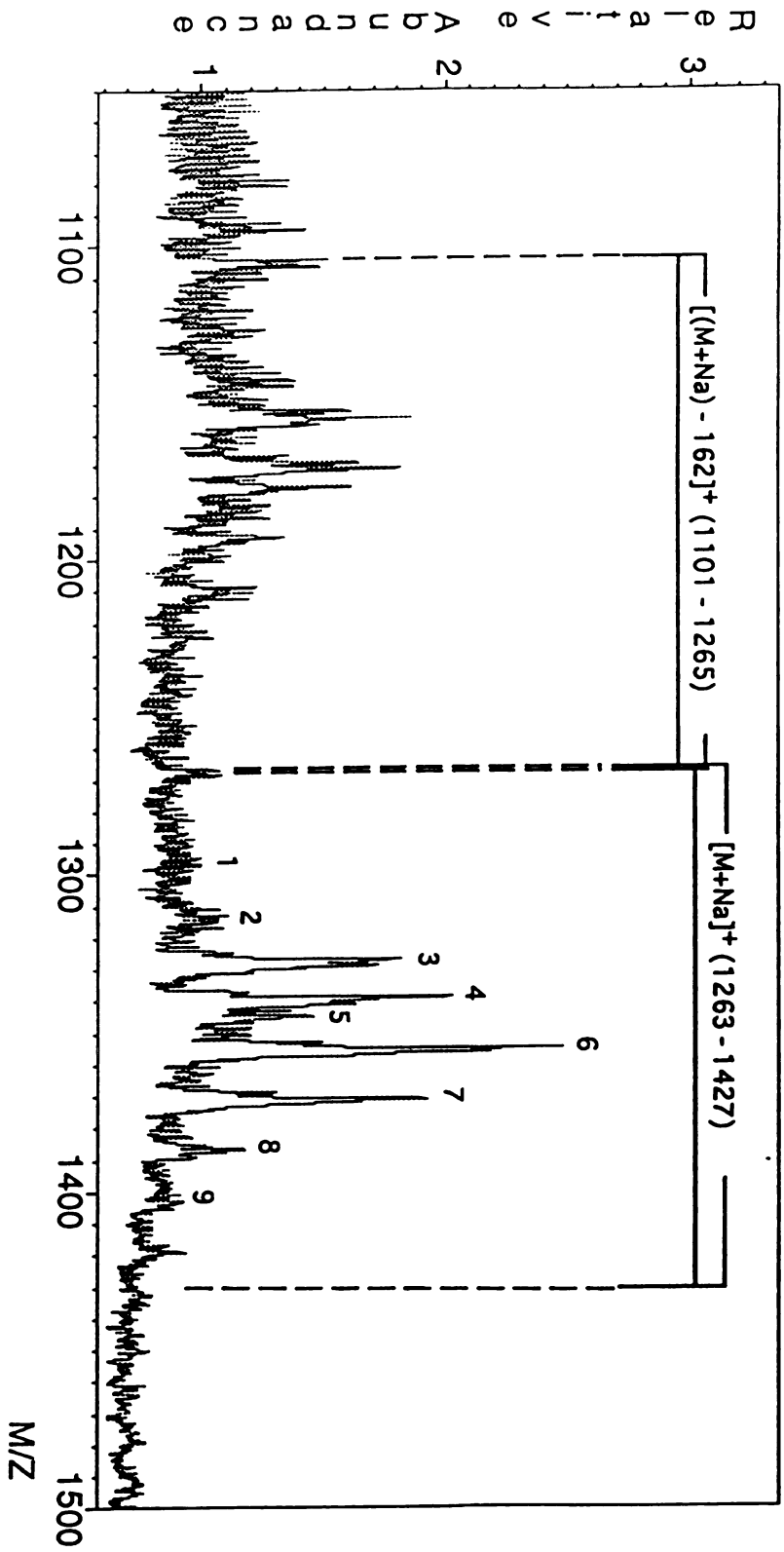
Relative Abundance
1
2
3
1100
1200
1300
1400
1500
M/Z
[(M+Na) - 162]+ (1101 - 1265)
[M+Na]+ (1263 - 1427)
1
2
3
4
5
6
7
8
9

Figure 11

Table 1. The calculated m/z vaues of ionic clusters based on the compositional analyses. MSFC; Membrane Spanning Fatty Acyl Components, Fy 1: Fatty acyl component 1, Fy 2; Fatty acyl componet 2. Small alphabets (**a, b.., l, m**) indicated the peak numbers in the GC/MS analyses (Figure 3). The asterisked small number in each column point out the peak number (1, 2, .., 9) of the ion fragments observed in FAB-MS. Almost all of the observed ionic clusters were predicted with the proposed lipid structures based on the structural model shown in Figure 12.

MSFC / (Fy1,FY2)	[(M+Na)-162]+				[M+Na]+			
	j(538)	l(564)	m(590)	k(534)	j(538)	l(564)	m(590)	k(534)
(b,b) (242,242)	(j,b,b) (1101)	(l,b,b) (1127)	(m,b,b) (1153)	(k,b,b) (1111)	(j,b,b) (1263)	(l,b,b) (1279)	*2 (m,b,b) (1315)	(k,b,b) (1273)
(b,c) (242,270)	(j,b,c) (1129)	(l,b,c) (1155)	(m,b,c) (1181)	(k,b,c) (1139)	*1 (j,b,c) (1291)	*2 (l,b,c) (1317)	*4 (m,b,c) (1343)	*1 (k,b,c) (1301)
(b,d) (242,296)	(j,b,d) (1155)	(l,b,d) (1181)	(m,b,d) (1207)	(k,b,d) (1165)	*2 (j,b,d) (1317)	*4 (l,b,d) (1343)	*7 (m,b,d) (1369)	*3 (k,b,d) (1327)
(b,e) (242,298)	(j,b,e) (1157)	(l,b,e) (1183)	(m,b,e) (1209)	(k,b,e) (1167)	(j,b,e) (1319)	*5 (l,b,e) (1345)	*7 (m,b,e) (1371)	*3 (k,b,e) (1329)
(c,c) (270,270)	(j,c,c) (1157)	(l,c,c) (1183)	(m,c,c) (1209)	(k,c,c) (1167)	(j,c,c) (1319)	*5 (l,c,c) (1345)	*7 (m,c,c) (1371)	*3 (k,c,c) (1329)
(c,d) (270,296)	(j,c,d) (1183)	(l,c,d) (1209)	(m,c,d) (1235)	(k,c,e) (1193)	*5 (j,c,d) (1345)	*7 (l,c,d) (1371)	*9 (m,c,d) (1397)	*6 (k,c,d) (1355)
(c,e) (270,298)	(j,c,e) (1185)	(l,c,e) (1211)	(m,c,e) (1237)	(k,c,e) (1195)	*5 (j,c,e) (1347)	*7 (l,c,e) (1373)	*9 (m,c,e) (1399)	*6 (k,c,e) (1357)
(d,d) (296,296)	(j,d,d) (1209)	(l,d,d) (1235)	(m,d,d) (1261)	(k,d,d) (1219)	*7 (j,d,d) (1371)	*9 (l,d,d) (1397)	(m,d,d) (1423)	*8 (k,d,d) (1381)
(d,e) (296,298)	(j,d,e) (1211)	(l,d,e) (1237)	(m,d,e) (1263)	(k,d,e) (1221)	*7 (j,d,e) (1373)	*9 (l,d,e) (1399)	(m,d,e) (1425)	*8 (k,d,e) (1383)
(e,e) (298,298)	(j,e,e) (1213)	(l,e,e) (1239)	(m,e,e) (1265)	(k,e,e) (1223)	*7 (j,e,e) (1375)	*9 (l,e,e) (1401)	(m,e,e) (1427)	*8 (k,e,e) (1385)

Table 1

Figure 12. Basic model structure of the monoglucosyldiacylglyceride diacyl glycerol in *S. ventriculi.* This frame was constructed based on the compositional analyses of the glucolipids. Letters point out the peaks in Figure 1. The numbers in parenthesis indicated the molecular weights of fatty acyl components obtained from the methanolysis of the glucolipids. MSFC; Membrane Spanning Fatty Acyl Components , Fy 1; a regular fatty acyl component

Fy 2; another regular fatty acyl component

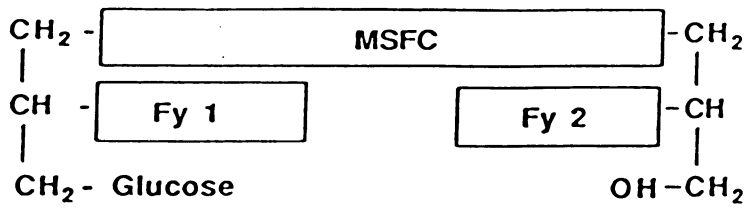

MSFC: j(538) =>OCO-$(CH_2)_{13}$-(CH_3)CH-CH(CH_3)-$(CH_2)_{13}$-OCO

l(564) =>OCO-$(CH_2)_{13}$-$(CH)_3$CH-CH(CH_3)-$(CH_2)_4$-CH=CH$(CH_2)_9$OCO

m(590)=>OCO$(CH_2)_9$CH=CH$(CH_2)_4$-(CH_3)CH-CH(CH_3)-$(CH_2)_4$CH=CH$(CH_2)_9$OCO

k(534)=>OCO$(CH_2)_9$CH=CH$(CH_2)_4$-(CH_3)CH-CH(CH_3)-$(CH_2)_{12}CH_2$CHO

FY 1; FY 2

(b) 242 => OCO-$(CH_2)_{12}$-CH_3

(c) 270 => OCO-$(CH_2)_{14}$-CH_3

(d) 296 => OCO$(CH_2)_9$CH=CH$(CH_2)_5$-CH_3

(e) 298 => OCO$(CH_2)_{16}$-CH_3

Figure 12

Most of the members of the cluster of peaks observed were predicted with this calculation. The asterisked small numbers in the columns in Table 1 points out the numbered peaks (1, 2,.., 9) observed in FAB-MS analyses (Figure 11). This combined with the structural data presented, confirmed that this lipid fraction is composed of a new family of monoglucosyl diglycerides containing bifunctional fatty acyl chains.

Biochemical Significance of Glucolipids Containing Bifunctional Fatty Acyl Chains

One possible mechanism for the synthesis of these unusual lipid components which was alluded to earlier (6, 7), is the random, pairwise, combination of fatty acyl chains in a tail-to-tail manner across the interface between the leaflets of the bilayer. Based on this scenario, we should expect to isolate intact membrane species of constant and invariant head group structure which contain fatty acyl components that reflect the distribution in the entire membrane. In this work, one such family of lipid species has been described. These results are powerful evidence in favor of a general adaptive response in *S. ventriculi* in which existing lipid species become chemically linked during certain stress conditions to transform the bilayer membrane into a bipolar monolayer membrane.

CONCLUSIONS

Recent research on the fatty acyl chains in the membrane lipids in *Sarcina ventriculi* has shown that unusually long chain, bifunctional fatty acyl components are the major components of the total lipid. These studies did not yield any information on the complete structures of the lipids species containing these fatty acids. In this study, the structures of a new family of glucolipids containing bifunctional acyl chains are described. These structures were determined using NMR (Nuclear Magnetic Resonance) spectroscopy, GC(Gas Chromatography)/MS (Mass Spectrometry), FTIR (Fourier transform Infrared) spectroscopy and FAB (Fast Atom Bombardment) mass spectrometric studies. One of the major bifunctional acyl components of the α-glucolipids was an ω-formylmethyl ester indicating the presence of a plasmalogen. The general structure of the lipid components is one in which the two head groups are separated by a membrane-spanning acyl species. One head group component is glycerol and the other is a glyceryl glucoside. Two regular chain fatty acids, one on the glycerol moiety of each head group, are also present and meet in the middle of the membrane, roughly equi-distant from each head group.

REFERENCES

1. Silvius, J. R., and McElhaney, R. N. (1979) *Chem. Phys. Lipids* **24**, 287-296
2. Silvius, J. R., and McElhaney, R. N. (1980) *Chem. Phys. Lipids* **26**, 67-77
3. Silvius, J. R., Mak, N., and McElhaney, R. N. (1980) in *Membrane Fluidity* (Kates, and Kuksis, A., Eds.) pp 213-222, Humana Press, Clifton, N.J.1.
4. Bazzi, M.D., and Nelsestuen, G.L. (1987) *Biochemistry* **26**, 5002-5008
5. Bell, R.M. (1986) *Cell* **45**, 631-632
6. Jung, S., Lowe E.S., Hollingsworth, I. R ., and Zeikus, J. G. (1993) *J. Biol. Chem.* 2828-2835
7. Jung, S., and Hollingsworth, I.R. (1993) in preparation (JBC submitted)
8. Morris, J. L. (1962) *Chem. & Ind.*. 1238-1240
9. Holme, J. D. and Peck, H. (1983) In *Analytical Chemistry* pp 436-467 Longman, Inc. New York
10. Shreve, O. D., and Heether, M. R., (1950) *Analytical Chemistry* **22**, 1261-1264
11. Canale-Parola, E. (1986) Genus *Sarcina Goodsir* 1842, 434^{AL}, p. 1100-1103. In P. A. Sneath, N. S. Mair, M. E. Shaarpe and J. G. Holt (ed.), Bergey's manual of systematic bacteriology, vol. 2. The Williams & Wilkins Co., Baltimore
12. Goodwin, S., and J. G. Zeikus. (1987) *J. Bacteriol.* **169**, 2150-2157

CHAPTER VI

A FAMILY OF VERY LONG CHAIN α,ω-DICARBOXYLIC ACIDS IS A STRUCTURAL COMPONENT OF MEMBRANE LIPIDS OF *CLOSTRIDIUM THERMOHYDROSULFURICUM*

INTRODUCTION

The optimum temperature for growth of the thermophilic eubacterium, *Clostridium thermohydrosulfuricum,* is 67-69°C The maximum temperature at which growth occurs is 76-78°C and the minimum temperature is 42°C (1). The structural basis for the stability of membranes of thermophilic bacteria such as *Clostridium* has been somewhat of an enigma because a number of physical studies, employing model membranes or natural membranes enriched in typical regular chain branched-chain fatty acids (the predominant type found in these organisms), have indicated that they act as membrane "fluidizers" rather that "stabilizers" (2,3,4). Based on these studies, the relatively obscure process of homeophasic adaptation (5), instead of homeoviscous adaptation (6, 7), was invoked in order to explain the roles of these branched fatty acids in the thermophilic membrane. The concept of homeophasic adaptation in the membrane of thermophilic bacteria was proposed mainly in an effort to explain how branched fatty acids components of regular length (C_{12}-C_{20}) could function in maintaining the stability of these membranes at such high temperatures. The process of homeophasic adaptation requires that the relative proportions of the different lipid phases (e.g. hexagonal, cubic etc.) always remain constant as the temperature changes. The difficulty with this concept is that there is no clear physical parameter one could use to follow these phase contributions. The possibility exists that there is some other major structural feature of the membrane of thermophilic bacteria which, when combined with the presence of the branched fatty acids, could easily explain membrane stability. In a recent study (1, 2) we reported an interesting adaptive mechanism in *Sarcina ventriculi* in which there was chemical cross-linking of the tails of fatty acids from opposite leaflets of the membrane bilayer in response to thermal , pH or solvent stress. This resulted in the formation of very long chain, transmembrane, dicarboxylic acid species. The possibility that mechanisms such as this may be possible in *Cl. thermohydrosulfuricum* was therefore explored. This seems reasonable in view of the

fact that *S. ventriculi* and *Cl. thermohydrosulfuricum* are not too distantly related. In this study, we explore the possibility that the mechanism used by *S. ventriculi* to adapt to high temperature might be employed by the thermophile *Cl. thermohydrosulfuricum* during its normal growth.

MATERIALS AND METHODS

Bacterial Cultures and Membrane Isolation

Cl. thermohydrosulfuricum 39E was isolated from Ocopus Spring at Yellowstone National Park (13) and is listed in the American Type Culture Collection (Rockville, Md.) as ATCC 33223. The cells were grown on TYE medium which contained yeast extract, trypticase, trace salts, and vitamins (TYE medium) with 0.5% of either xylose or glucose as the fermentable carbohydrate in stringent anaerobic condition at 65°C (1). Bacterial membranes were isolated as described before (8).

Total Fatty Acid Analysis

To 1 ml of a membrane suspension in water was added 3 ml of chloroform followed by 15 ml of a 5% methanolic HCl solution. The suspension was heated at 72°C for 12hrs and 3 ml portions of chloroform solution were added after every 6 hrs. with mild sonication for 5 minutes after each addition. The mixture was then concentrated to dryness on the rotary evaporator and the fatty acid methyl esters isolated by extraction several times with chloroform. The fatty acid methyl esters prepared above were subjected to gas chromatography analysis on a 25 m J&W Scientific DB1 capillary column using helium as carrier gas. The temperature program started at 150°C with 0.00 min. hold time and a 3.0 deg./min. temperature ramp to a final temperature of 200°C with a hold time of 0.00 min. There was another temperature ramp at a rate of 4.0 deg./min. to a final temperature of 300°C. The temperature was held at 300°C for 30 min. GC/MS analysis was performed on a Jeol JMS-AX505H spectrometer interfaced with a Hewlett-Packard 5890A Gas Chromatograph.

Isotope Labeling

Methyl esters of fatty acid obtained by acid methanolysis were deuterium labelled by treatment with 5% D-4 methanolic-HCl solution for 6 hrs at 72°C. The deuterated methyl esters of fatty acid were extracted and analyzed as described before.

Isolation of α,ω-13,16-Dimethyloctacosanedioate Dimethyl Ester

The mixture of fatty acid methyl ester was applied to preparative silver TLC (thin layer chromatography) plates which were eluted with chloroform/hexane (1.5:1.0,v/v) solutions. Bands were visualized by treatment with Iodine vapor. One of the fractions containing the dicarboxylic acid dimethyl esters, determined by GC analysis of all the bands, was subjected to flash column chromatography (14). The column was sequentially eluted with 3 times the column void volume (V_C) of a chloroform/hexane (1.5:1,v/v) mixture, 2 V_C of chloroform/hexane (4:1, v/v) and V_C of chloroform at a flow rate of 20 ml/min. Separated components were conveniently detected by spotting 5-10 ul of each fraction on TLC plates followed by elution with chloroform and charring. Similar fractions were pooled and concentrated on a rotary evaporator. Each product was dissolved in hexane and then subjected to further analyses.

DQF-COSY and DEPT Experiments

Proton NMR spectra were recorded at 500 MHz on solutions in $CDCl_3$. Correlation data was obtained by 2D DQF-COSY (15) experiment. ^{13}C NMR spectra were recorded at 125 MHz on solutions in $CDCl_3$. DEPT (Distortionless Enhanced by Polarization Transfer) experiments were performed for establishing ^{13}C chemical shift assignments. Chemical shifts are quoted relative to the chloroform resonance taken as 7.24 ppm for proton and 77 ppm for ^{13}C measurements, respectively.

Fourier Transform Infrared Spectroscopy

Spectra were obtained with a Nicolet model 710 FT-IR spectrometer in a 10% (w/v) solution of dicarboxylic acid dimethyl ester in chloroform.

RESULTS AND DISCUSSION

Total Fatty Acids Analyses of *Cl. thermohydrosulfuricum*

The total ion chromatogram from the gas chromatography/mass spectrometric analysis of fatty acids methyl esters extracted from cells grown at 67°C is shown in Figure 1. The peaks from 1 to 6 are due to typical membrane fatty acyl components ranging from 14 to 17 carbons. Major regular fatty acids are *iso*-pentadecanoic acid (peak 3, *iso*-$C_{15:0}$) and *iso*-heptadecanoic acid (peak 5, *iso*-C17:0). The peaks from **A** to **D**, however, correspond to unusual components of apparent lengths much greater than the usual lengths.

Mass Spectrometric Analyses of C_{30} - Dicarboxylic Dimethyl Ester

Peak **B** is the most abundant fatty acyl component (about 36 %) of the membrane of *Cl. thermohydrosulfuricum*. The electron impact mass spectrum of Peak **B** is shown in Figure 2. Figure 2A shows major ions at m/z 510, 478 and 446. These corresponded to the molecular ion of a C_{30}-α,ω-dicarboxylic dimethyl ester (M^+) with the sequential losses of methanol (CH_3OH) and methoxy (CH_3O) groups, respectively. The predominant ion at m/z 297 suggested dimethyl branching and represents the structure obtained by fragmentation at a secondary carbon (Figure 3A). The ion m/z 265 was assigned to the loss of methanol (CH_3OH) from the ion m/z 297. The proposed positions for the placement of the methyl groups was supported by the presence of the strong peak at m/z 255 corresponding to the loss of propene (CH_2=$CHCH_3$) from the ion m/z 297 by way of a single bond inductive cleavage mechanism (Figure 3B) (17). The ion at m/z 199 was similarly assigned to the loss of propene (CH_2=$CHCH_3$) from the other secondary cationic fragment at m/z 241. The characteristic McLafferty fragment ion at m/z 74 ($CH_3OC(OH)$=CH_2) was also detected. Figure 2B shows the electron impact mass spectrum of the deuterium-labeled molecule obtained by methanolysis with the D-4

Figure 1. Total ion chromatogram of Gas Chromatography/Mass Spectrometry analysis for the esterified fatty acyl components of the membrane of *Cl. thermohydrosulfuricum.* The later eluting cluster of peaks is due to very long chain α,ω-bifunctional fatty acids.

1. $C_{16:1}$ *iso*-branched fatty aldehyde ($OHC(CH_2)_{12}(CH_3)CHCH_3$)
2. $C_{14:0}$ *iso*-branched carboxylic acid methyl ester ($OCH_3CO(CH_2)_{10}(CH_3)CHCH_3$)
3. $C_{15:0}$ *iso*-branched carboxylic acid methyl ester ($OCH_3CO(CH_2)_{11}(CH_3)CHCH_3$)
4. $C_{16:0}$ *iso*-branched carboxylic acid methyl ester ($OCH_3CO(CH_2)_{12}(CH_3)CHCH_3$)
5. $C_{17:0}$ *iso*-branched carboxylic acid methyl ester ($OCH_3CO(CH_2)_{13}(CH_3)CHCH_3$)
6. unknowns

A. $C_{29:0}$ α,ω-dicarboxylic dimethyl ester

B. $C_{30:0}$ α,ω-dicarboxylic dimethyl ester

C. $C_{31:0}$ α,ω-dicarboxylic dimethyl ester

D. $C_{32:0}$ α,ω-dicarboxylic dimethyl ester

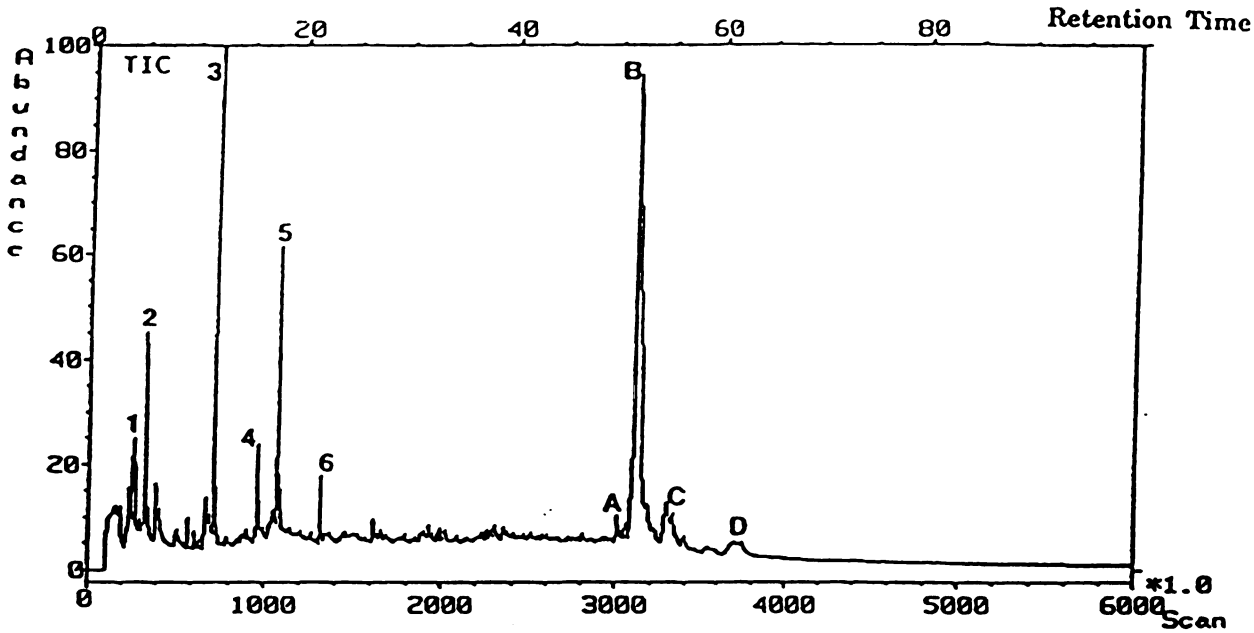
Retention Time
0
20
40
60
80
Abundance
100
80
60
40
20
0
TIC
1
2
3
4
5
6
A
B
C
D
0
1000
2000
3000
4000
5000
6000
*1.0
Scan

Figure 1

Figure 2. Electron impact mass spectrum (70ev) of peak B without (A) and with (B) isotope labeling. (A) Major ions appear at m/z 510, 478, and 447. These corresponded to molecular ion (M^+) with the sequential losses of methanol and a methoxy group, respectively. The ion at m/z 255 is due to the single bond inductive cleavage of the major fragment ion at m/z 297. (B) It shows the EI spectrum of deuterium labeled molecules obtained by deuteration with D-4 methanolic HCl solution. The presence of two carboxylic and two branching methyl groups was confirmed by isotope labeling.

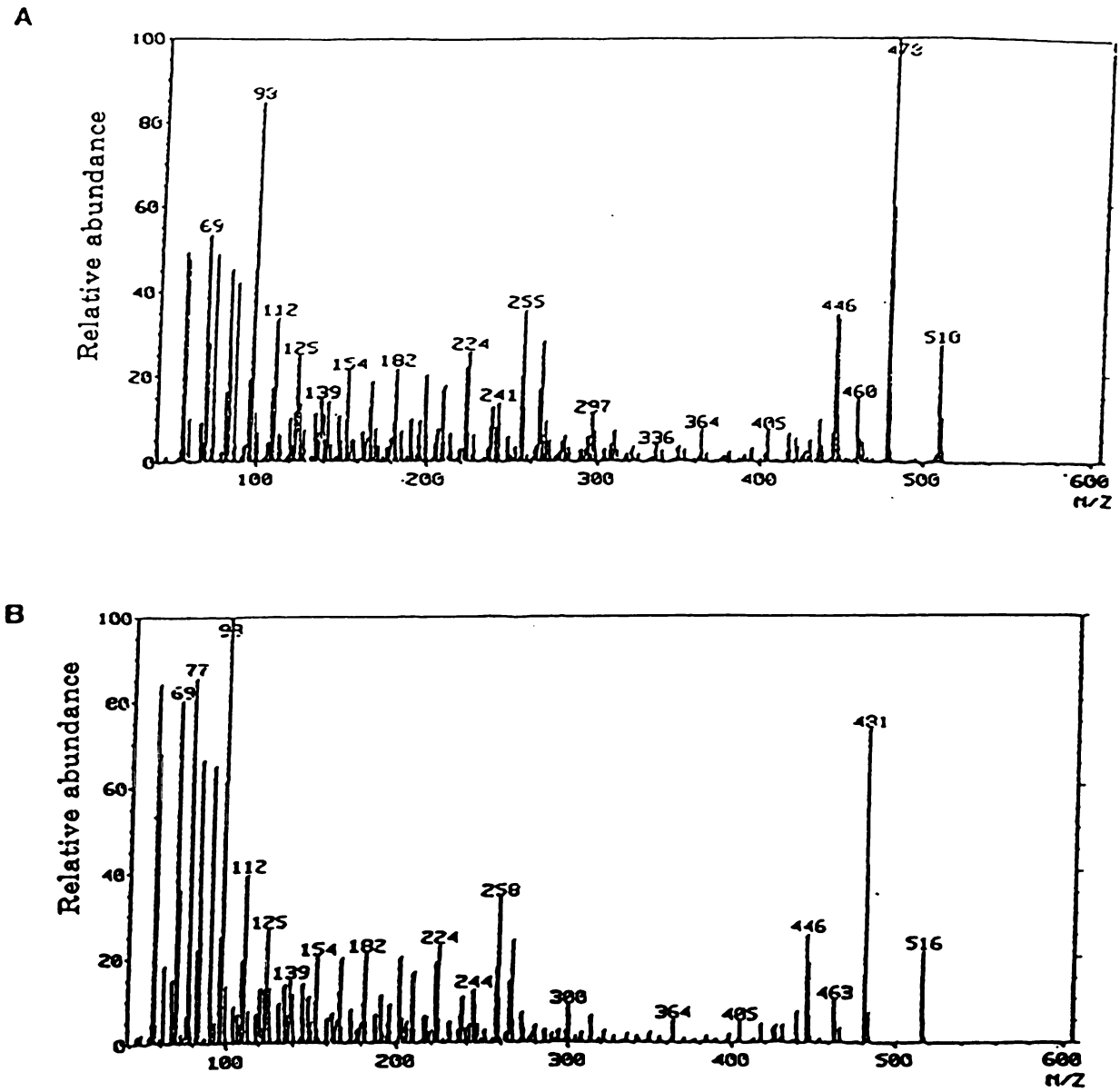
A
Relative abundance
100
80
60
40
20
0
93
69
112
125
139
154
182
224
255
241
297
336
364
405
446
460
473
516
100
200
300
400
500
600
M/Z
B
Relative abundance
100
80
60
40
20
0
93
77
69
112
125
139
154
182
224
258
244
300
364
405
431
446
463
516
100
200
300
400
500
600
M/Z

Figure 2

Figure 3. Analysis of mass spectral fragmentations of peak B. (A) Mass fragmentation pattern of peak **B.** 18: water, 31: methoxy, 32: methanol, 42: propene, 56: butane (B) Single bond inductive cleavage fragmentation mechanism. It produced m/z 255 ion as a major product.

A

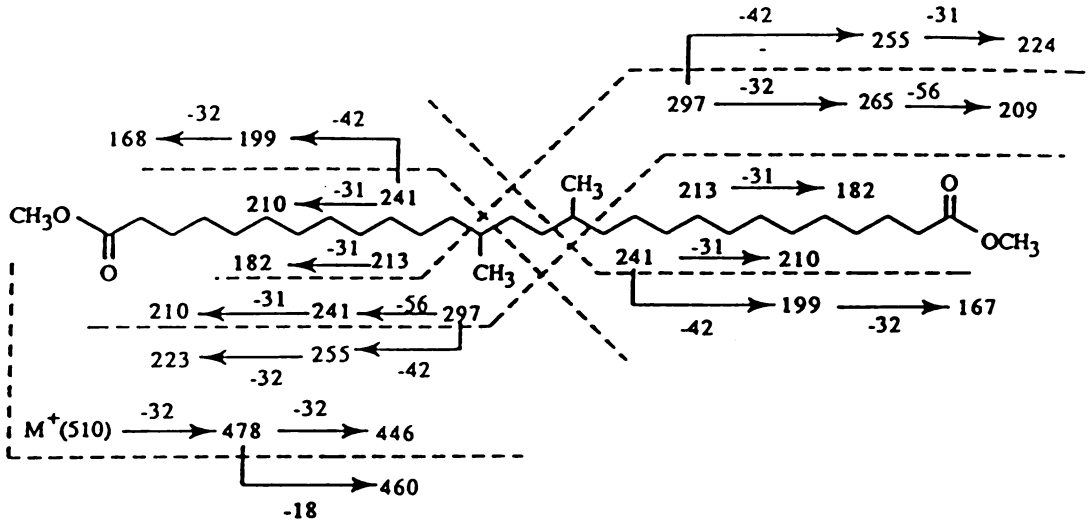
-42
255
-31
224
297
-32
265
-56
209
-32
168
199
-42
CH3
213
-31
182
O
OCH3
210
-31
241
CH3O
O
182
-31
213
CH3
241
-31
210
210
-31
241
-56
297
199
167
-42
-32
223
255
-32
-42
M+(510)
-32
478
-32
446
460
-18

B

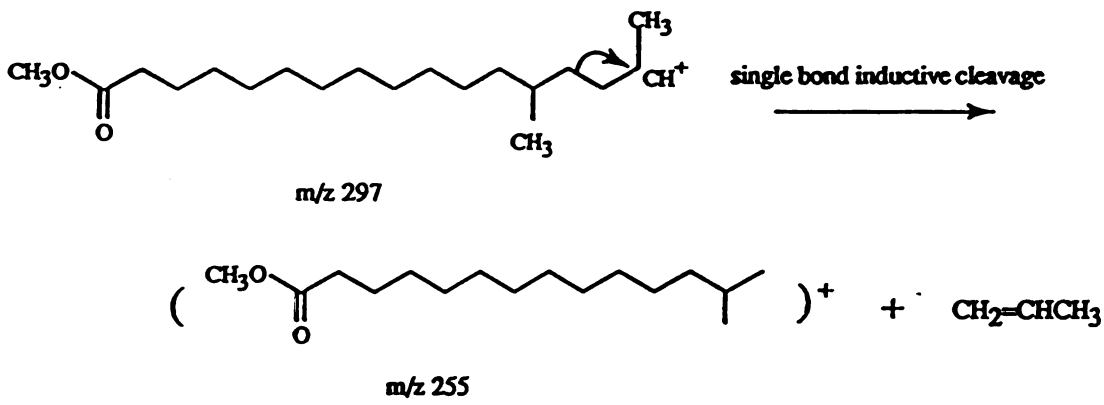
CH3
CH3O
CH+
single bond inductive cleavage
O
CH3
m/z 297
CH3O
O
)+
+
CH2=CHCH3
m/z 255

Figure 3

methanol/HCl solution (to produce the trideuterated methyl ester). The most striking change was the shift of molecular ion by 6 mass units confirming the presence of two methoxy groups. Two trideuterio-methanol (CD_3OH) losses from the molecular ion (516 m/z) to give ions at m/z 481 and 446 were also observed. The ions at m/z 258 ($CD_3OCO(CH_2)_{11}$ $CH(CH_3)CH_2$) and 300 ($CD_3OCO(CH_2)_{11}CH(CH_3)CH_2CH_2$ $CH(CH_3)$) corresponded to deuterated m/z 255 ($CH_3OCO(CH_2)_{11}CH(CH_3)CH_2$) and 297 ($CH_3OCO(CH_2)_{11}CH$ $(CH_3)CH_2CH_2CH$ (CH_3)), respectively. Figure 3A and Table 1 explains the origins of most other ionic fragmentation products.

NMR / FTIR Analyses of C_{30} - Dicarboxylic Dimethyl Ester

The ^1H NMR spectrum (Figure 4A) of peak **B** contained signals at 0.83 and 1.25 ppm characteristic of the methyl and methylene groups, respectively of the long chain fatty acyl components. Ester methoxy groups (CH_3O-) were assigned to a singlet at δ 3.65. The correlation of the peaks in the region between 0 and 2.6 ppm was investigated by 2D NMR (DQF COSY) spectroscopy (Figure 5). Correlation analysis showed the relationship between peaks such as peak A with D, peak D with A and B, peak E with F and C and peak C with B and E (Figure 4). The doublet at 0.83 ppm (J=6.3Hz) was assigned to the branched methyl groups of the fatty acyl chain. Resonance at δ 1.61 were assigned to the protons of the β-carbons of the molecule. Resonance at δ 2.30 (t, J=7.5Hz) was assigned to the methylene function α to the carbonyl group ($-CH_2-CO$). The ^{13}C NMR spectrum (Figure 4B) showed the ester carbonyl carbon at δ 174.2, methoxy carbon at δ 50.9, and branching methyl carbons at δ 19.2. Moreover, all these resonances were present as singlets, indicating magnetic equivalence due to molecular symmetry. In order to confirm the number of branched methyl carbons, DEPT (Distortionless Enhancement by Polarization Transfer) experiments were performed (16). Figure 7 shows the DEPT spectrum after making all signals positive. All 32 carbons (16 pairs) were assigned by this analysis. The presence of a signal for one methine carbon

Table 1. Analysis of electron impact mass spectral fragments of peak B

Structure of ionic fragments	mass(m/z)	deuteriated mass(m/z)
$CH_3OCO(CH_2)_{11}CH(CH_3)CH_2CH_2(CH_3)CH(CH_2)_{11}OCOCH_3$	510	516
$CH_3OCO(CH_2)_{11}CH(CH_3)CH_2CH_2(CH_3)CH(CH_2)_{10}CH=CO$	478	481
$CO=CH(CH_2)_{10}CH(CH_3)CH_2CH_2(CH_3)CH(CH_2)_{10}CH=CO$	446	446
478 - 18 (H_2O)	460	463
$CH_3OCO(CH_2)_{11}CH(CH_3)CH_2CH_2CH(CH_3)$	297	300
$CO=CH(CH_2)_{10}CH(CH_3)CH_2CH_2CH(CH_3)$	265	268
$CH_3OCO(CH_2)_{11}CH(CH_3)CH_2$	255	258
$CH_3OCO(CH_2)_{11}CH(CH_3)$	241	244
$OC(CH_2)_{11}CH(CH_3)CH_2$	224	224
$CH_3OCO(CH_2)_{11}$	213	216
$OC(CH_2)_{11}$	182	182
$CH_3OC(OH)=CH_2$	74	77
$CH_3OCO(CH_2)_n$; n=1~13	73 + 14*n	76 + 14*n
$CO=CH(CH_2)_n$: n=1~13	55+14*n	55+14*n
$CH_3-(CH_2)_n$: n= 3~12	57+14*n	57+14*n
$CH_2=CH-(CH_2)n$; n=2~11	55+14*n	55+14*n

Figure 4. ^{1}H and ^{13}C NMR spectrum of peak B. (A) ^{1}H NMR spectrum of peak B It contained signals at 0.83 ppm (d, J=8.3Hz) and 1.25 ppm characteristic of the methyl and methylene groups of long chain acyl components. Resonance at 2.30 ppm (t, J=7.5Hz) and at 3.65 ppm (s) represented methylene groups of α to the carbonyl and ester methoxy group, respectively. The multiplets at 1.61 ppm was assigned to the protons of the β carbons of a molecule. The signal at δ 7.24 was assigned to the chloroform. (B) The 125 MHz ^{13}C NMR spectrum of peak B. The presence of a methyl ester and branching methyl group are confirmed by signals at 50.9 and 19.2 ppm respectively. The signal at 174.2 ppm was assigned to the carbonyl carbon of the ester group.

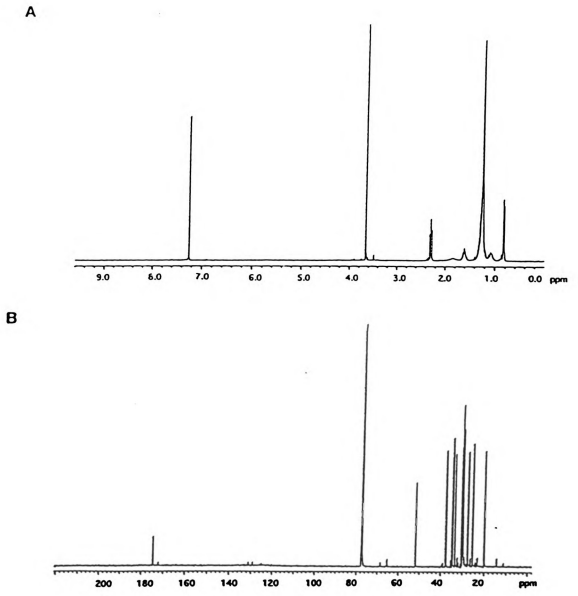
A
9.0
8.0
7.0
6.0
5.0
4.0
3.0
2.0
1.0
0.0
ppm
B
200
180
160
140
120
100
80
60
40
20
ppm

Figure 4

Figure 5 The DQF-COSY spectrum (in the region between 0 to 2.6 ppm) of peak B, in $CDCl_3$ at 500MHz. Correlation analysis showed the relationship among the peaks such as peak A with D, peak D with A and B, peak E with F and C and peak C with B and E (Figure 6). The doublet at 0.83 ppm (J=6.3Hz) was assigned to the branched methyl groups of the fatty acyl chains and resonance at δ 1.61 as the protons of the β-carbons of the molecule. Resonance at δ 2.30 (t, J=7.5Hz) was assigned to the methylene groups α to the carbonyl group ($-CH_2-CO$).

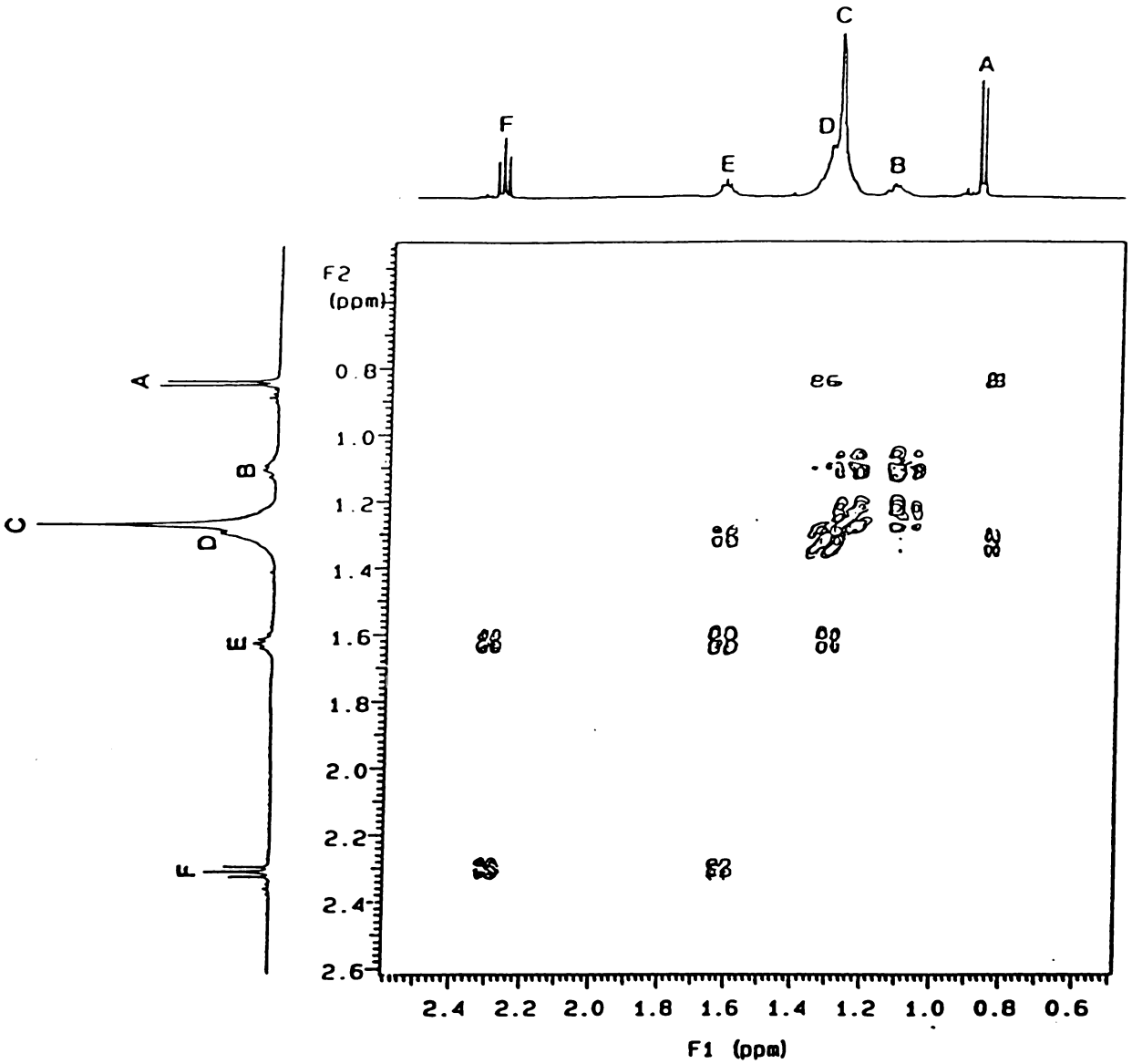
C
A
F
D
E
B
F2
(ppm)
A
B
C
D
E
F
0.8
1.0
1.2
1.4
1.6
1.8
2.0
2.2
2.4
2.6
2.4 2.2 2.0 1.8 1.6 1.4 1.2 1.0 0.8 0.6
F1 (ppm)

Figure 5

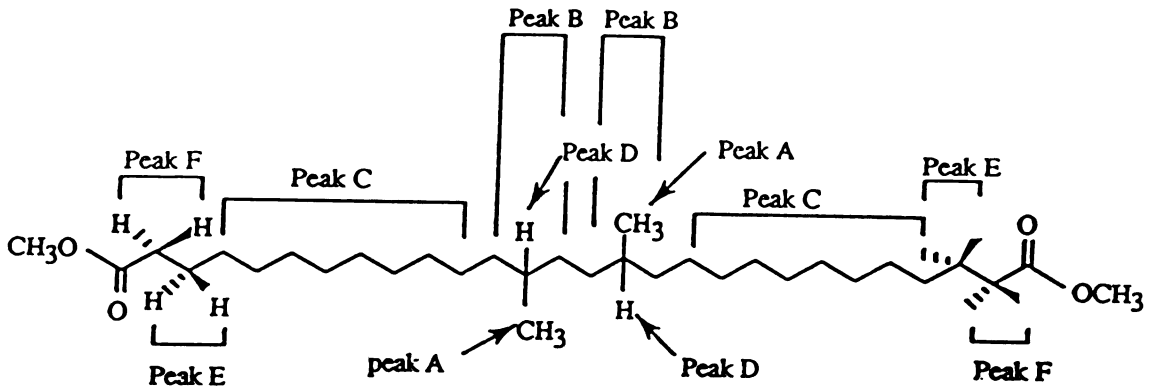

Figure 6. The correlation analysis of DQF-COSY spectrum of peak B.

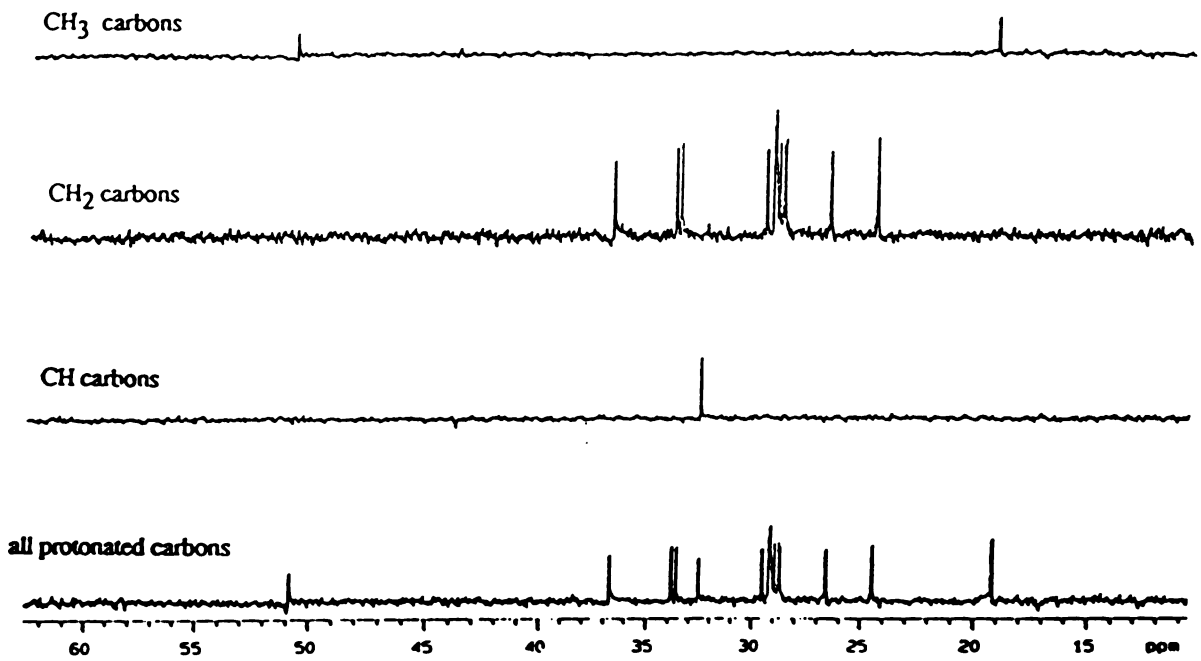

Figure 7. DEPT spectrum of peak B in $CDCl_3$ after making all peaks positive. The presence of one methine carbon (CH) and two methyl carbons (CH_3) confirmed the 2 branched methyl groups and two methoxy groups in the structure.

(CH) confirmed the presence of the 2 branching methyl groups in the structure. Figure 8 shows a FTIR spectrum. It contains very strong signals for methylene asymmetrical stretching at 2928 cm^{-1} and symmetrical stretching at 2856 cm^{-1}. The asymmetric stretching of methyl groups occur at 3017 cm^{-1}. The symmetric bending vibration of methyl groups appear at 1378 cm^{-1} and asymmetric bending at 1458 cm^{-1}. The absorption band at 1378 cm^{-1} arises from the asymmetrical bending of the methyl C-H bonds. The scissoring band of the methylene groups occur at 1463 cm^{-1}. The methylene twisting and wagging vibrations occur at 1119 - 1378 cm^{-1}. The characteristic C=O absorption band of the aliphatic ester group appeared at 1733 cm^{-1}. There was no evidence for alky chain unsaturation in the molecular structure.

Mass Spectrometric Analyses of C_{29}, C_{31} and C_{32} Dicarboxylic Dimethyl Esters

Figure 9. shows the electron impact (70eV) mass spectrum of peak A. Major ions appear at m/z 496, 464 and 432. These corresponded to the molecular ion of a C_{29}-α,ω-dicarboxylic dimethyl ester (M^+) with the sequential losses of two methanol (CH_3OH). The major ion m/z 281 represents the structure obtained by the loss of one hydrogen molecule on the secondary cations at m/z 283. The ion m/z 255 was assigned to the loss of propene(CH_2=$CHCH_3$) from the ion at m/z 297 by way of a single bond inductive cleavage mechanism (17). The ion at m/z 241 was similarly assigned to the loss of propene (CH_2=$CHCH_3$) from the secondary cationic fragment at m/z 283. The characteristic McLafferty fragment ion at m/z 74 ($CH_3OC(OH)$=CH_2) was also detected. Figure 9B shows the electron impact mass spectrum of the deuterium-labeled molecule obtained by methanolysis with D-4 methanol/HCl solution to produce the trideutrated methyl ester. The most striking change was the shift of the molecular ion by 6 mass units, which confirmed the presence of two methoxy groups in the molecule. The loss of two molecules of trideuterio-methanol (CD_3OH) from the molecular ion (502 m/z) to give ions at m/z 467

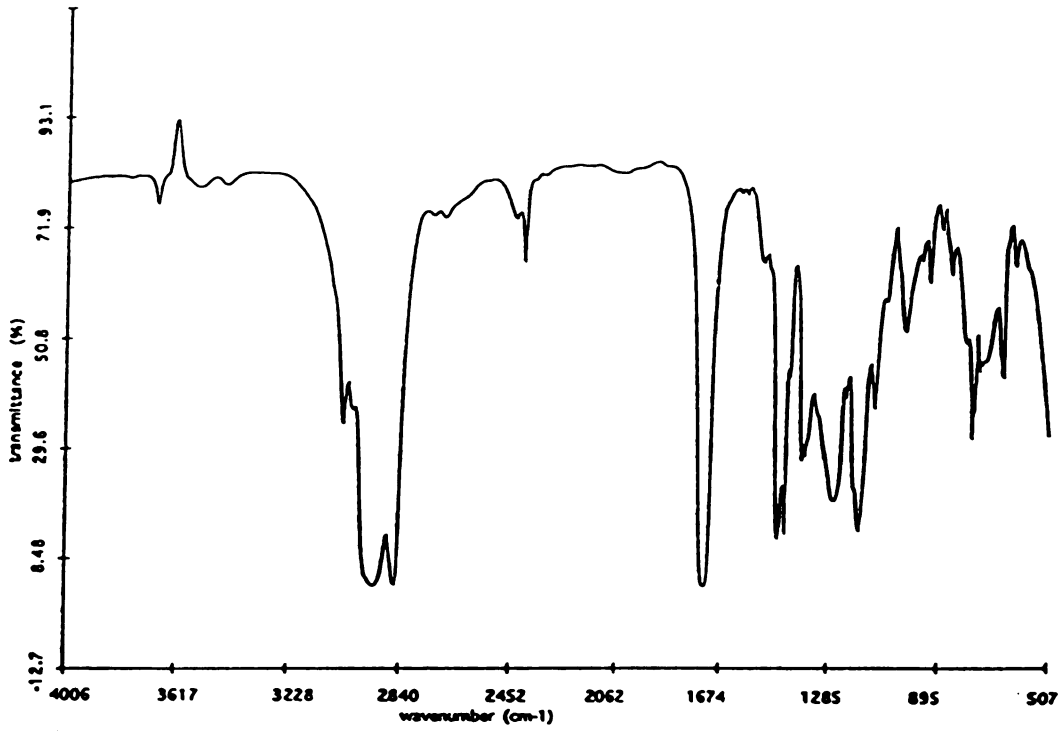

Figure 8. Fourier Transform Infrared spectrum of peak B. It shows strong methylene stretching at 2856 cm^{-1} (symmetrical), 2928 cm^{-1}(asymmetrical). The bending vibrations of the C-H bonds in the methylene group occurred around 1463 cm^{-1} (scissoring) and 1119-1378 cm^{-1} (twisting and wagging). The characteristic C=O absorption band of the aliphatic ester group at 1733 cm^{-1}. There was no evidence of unsaturation or of oxygen combined in hydroxy or simple ether linkages.

Figure 9. Electron impact mass spectrum (70ev) of peak A without (A) and with isotope labeling (B). (A) EI spectrum contained major ions at m/z 496, 464 and 432. These corresponded to the molecular ion (M^+) with the sequential losses of two methanol molecules. The characteristic McLafferty fragment of aliphatic esters appears at 74 (m/z). (B) It shows the EI spectrum of deuterium labeled molecules obtained by deuteration with D-4 methanolic-HCl solution. The presence of two carboxylic and two branching groups was confirmed by isotope labeling.

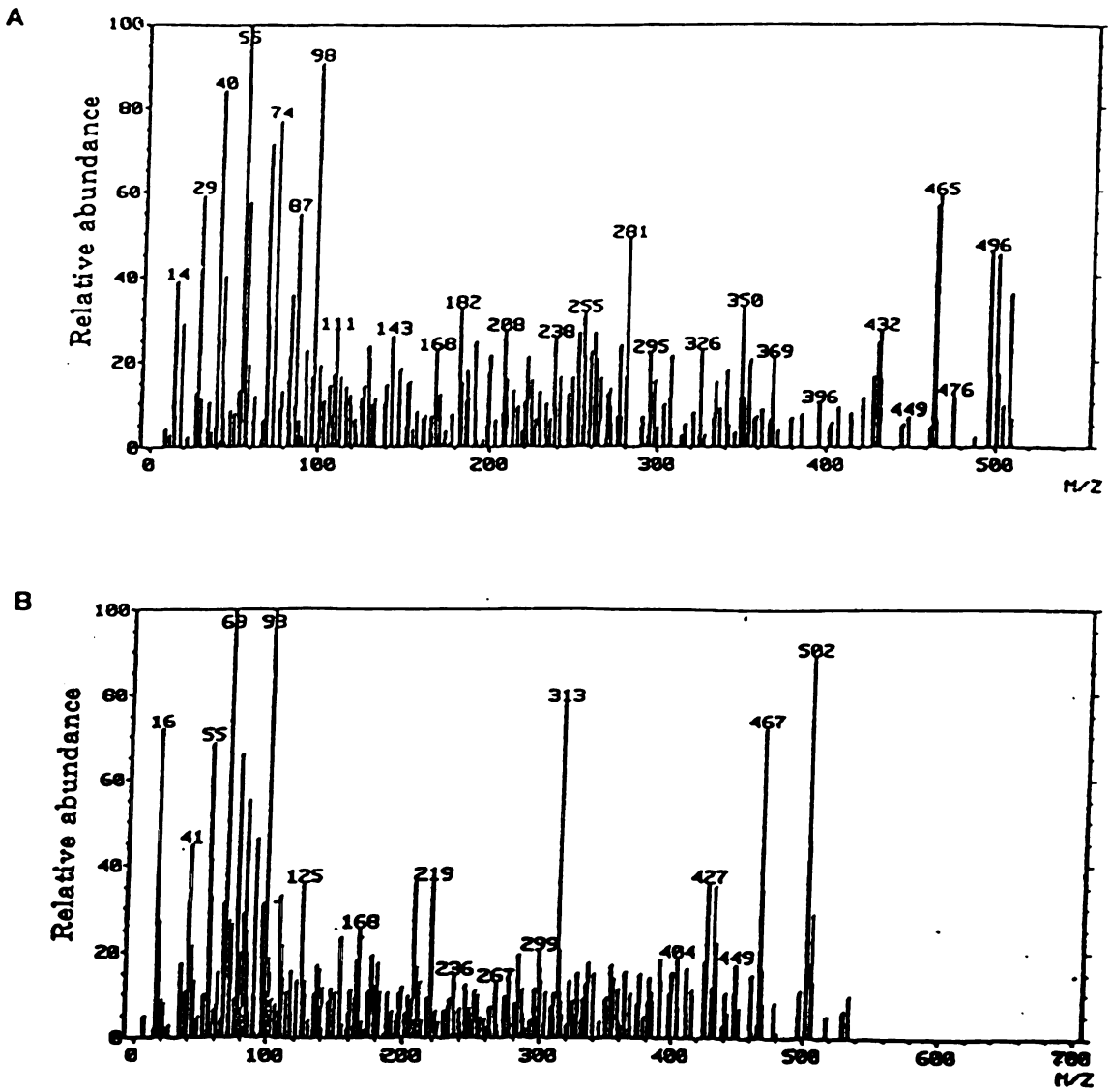
A
Relative abundance
100
80
60
40
20
0
0
100
200
300
400
500
M/Z
14
29
40
55
74
87
98
111
143
168
182
208
238
255
281
295
326
350
369
396
432
449
465
476
496
B
Relative abundance
100
80
60
40
20
0
0
100
200
300
400
500
600
700
M/Z
16
41
55
69
93
125
168
219
236
267
299
313
404
427
449
467
502

Figure 9

and 432 was also observed. Figure 10. shows most of the other fragments and their origin. Figure 11A. shows the electron impact mass spectrum of peak C. Major ions appeared at m/z 524, 492 and 461. These correspond to the molecular ion of a C_{31}-α,ω-dicarboxylicacid dimethyl ester (M^+) with the sequential losses of methanol (CH_3OH) and a methoxy (CH_3O) group, respectively. The major ion at m/z 478 and 447 corresponded to the sequential loss of methanol and methoxy groups, respectively from the second cationic fragment at m/z 509. The ion at /mz 509 is due to the loss of a methyl group from the molecular ion (M^+). The major ion m/z 311 represents the structure obtained by fragmentation of the alkyl chain to generate secondary cations . The ion m/z 269 was assigned to the loss of propene (CH_2=$CHCH_3$) from the ion m/z 311 by way of single bond inductive cleavage mechanism . The strong peak at m/z 255 corresponds to the loss of propene (CH_2=$CHCH_3$) from the ion at m/z 297. The characteristic McLafferty fragment ion at m/z 74 ($CH_3OC(OH)$=CH_2) was also detected. Figure 11B shows the electron impact mass spectrum of the deuterium-labeled molecule obtained by methanolysis with D-4 methanol/HCl solution (to produce the trideuterated methyl ester). The most striking change was again the shift of the molecular ion by 6 mass units, confirming the presence of two trideuterio-methyl groups. Loss of two molecules of CD_3OH from the molecular ion (530 m/z) to give ions at m/z 495 and 447 was also observed. Figure 12 shows the origin of the other fragmentation products.

The electron impact mass spectrum of peak D is shown in Figure 13A. Major ions appeared at m/z 538, 506 and 475. These correspond to the molecular ion of a C_{32}-α,ω-dicarboxylic dimethyl ester (M^+) with the sequential losses of methanol (CH_3OH) and a methoxy (CH_3O) group, respectively. The ions at m/z 297 and 325 arise from fragmentation of the alkyl chain to form secondary cations. The ion at m/z 265 was assigned to the loss of methanol (CH_3OH) from the one at m/z 297. The ion at m/z 294 was assigned to the loss of a methoxy group from the secondary cation at m/z 325. The strong peak at m/z 255 corresponded to the loss of propene (CH_2=$CHCH_3$) from the ion

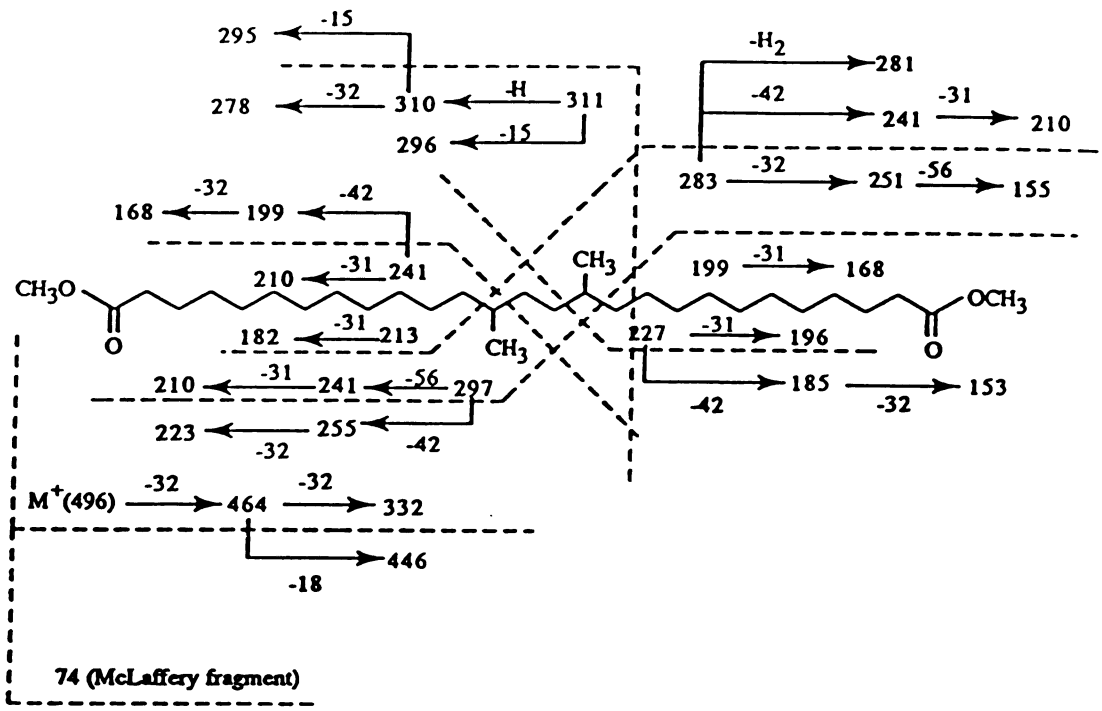

Figure 10. Mass fragmentation pattern of peak A. 15: methyl, 18: water, 31: methoxy, 32: methanol, 42: propene, 56: butane, 74: McLafferty fragment

Figure 11.Electron impact mass spectrum (70ev) of peak C without (A) and with isotope labeling (B). (A) EI spectrum contained major ions at m/z 524, 492 and 461. These corresponded to the molecular ion (M^+) with the sequential losses of methanol and a methoxy group, respectively. The major ion at m/z 478 was due to the loss of a methoxy group from the fragment at m/z 509 which was produced after the loss of methyl group from the molecular ion (M^+). Another major ion at m/z 446 was due to the loss of methanol from the ionic fragment at m/z 478. The characteristic McLafferty fragment of aliphatic ester appears at 74 (m/z). (B) It shows the EI spectrum of deuterium labeled molecules obtained by deuteration with D-4 methanolic-HCl solution. The presence of two carboxylic and two branching groups was confirmed by isotope labeling.

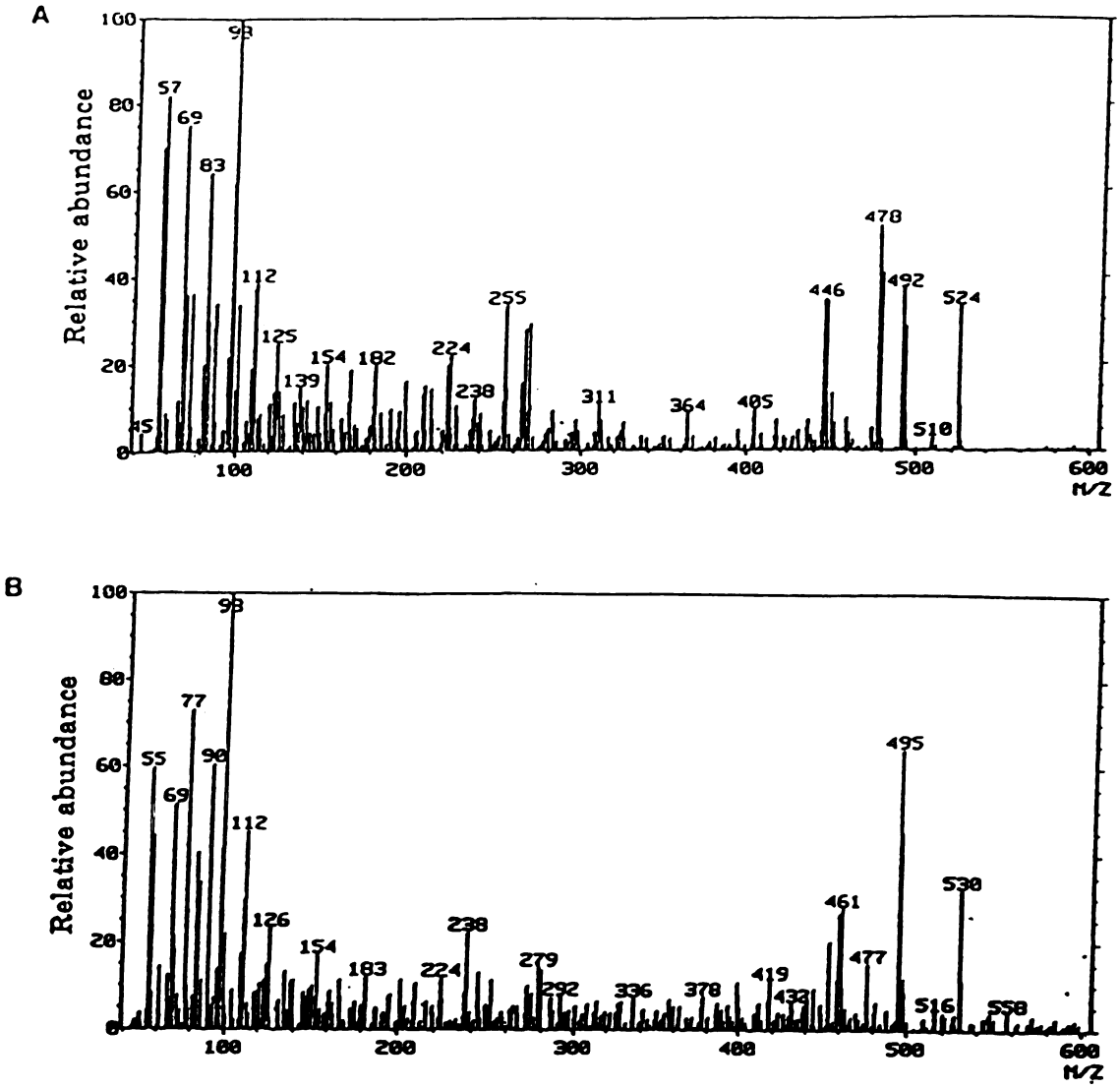
A
Relative abundance
100
80
60
40
20
0
98
57
69
83
112
125
139
154
182
224
238
255
311
364
405
446
478
492
524
510
15
100
200
300
400
500
600
M/Z
B
Relative abundance
100
80
60
40
20
0
98
77
55
90
69
112
126
154
183
224
238
279
292
336
378
419
433
461
477
495
530
516
558
100
200
300
400
500
600
M/Z

Figure 11

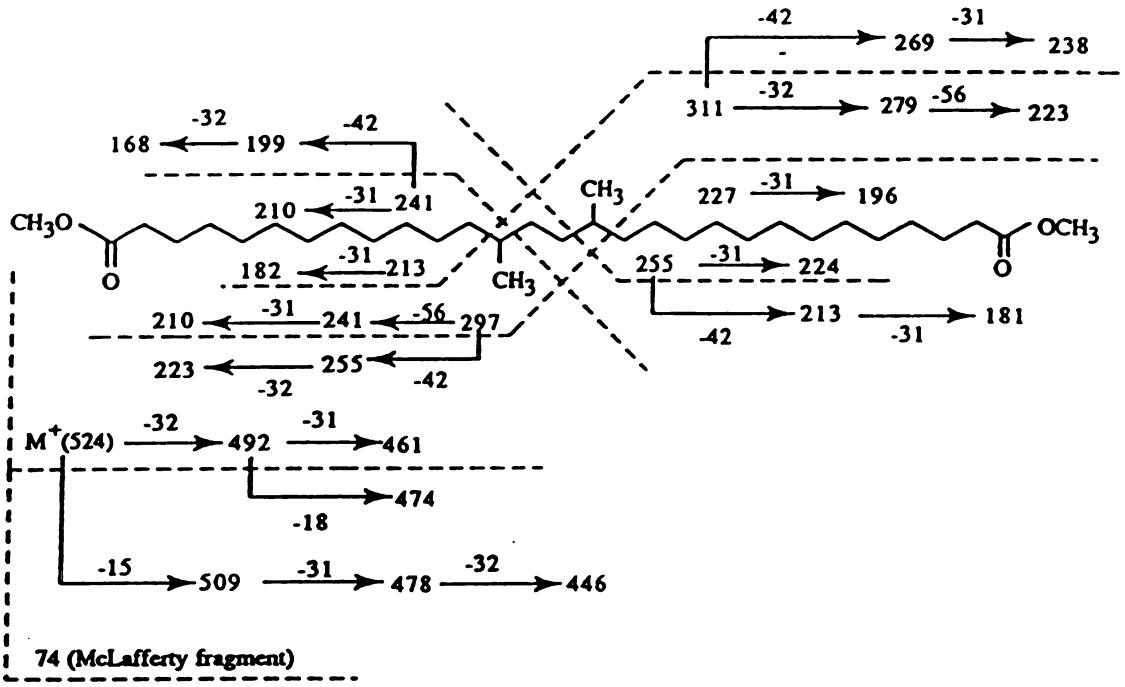

Figure 12. Mass fragmentation pattern of peak C. 15: methyl, 18: water, 31: methoxy, 32:methanol, 42: propene, 56:butane, 74: McLafferty fragment

Figure 13. Electron impact mass spectrum of peak D without (A) and with isotope labeling (B). (A) EI spectrum contained major ions at m/z 538, 506 and 475. These corresponded to molecular ion (M^+) with the sequential losses of methanol and a methoxy group respectively. The ions at m/z 255 and 283 are due to the single bond inductive cleavage of the major fragment ions at m/z 297 and 325, respectively. (B) It shows the EI spectrum of deuterium labeled molecules obtained by deuteration with D-4 methanolic-HCl solution. The presence of two carboxylic and two branching methyl groups was confirmed by isotope labeling.

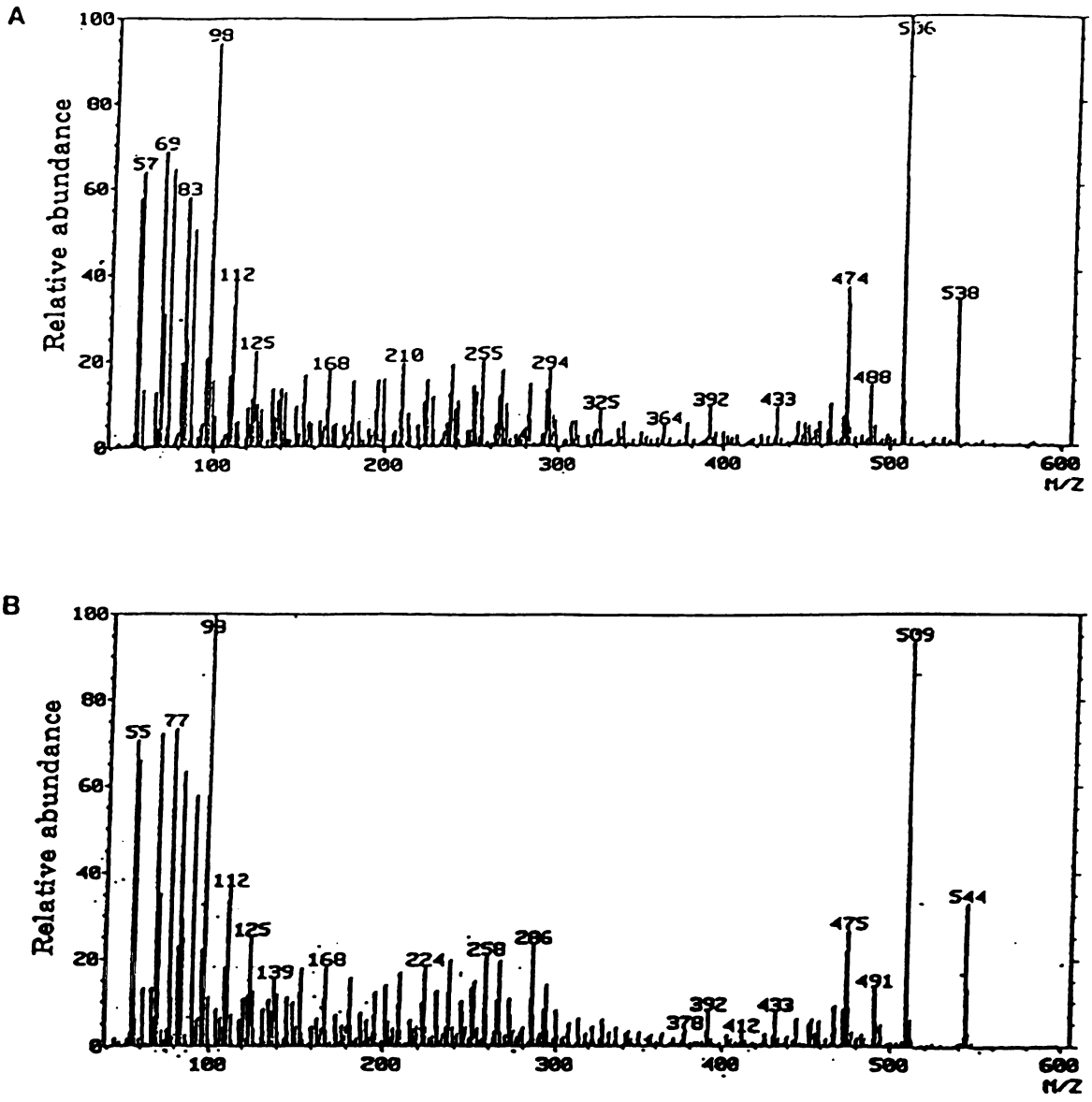
A
Relative abundance
100
80
60
40
20
0
98
69
57
83
112
125
168
210
255
294
325
364
392
433
474
488
506
538
100
200
300
400
500
600
M/Z
B
Relative abundance
100
80
60
40
20
0
98
55
77
112
125
139
168
224
258
286
378
392
412
433
475
491
509
544
100
200
300
400
500
600
M/Z

Figure 13

m/z 297 by way of a single bond inductive cleavage mechanism. The ion at m/z 283 was similarly assigned to the loss of propene (CH_2=$CHCH_3$) from the secondary cationic fragment at m/z 325. The characteristic McLafferty fragment ion at m/z 74 ($CH_3OC(OH)$=CH_2) was also evident. Figure 13B shows the electron impact mass spectrum of the deuterium-labeled molecule obtained by methanolysis with the D-4 methanol/HCl solution to produce the trideuterated methyl ester. The shift of the molecular ion by 6 mass units confirms the presence of two methoxy groups. Loss of two molecules of trideuterio-methanol (CD_3OH) from the molecular ion (544 m/z) to give ions at m/z 509 and 475 was also evident. The ions at m/z 258 ($CD_3OCO(CH_2)_{11}$ $CH(CH_3)CH_2$) and 286 ($CD_3OCO(CH_2)_{13}CH(CH_3)CH_2$) correspond to deuterated forms of m/z 255 ($CH_3OCO(CH_2)_{11}CH(CH_3)CH_2$) and 283 ($CH_3OCO(CH_2)_{13}CH$ $(CH_3)CH_2$), respectively. The other fragmentation products are shown in Figure 14. Figure 15 shows the structures of the members of the new family of α,ω-dicarboxylic acids in *Cl. thermohydrosulfuricum*. They are α,ω-13,16-dimethylheptacosanedioate dimethyl ester (C29) α,ω-13,16-dimethyloctacosane dimethyl ester (C30), α,ω-13,16-dimethylnona cosanedimethyl ester (C31) and α,ω-13,16-dimethyltriacotane dimethyl ester (C32).

The General Significance of These α,ω-Dicaboxylic Acyl Components

A recent study of the membrane of a strict anaerobic, facultative acidophilic eubacterium, *Sarcina ventriculi* demonstrated that α,ω-dicarboxylic fatty acyl components are synthesized as a general response to the perturbation of the membrane structure by the addition of exogenous organic solvents or increasing temperature (8). Interestingly, the membrane of *Clostridium thermohydrosulfuricum* contains similar α,ω-dicarboxylic fatty acyl components to those formed in*S. ventriculi*. The critical difference is the position of internal methyl branches. It appears the synthetic mechanism of formation of α,ω-dicarboxylic fatty acyl components is similar to that found in *S. ventriculi*. The proposed mechanism is by way of tail-to-tail (ω-1) coupling of the lipid bilayer across from the

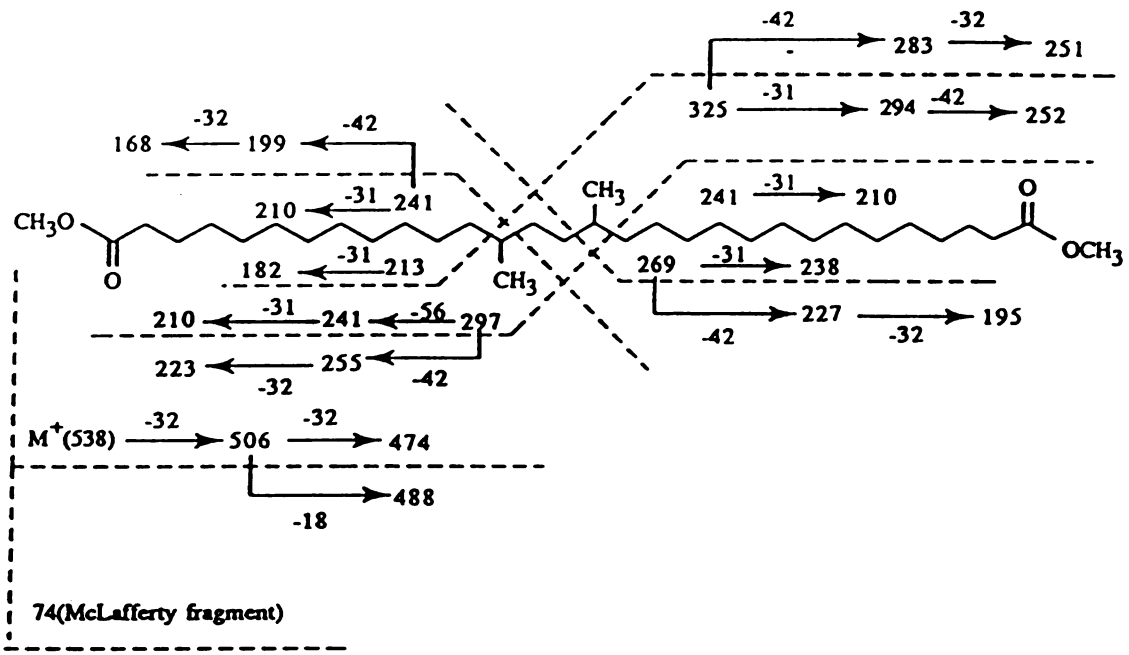

Figure 14. Mass fragmentation pattern of peak D. 15: methyl, 18: water, 31: methoxy, 32: methanol, 42: propene, 56: butane, 74: McLafferty fragment

opposite sides of the membrane. The difference in the position of internal methyl branches can be easily rationalized if one considers the fact that there are predominantly *iso*-branched regular fatty acids in this organism. Figure 15 shows the possible correlation between the α,ω–dicarboxylic acids and the regular fatty acids. The most abundant regular chain fatty acid in *Cl. thermohydrosulfuricum* is the *iso*-pentadecanoic acid. This fatty acid could be used as a general frame for the coupling step (ω-coupling) to synthesize the α,ω–dicarboxylic acids. The family of archaebacteria that can easily grow at extremely high thermal condition (more than 100°C) provides an interesting analogy. These organisms contain the diether lipid as well as tetraether lipid groups in their membranes The tetraether lipids are thought to be made by way of the tail-to-tail coupling mechanism (10,11,12). The fact that *Cl. thermohydrosulfuricum* or *S. ventriculi* are eubacteria strongly supports the idea that the tail-to-tail coupling mechanism of the membrane lipids is very general throughout the bacterial kingdom.

Figure 15. The determined structures of a family of very long chain α,ω-dicarboxylic dimethyl esters. A: α,ω-13,16-dimethylheptacosanedioate dimethyl ester (C29) B: α,ω-13,16-dimethyloctacosane dimethyl ester (C30), C: α,ω-13,16-dimethylnonacosane dimethyl ester (C31), D: α,ω-13,16-dimethyltriacotane dimethyl ester (C32) All assigned α,ω-dicarboxylic acids could be constructed by ω-coupling of opposite fatty acyl groups of the membrane.

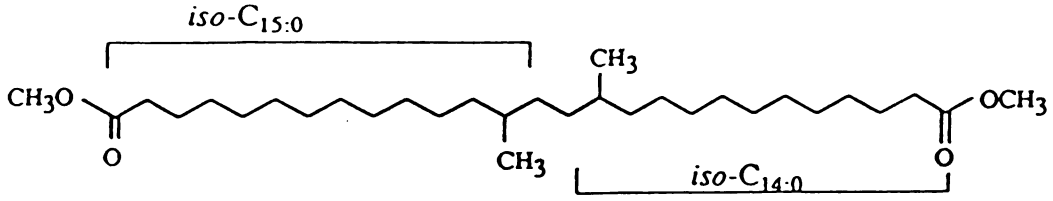

A

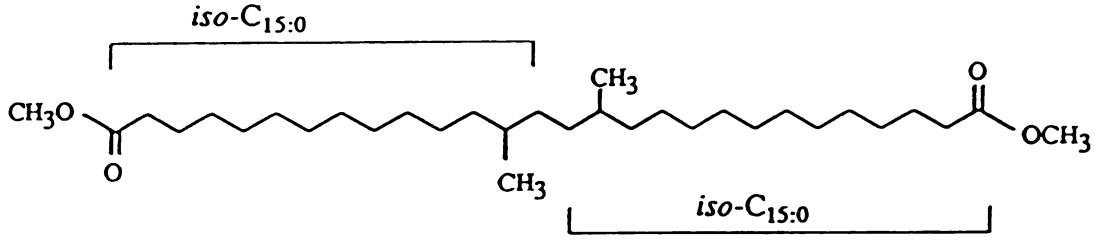

B

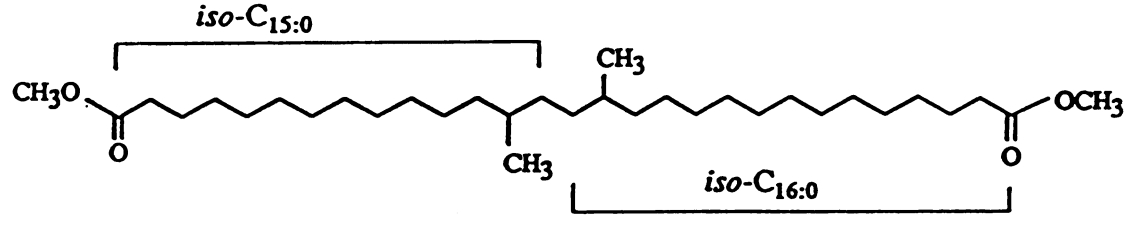

C

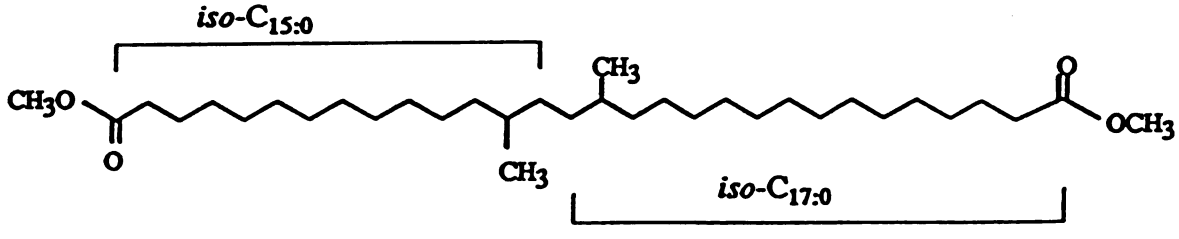

D

Figure 15

CONCLUSIONS

A new family of α,ω-dicarboxylic, very long chain fatty acids was isolated and characterized from the lipids of thermophilic anaerobic eubacterium, *Clostridium thermohydrosulfuricum*. After the isolation of the membrane, the fatty acyl components were released by converting them to their methyl ester forms by acid-catalyzed methanolysis. The esterified fatty acyl components were purified by a variety of chromatographic techniques and analyzed by GC and GC/MS. One of the isolated, esterified, α,ω-dicarboxylic, very long chain fatty acids was characterized by mass spectrometry, ^{1}H NMR and ^{13}C NMR spectroscopy and Fourier transform infrared spectroscopy. NMR experiments employed included double quantum filtered correlated spectroscopy (DQF-COSY) to assign proton spin-spin coupling and polarization transfers (DEPT) to measure the multiplicity of carbon signals split by protons. The other components were identified by mass spectrometry. The new long chain fatty acid methyl esters are α,ω-13,16-dimethylheptacosanedioate dimethyl ester (C_{29}), α,ω-13,16-dimethyloctacosane dimethyl ester (C_{30}), α,ω-13,16-dimethylnonacosanedimethyl ester (C_{31}) and α,ω-13,16-dimethyltriacotane dimethyl ester (C_{32}). This family of α,ω-dicarboxylic fatty acids accounts for about 40 % of fatty acyl components of the membrane of *Clostridium thermohydrosulfuricum*. Interestingly almost all (>90%) of the very long chain, α,ω-dicarboxylic fatty acid was α,ω-13,16-dimethyloctacosanedioic acid. A careful study of the structures of the family of α,ω-dicarboxylic acids indicated that the synthetic mechanism for their formation involves the tail-to-tail (ω) coupling of regular *iso*-branched fatty acids across opposite sides of the membrane bilayer.

REFERENCES

1. Lovitt. R. W, Longin, R., and Zeikus, J. G. (1984) *Appl. Environ. Microbiol.* **48**, 171-177
2. Silvius, J. R., and McElhaney, R. N. (1979) *Chem. Phys. Lipids* **24**, 287-296
3. Silvius, J. R., and McElhaney, R. N. (1980) *Chem. Phys. Lipids* **26**, 67-77
4. Kannenberg, E., Blume, A., McElhaney, R. N. and Poralla, K. (1983) *Biochim. Biophys. Acta* **733**, 111-116
5. Silvius, J. R., Mak, N., and McElhaney, R. N. (1980) in *Membrane Fluidity* (Kates, H, and Kuksis, A., Eds.) pp 213-222, Humana Press, Clifton, N.J.
6. Sinensky, M. (1974) *Proc. Natl. Acad. Sci.* USA **71**, 522-525
7. Okuyama, H., Fukunaga, N., and Sasaki, S. (1986) *J. Gen. Appl. Microbiol.* **32**, 473-482
8. Jung, S., Lowe E.S., Hollingsworth I. R., and Zeikus, J. G. (1993) *J. Biol. Chem.* **268**, 2828-2835
9. Chan, M., Himes, R. H., and Akagi, J. M. (1971) *J. Bacteriol.* **106**, 876-881
10. Langworthy, T. A. (1982) *Curr. Top. Membr. Transp.* **17**, 45-77
11. Langworthy, T. A. (1977) *Biochim. Biophys. Acta* **487**, 37-50
12. Ross, H. N. M., Collins, M. D., Tindall, B. J., Grandt, W.D. (1981) *J. Gen. Microbiol.* **123**, 75-80
13. Zeikus, J. G., Ben-Bassat, A., and Hegge, P. W. (1980) *J. Bacteriol.* **143**, 432-440
14. Still, W.C., Kahn, M., and Mitia, A. (1978) *J. Org. Chem.* **43**, 2923-2926
15. Rance, M., Sorensen, O. W., Bodenhausen, G., Wagner, G., Ernst, R. R. and K. Wuthrich (1983) *Biochem, Biophys. Res. Commun.* **113**, 967-974
16. Derome, A. E. (1988) In *Modern NMR Techniques for Chemistry Research* (Baldwin, J. E. ed.) pp 143-151, Pergamon Press, New York
17. McLafferty, F. W. (1980) In *INTERPRETATION OF MASS SPECTRA* (Turro, N. J. ed.) pp141-146, University Scirnce Books, California

18. Salem, L. (1962) *Can. J. Biochem. and Physiol.* **40**, 1287-1298

19. Langworthy, T. L. (1985) in *The Bacteria* (Woese, C.R, and Wolfe, R. S. eds.) p459 , Academic Press, New York

20. De Rosa, M., Gambacorta, B., and Nicolaus, B. (1980) *Phytochemistry* **19**, pp791-795

CHAPTER VII

COMPUTATIONAL STUDIES ON THE EFFECT OF THE TRANSMEMBRANE ALKYL CHAINS ON THE STRUCTURE AND DYNAMICS OF MEMBRANE

INTRODUCTION

Our research on the structural transition of membrane from the bilayer to a bipolar monolayer form via ω-1 or ω-linked acyl chains raises interesting questions about the physiological role for this phenomenon (1, 2, 3). In *Sarcina ventriculi* this phenomenon was responsible for the general adaptive response to the various forms of environmental stress such as increasing the growth temperature, the addition of exogenous solvents and lowering the pH (1).

Elevated temperature as well as the addition of the alcoholic solvents increased the freedom of motion of the lipids. The reported adaptive response to this is to regulate the fluidity of the membrane by changing the relative amounts of unsaturation of the acyl chains or by increasing chain length of the acyl groups by 2 or 4 carbons (4, 5, 6). The presence of very long bifunctional lipids in the membrane of *S. ventriculi* could have arisen by coupling the tails of fatty acids of membrane lipids from the same side of the bilayer. This, incidently, was ruled out by freeze-fracture studies which demonstrated that the leaflets could not be separated and that therefore the very long chain fatty acids were transmembrane (Figure 1).

Our important question which arises from this research is what is the effect of transmembrane lipids on membrane fluidity and dynamics. Membrane fluidity studies are usually performed with spin probes using electron paramagnetic resonance spectroscopy (7, 8). One critical disadvantage of this method is that probe molecules might change the local fluidity of the system.

The theoretical and computational methods offer tremendous insight into molecular processes and make real-time simulation possible. Molecular mechanics and molecular dynamics simulation techniques have proven to be especially suited to the study of biological macromolecules and their assemblies. This is very evident from the vast

Figure 1. Electron micrograph of *S. ventriculi* cells grown at pH 7.0 (A) and at pH 3.0 (B) after freeze fracturing and coating. (A) Note the concave/convex surfaces (arrows) characteristic of fracture between bilayer leaflets. (B) Note that cleavage through the cytoplasm is the only form of cleavage observed.

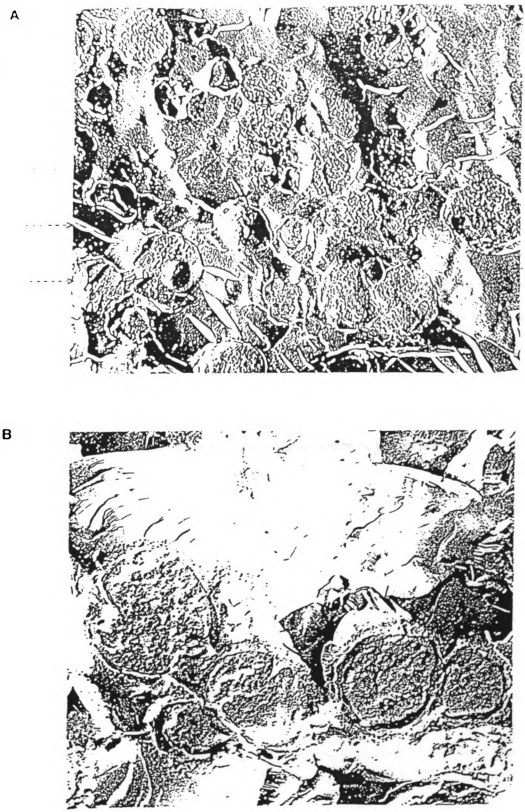

Figure 1

amount of work done on the proteins, nucleic acids and lipids during the last decades (9,10,11,12). These techniques were used for studying the effects of transmembrane alkyl species on membrane structure and dynamics. RMS (Root Mean Square) distance and specific angle fluctuation were investigated for alkyl chain atoms and bonds respectively.

Three different systems were studied. Firstly, a molecular dynamics simulation (10ps) of two free, opposed, unconnected hydrocarbon chains (bilayer form) was performed. The simulation was repeated after coupling the ends of chains (linked monolayer form). Secondly, 10 ps dynamic simulation was also performed for two opposed, unconnected and two connected phospholipid molecules with fixed headgroups. The third system studied was an array of phospholipids (phosphatidyl cholines, *sn*-1 for $C_{18:0}$, *sn*-2 for $C_{16:1}$) arranged in a bilayer membrane. Simulated annealing dynamics (13, 14) was used for the prediction of molecular geometry of the acyl chains before and after the transition of the bilayer to bipolar monolayer. In this case, 32 of the bilayer lipids (50 %) were changed to monolayer form by coupling only one alkyl chain to the opposing one cross the bilayer. Using results obtained from these studies, it was possible to rationalize the effects of transmembrane lipids on the structure of the membrane.

MODELS AND METHODS OF SIMULATION

Models for Simulations

For the simulation of free hydrocarbon chain, two octadecane (C_{18}) molecules were used . For the second model, two typical phosphatidyl choline lipids with *sn*-1 $C_{18:0}$ and *sn*-2 $C_{16:0}$ were used. For the membrane simulation, 64 phosphatidyl choline lipids with *sn*-1 $C_{18:0}$ and *sn*-2 $C_{16:1}$ were used. For the transition to the monolayer form, 50% of lipids were randomly connected across the bilayer at the ω-1 positions.

Force Fields for Energy Calculation

All molecular mechanics and dynamics calculations were performed under the Dreiding-II force filed (15). The forms of potential energy functions for bond stretching, angle bending and torsions are given as

$E_{bs} = 1/2k_{bs}(r-r_e)^2$ ---------- (a)

$E_{ab} = 1/2k_{ab}(\theta-\theta_e)^2$ ---------- (b)

and $E_{ijkl} = 1/2V_{jk}(1 - \cos[\mu_{jk}(\phi - \phi_e)^2]$ ---------- (c)

where k_{bs} and k_{ab} are the force constants for bond stretching and angle bending; r_e and θ_e are the equilibrium bond length and bond angle. E_{ijkl} represents the torsional interaction potential between two bonds ij and kl connected through a common bond jk. In eq. (c) ϕ is the dihedral angle (angle between ijk and jkl plane) V_{jk} is the rotational barrier. n_{jk} is the multiplicity and ϕ_e is the equilibrium value of the dihedral angle. The van der Waals interactions are represented through a 12-6 Lennard-Jones potential.

$E_{LJ} = D_o(\rho^{-12} - 2\rho^{-6})$ ---------- (d)

Where ρ is the radial distance scaled by van der Waals radius R_o, $\rho=R/R_o$ and D_o is the depth of the potential at minimum, R_o. The electrostatic interactions are calculated by using

$E_Q=332.0637Q_iQ_j/\varepsilon R_{ij}$ ---------- (e)

Where Q_i and Q_j are charges in electron units, R_{ij} is the distance in Angstroms. ε is the dielectric constant, and 332.0637 converts E_Q to kcal/mol. Interactions are not calculated between atoms bonded to each other (1, 2 interactions) or involved in angle terms (1, 3 interactions) since these are assumed to be contained in the bond and angle interaction. For charge calculation the Gasteiger estimates (16) were used. In calculating the non-bond interactions, a cut-off distance of 9.0 Å was used along with a switching function. Switching function smoothly reduces the interaction potential and forces to zero using on-distance at 8.0 Å and off-distance 8.5 Å. The force field parameters are kept as simple as possible.

Methods for Simulations

All molecular mechanics and dynamics calculations were performed using the BIOGRAF 3.0 software package (Molecular Simulations, Inc.) on a Silicon Graphics Iris 4D super-minicomputer. Initial constructed models were relaxed with 500 steps of conjugate gradient minimization methods (17) and relaxed with 500 steps of molecular dynamics, and reminimized with 5000 steps of conjugate gradients methods. The global minimum structure of the 64 lipids systems was obtained after the reminimization of the structures obtained by 5 cycles of annealed dynamic simulation with the initial 300K to 600K temperature program from the initial minimized structure. A 1 fs (10^{-15} s) time step was used in the integration for dynamic calculations. These minimized structures were used as the initial coordinates for the molecular dynamics calculations for 10 ps in the adiabatic conditions. The equations of motions in MD simulations were integrated with the Verlet algorithm (18). For the dynamic simulations of 2 lipids (second model), a point in the head group was fixed during the dynamics simulation. This is a reasonable assumption because the motional dynamics (translational diffusion) of the head group relative to the vibrational motions of the hydrocarbon chains is static over the relevant time scale (10 ps) (19).

RESULTS AND DISCUSSION

RMS Distance Fluctuation for Two Hydrocarbon Chain Model during 10 ps MD Simulations

Figure 2A shows the trajectory snapshots for every 0.5 ps at the dynamic simulations for two C_{18} molecules over 10 ps. Each end of the free octadecane molecules showed a high degree of freedom of molecular motion. Figure 2B shows the snapshots of the trajectory files obtained every 0.5 ps from the end-to-end condensed form (one C_{36} hydrocarbon). As expected, coupling of the ends of the molecules led to considerable restriction of the motion of the chain. As shown in Figure 2B, the relative displacements of the alkyl chain atoms are severely restricted. Figure 3 shows the RMS (Root Mean Square) distance fluctuation based on the molecular coordinate of the initial minimized structure (0 ps). As shown in Figure 3, the tail-linked form (C_{36} chains) has smaller values of RMS distance fluctuation than free form (C_{18} atoms). This relative rigidity of the C36 alkyl chains immobilized at each end can, in principle, be transmitted to neighboring chains via dispersion forces. This possibility was explored using a model system with two phopholipid molecules.

RMS Distance and Angle (Φ) Fluctuations for Two Lipid Model during 10 ps MD Simulations

Figure 4 shows the pictures of snap shots of the trajectory files obtained every 0.4 ps during the 10 ps MD simulation. The unconnected lipids displayed a much wider spectrum of motion (Figure 4A) compared to the ω-1 linked form (Figure 4B). Figure 5 shows a simplified picture of the motional spectrum of the lipids, Φ_m indicate the maximum angle sunbtended by the two alkyl chains at the head group. It is a measure of the extent to which the two alkyl chains are splayed. Figure 5A is an amplitude of Φ_m for

Figure 2. Computer generated pictures of the trajectory snapshots of two octadecane molecules for the 10 ps molecular dynamic simulations. Figure 2A shows the trajectory snap shots for every 0.5 ps (pico second) dynamic simulations for two C_{18} molecules. Each end of the free octadecane molecules showed high degree of freedom of molecular motions. Figure 2B shows the snapshots of the trajectory files obtained every 0.5 ps from the tail-linked (ω-1 linked) form (one C_{36} hydrocarbons). There were no fixed points during the simulation.

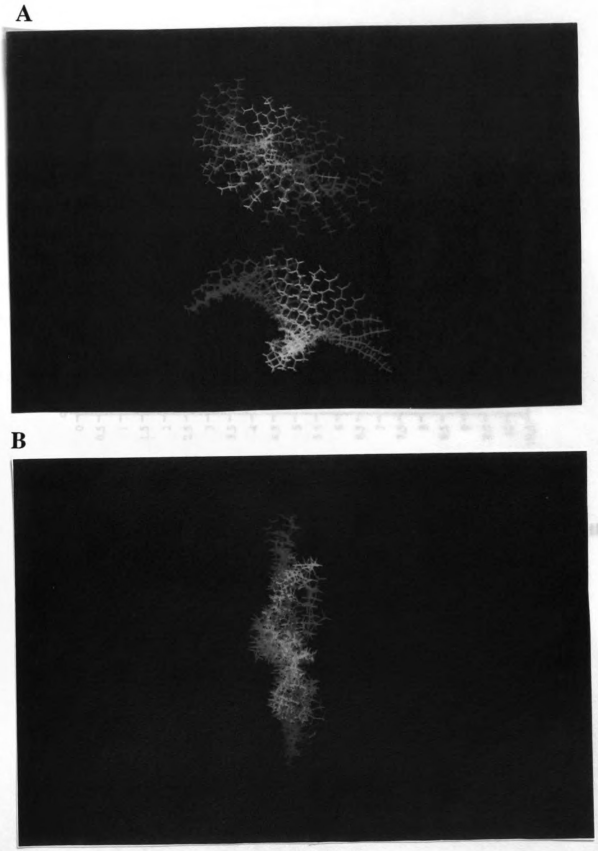

Figure 2

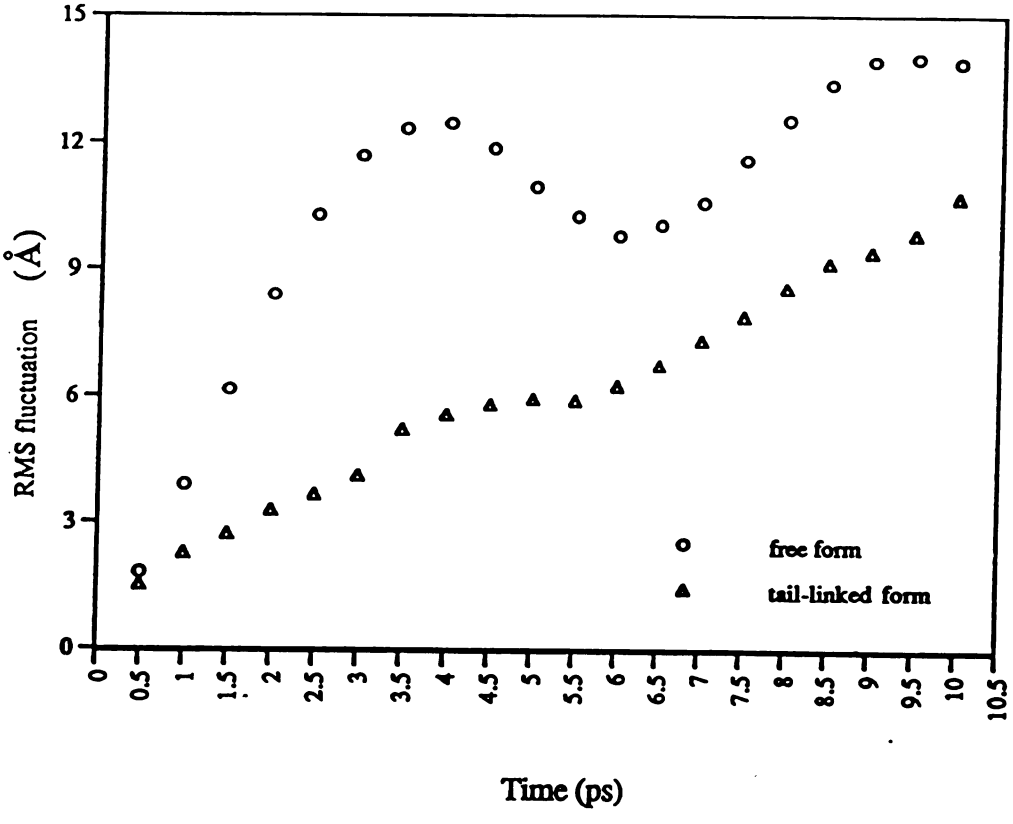

Figure 3. RMS (Root Mean Square) distance fluctuation based on the initial minimized structure as a reference coordinate.

Figure 4. Computer generated pictures of the snapshots of the trajectory files obtained every 0.4 ps during the 10 ps MD simulations. One point in the lipid head group was fixed during the MD simulations. (A) Bilayer form of the two lipids (B) Monolayer form (One of the acyl chains linked at the ω-1 positions).

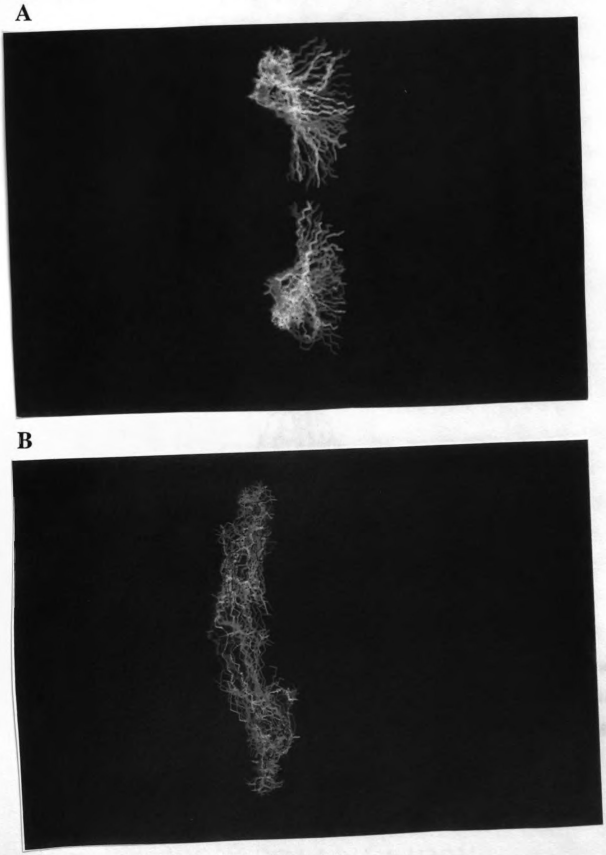

Figure 4

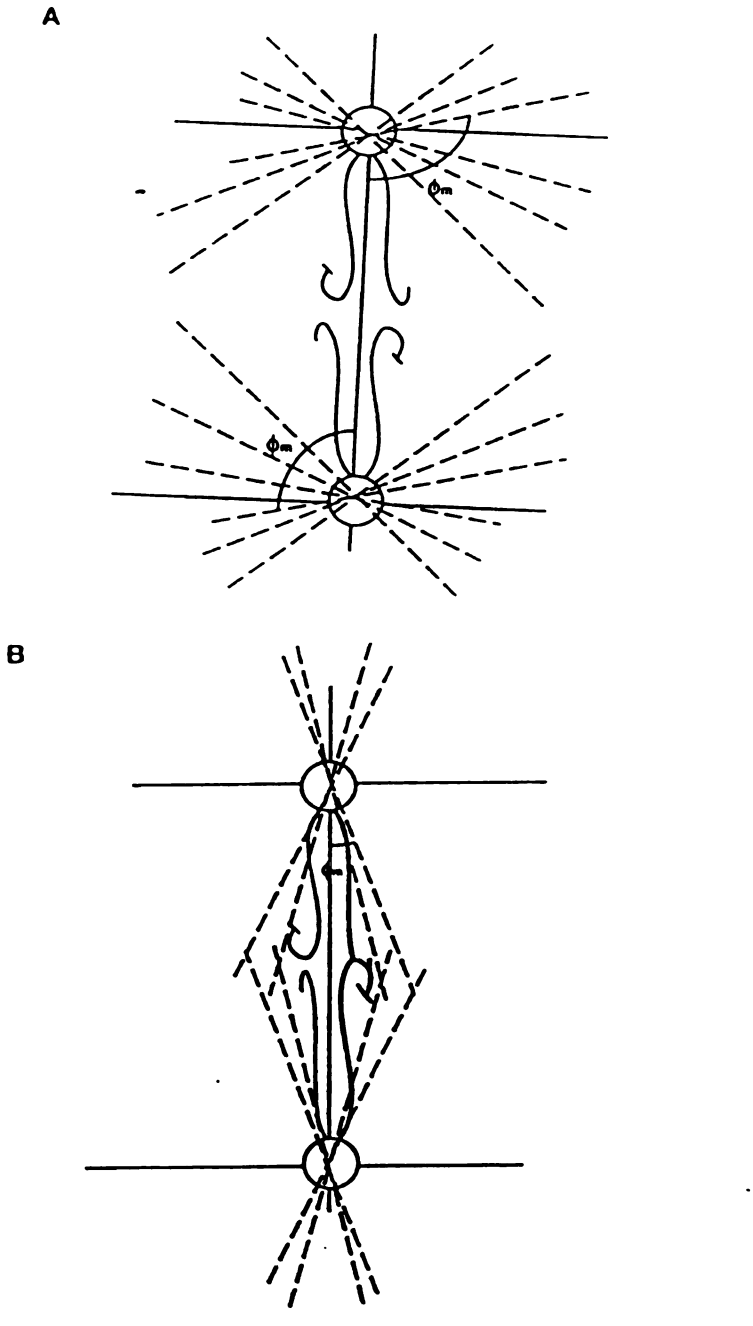

Figure 5. Simplified pictures of the motional spectrum of the lipids. Φ_m indicated the maximum angle subtended by the two alkyl chains at the head group. It is a measure of the extent to which the alkyl chains are sprayed. (A) Bilayer form (B) Monolayer form

the unconnected lipid chains and Figure 5B describes the situation when one alkyl chain of one lipid species is connected to an opposing alkyl chain of the other. Figure 6 shows the angle fluctuation (Φ) between the bilayer form and monolayer form. During the first 3 ps, both systems showed similar angular motional dynamics. However, after the 4 picosecond point, the angular fluctuation differences between them dramatically increased. The simulation indicated that the monolayer form has very restricted angular motional dynamics because of the linkage at the center. Early similarity of the angular fluctuations between them was due to the intrinsic angular fluctuation around the connected centers. It also indicated that transmembrane acyl chains could strongly restrict the isotropic rotations of neighboring lipids in the membrane.

Figure 7 shows the RMS fluctuation of each carbon atom in one chain (*sn*-1; C18) as a function of MD simulation time. It confirmed that as time went on, the degree of motional freedom in one chain became greater towards the end of the chain. Hence, at the end of MD simulation (10 ps) there was an almost a linear relationship between the chain length (carbon number) and the magnitude of the degree of motional freedom. A similar phenomenon was observed in the other chain (*sn*-2 C16) of the same lipids (Figure 8). Figure 9 shows the RMS fluctuation pattern of the carbon atoms of the "transmembrane" alkyl chains for two opposed lipids when two chains are connected to form a transmembrane system. Because of symmetry, only half of the molecules is considered, the half of the transmembrane (C36) acyl chains. The front portion of the chain (C1-C4) shows the big amplitude of the motional fluctuation relative to the center of the chain. The magnitude of the amplitude became small as the number of carbon increases. Finally, after 10 ps, all of the first 18 carbon atom of the chain showed similar values of RMS distance fluctuation. The other free chain (C16) displayed an interesting pattern of the RMS distance fluctuation (Figure 10). It displayed an oscillatory pattern of small magnitude (30 % of that observed when both chains are unconnected) because of attraction to the relatively immobile "transmembrane" chain. This result proves that transmembrane lipid chains can

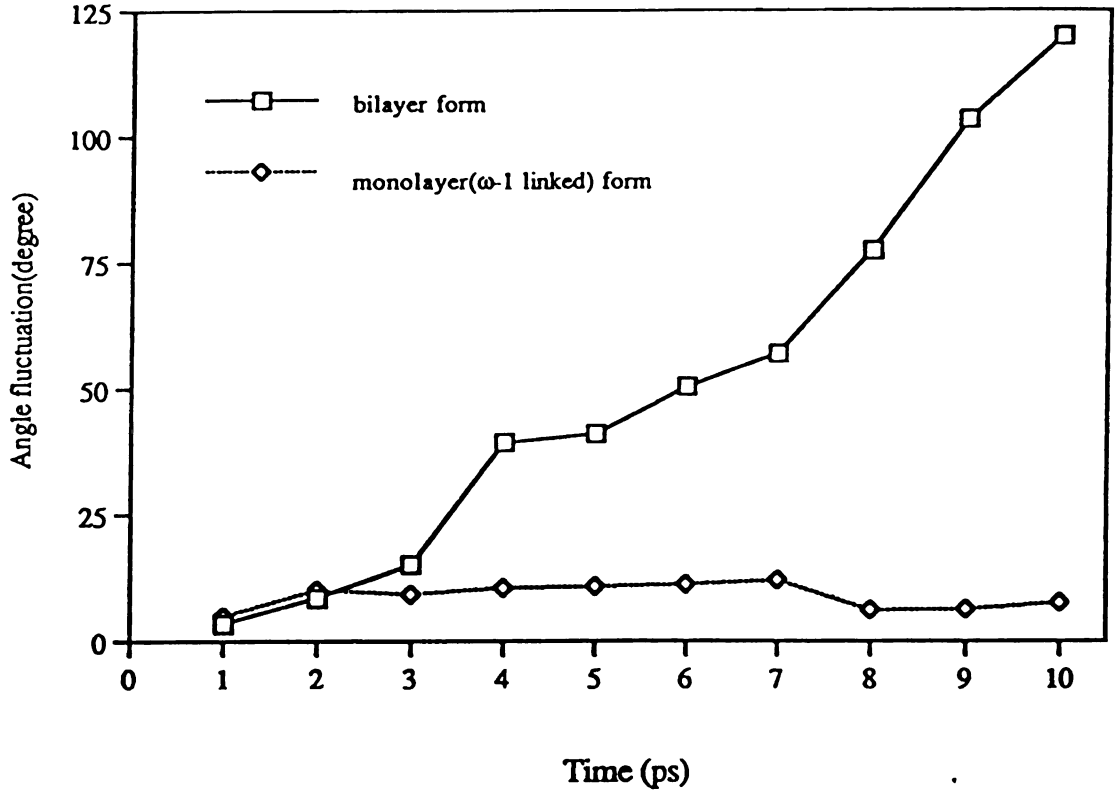

Figure 6. Angle fluctuation between the bilayer form and monolayer form during the MD simulations. The angle ϕ is determined by the trajectories of the lipids referred to the initial position (0 ps). The monolayer form showed very restricted angular motional fluctuations because of linked structure at the center.

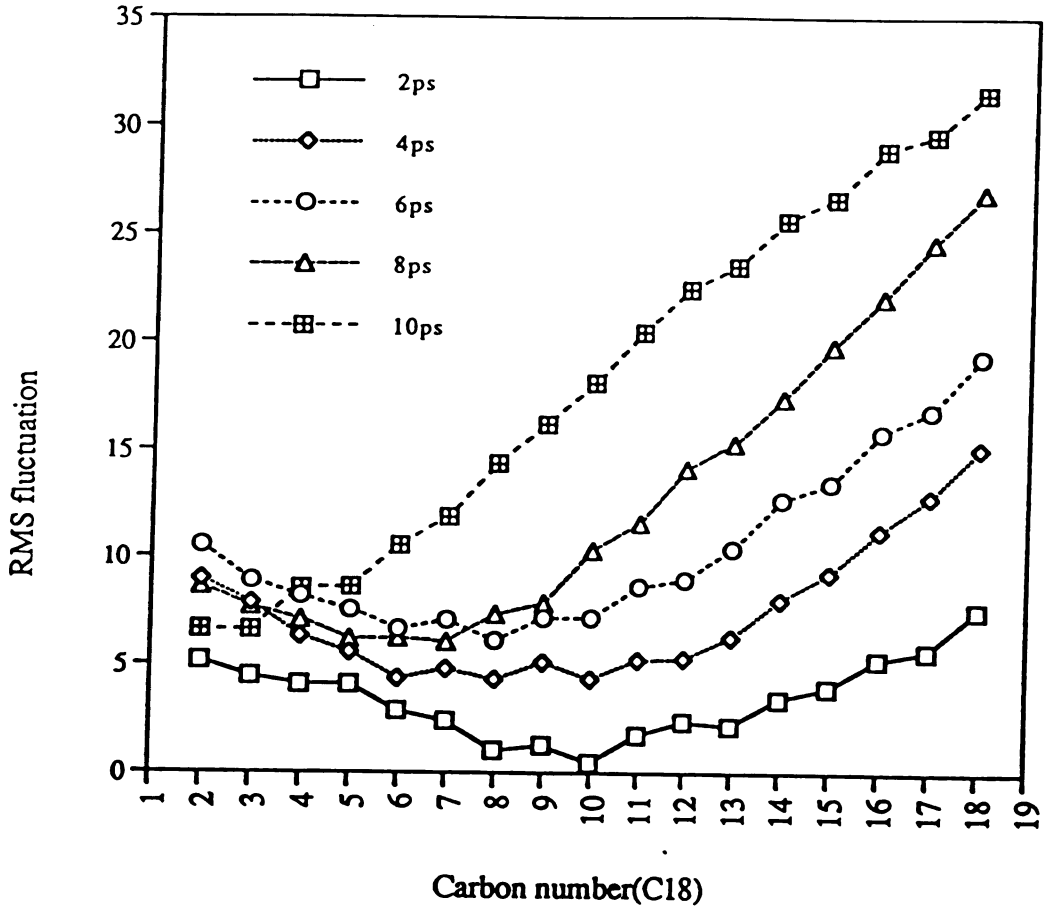

Figure 7. RMS (Root Mean Square) distance fluctuation of each carbon atom in a *sn*-1 chain (C18) of the typical bilayer lipid as a function of MD simulation time. The degree of motional freedom in the chain became greater towards the end of the chain.

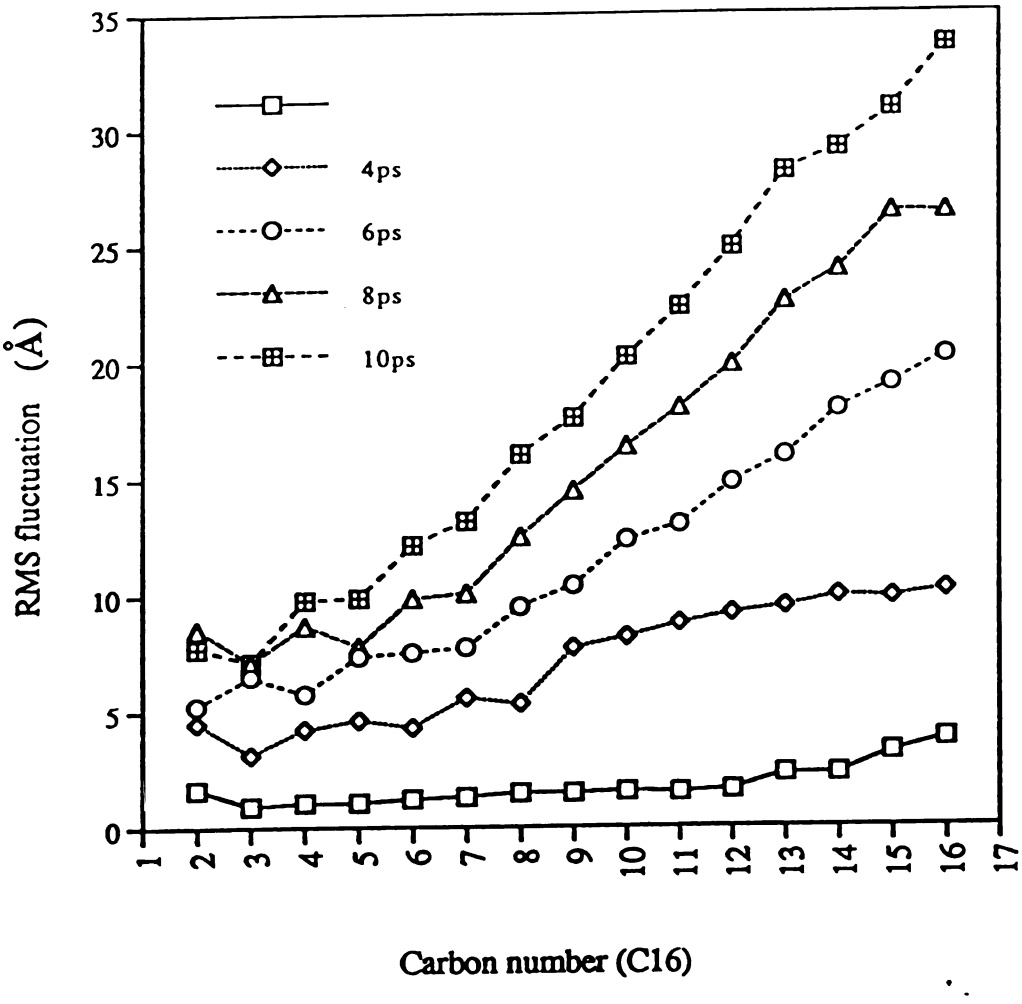

Figure 8. RMS (Root Mean Square) distance fluctuation of each carbon atom in a *sn*-2 chain (C16) of the typical bilayer lipid as a function of MD simulation time. The degree of motional freedom in the chain became greater towards the end of the chain.

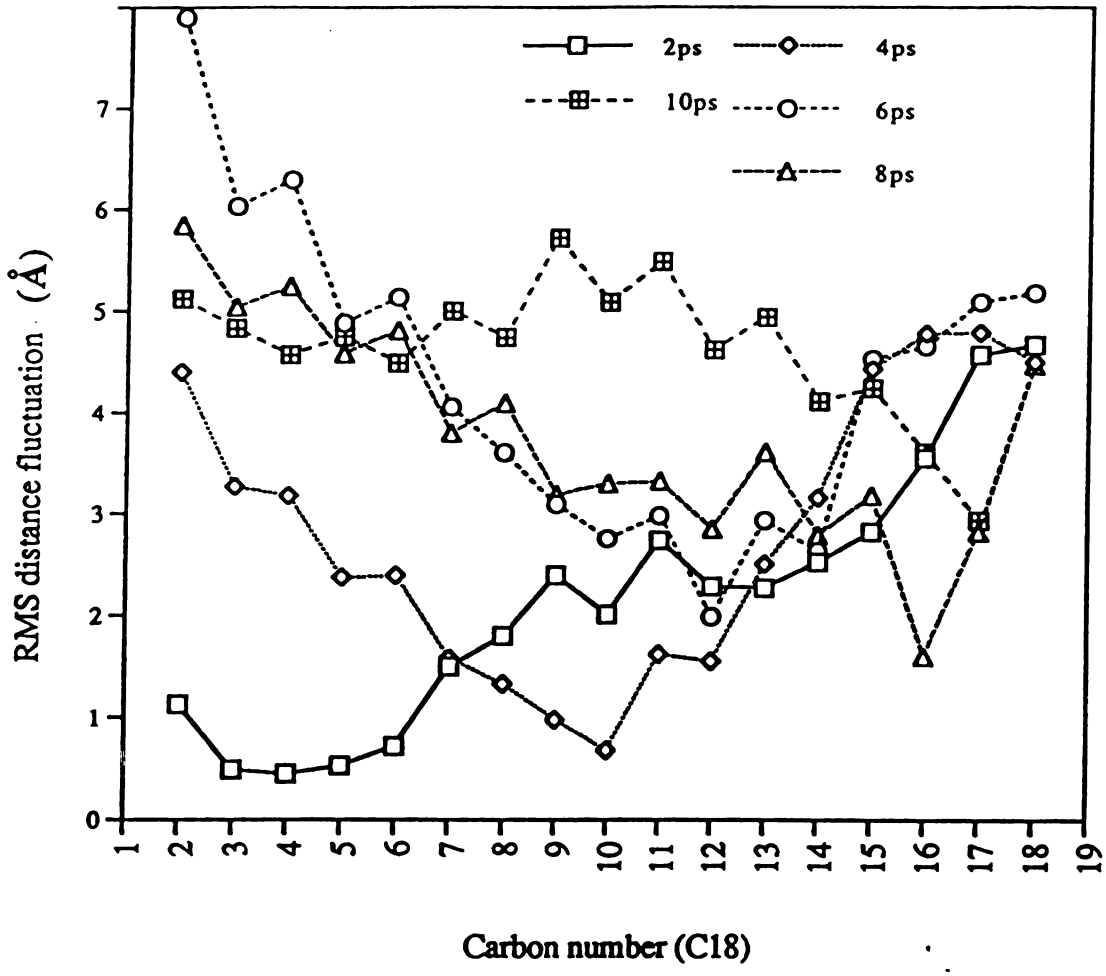

Figure 9. RMS distance fluctuation of the half of the transmembrane monolayer (C36) acyl chain (*sn*-1). It shows some kinds of oscillation of the degree of motional freedom.

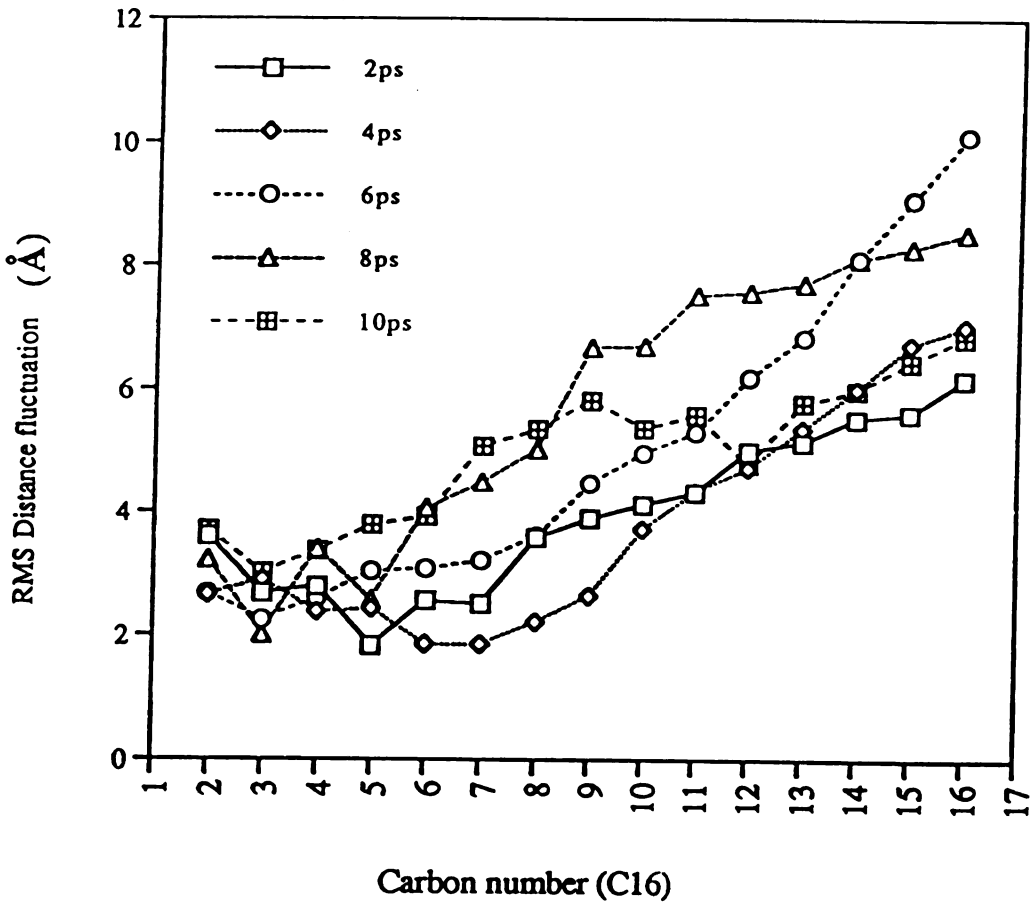

Figure 10. RMS distance fluctuation of the other free chain (*sn*-2, C16) in the monolayer lipid form. It also showed some oscillation pattern of the magnitude of the fluctuation probably due to the motional restriction of the *sn*-1 transmembrane acyl chain. It confirmed that the geometric transition to the ω-1 linked acyl chain modulated the fluctuation of the other acyl chain of the same lipid.

modulate the fluctuation of other free acyl chains in close proximity. Average values of the atomic fluctuation of the lipid chains (C16) were also studied. Figure 11 shows how the amplitude of the fluctuation of the atomic distance changed as time went on from 1 ps, 5 ps to 10 ps. This fact strongly confirmed that the transition to the monolayer from the bilayer makes an important contribution to the reduction of the amplitude of the motional fluctuation. Finally, total RMS distance fluctuation of the lipid was investigated based on the initial lipid coordinates as the reference in Figure 12. Early similarity was broken after the 3 ps. These kinds of data eventually explained the molecular viewpoints of the homeoviscous adaptation of the monolayer form lipid.

Effect of the Transmembrane Alkyl Chains on the Structure and Dynamics of Membrane.

In annealed dynamics, the energy of the structure is minimized gradually without allowing it to be trapped in a conformation that has a lower energy that nearby conformations but higher energy than more distant conformations (*i.e.* a local energy minimum). The structure with the lowest potential energy from the annealing cycle is minimized after the end of the cycle and then written to a trajectory file. Figure 13 shows reminimized structures after the annealed MD simulations (5 annealing cycles) for model membranes of the pure bilayer type (A) and 50 % bipolar monolayer type (B). The typical bilayer phase of the membrane is shown in (A). Here, the width of the bilayer is around 38 Å, the typically observed value. In contrast, the ω-1 linked systems of the bilayer is much more compact and significantly more narrow (around 24 Å). Figures 14A and B show views of the two membrane model systems using different representations (ball-stick model for A and vector model for B). Both structures indicate a clear contraction of the membrane in going from the separated to linked forms. Approximately a 30 % contraction of the membrane width was observed in going from the separated to cross-linked model membranes.

Figure 11. Fluctuation amplitude of the atomic distance of the lipids during the MD simulations at 1 ps (A), 5 ps (B) and 10 ps (C). Transition to the monolayer from the bilayer made an important contribution for lowering the amplitude of the motional fluctuation.

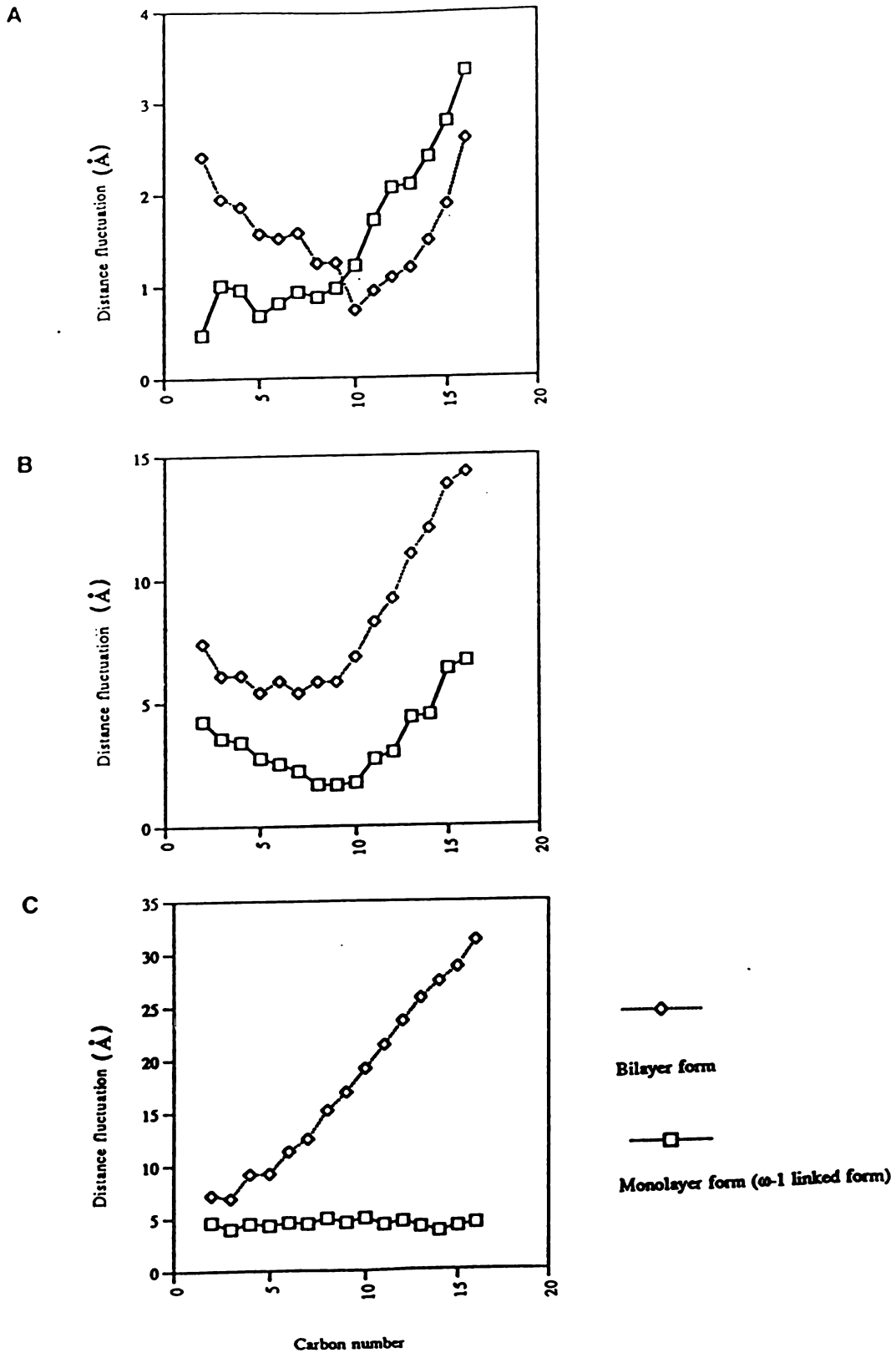
A
B
C
Distance fluctuation (Å)
Carbon number
Bilayer form
Monolayer form (ω-1 linked form)

Figure 11

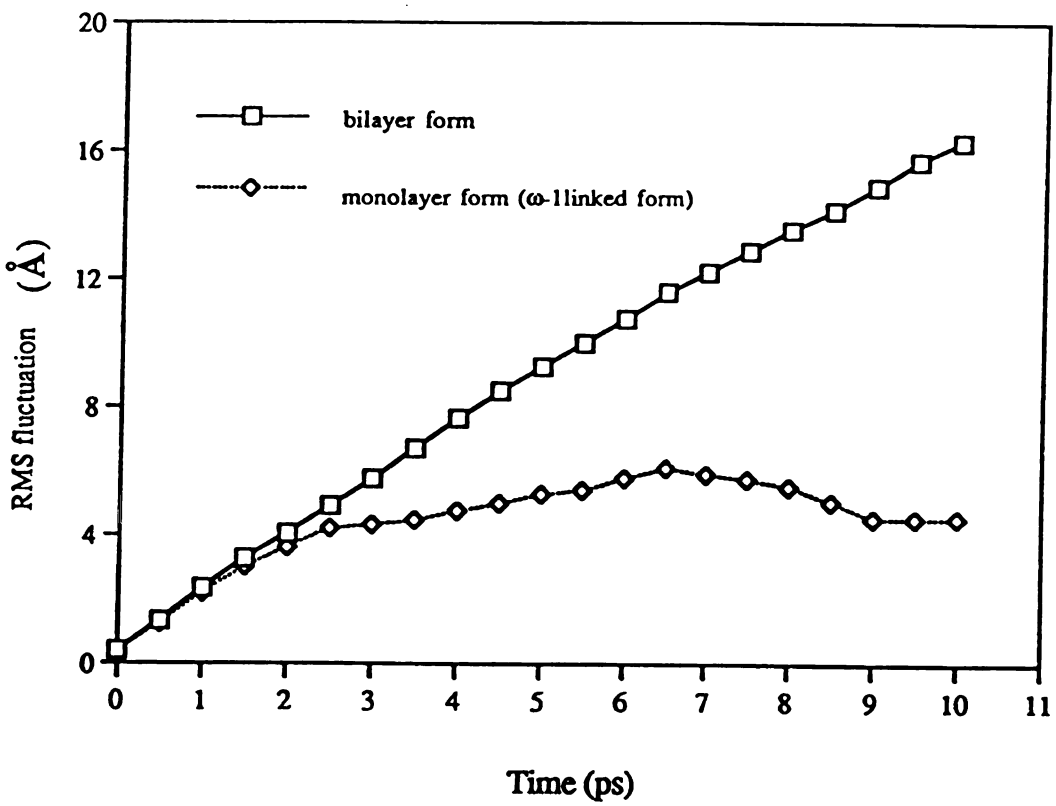

Figure 12. RMS distance fluctuation of the lipid based on the initial lipid coordinates (0 ps) as the reference.

Figure 13. Computer generated pictures of the reminimized structures after the annealed MD simulations (5 annealing cycles) before (A) and after (B) the transition from the bilayer to monolayer form. Typical bilayer phase (Liquid crystalline phase) of the membrane was shown in (A).

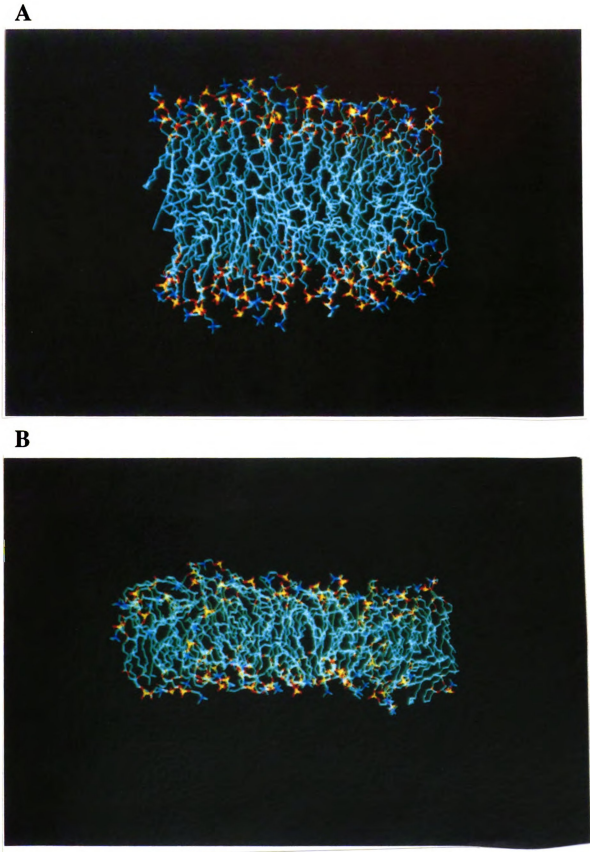

Figure 13

Figure 14. Comparison of the two structures before (right) and after (left) the transition to monolayer in different models (in ball-stick model for (A), vector model for (B)). It shows the clear contraction of the membrane after the transition.

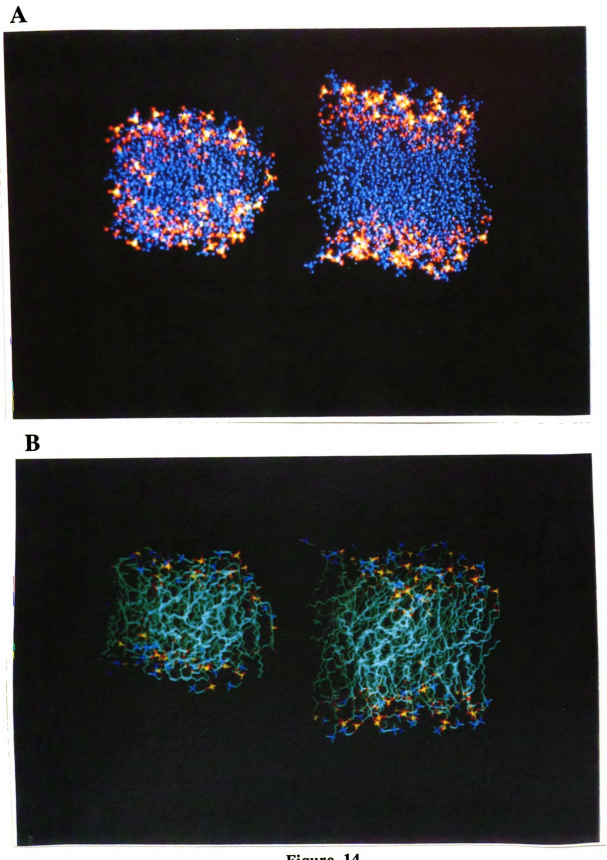

Figure 14

Figure 15A shows the energy-minimized structures of the two connected and two unconnected lipids. The head-to-head distance of the two opposed lipids with the linked acyl chains is significantly smaller than is the case when the lipids are unconnected. This contraction serves to increase the chain-chain interaction (van der Waals interaction) between the tails of the two unconnected lipid chain. There is, therefore, an increased electronic density at the middle of the lipid bilayer (Figure 16). This would also lead to increased interdigitation of the alkyl chains at the middle of the bilayer. Since the Keough's group proposed the interdigitation of the acyl chains of the lipids for membrane packing (20), much research has been performed to prove that interdigitations of the natural membranes could be a general and significant phenomenon (21, 22, 23). Interdigitation of the acyl chains is due to the motional dynamics of the electronic distribution of the acyl chains of the lipids. Figure 15B shows the portions of the monolayer lipids inside the membrane obtained after the transition. Inter- and intradigitation of the acyl chains were clearly shown. The total change of the membrane shape, *i.e.*, contraction of the membrane can be explained by the enhanced inter- and intradigitation of the acyl chains. Figure 17 shows the progressive intra- and interdigitation of the acyl chains of the membrane.

Figure 15. Inter- and intradigitation of the acyl chains shown in the transmembrane structures obtained after the annealed dynamic simulations. (A) A computer generated picture of the energy-minimized structures of a single lipid before (left) and after (right) the transition. The lipid with the linked acyl chains made an initial contraction of its size. (B) A computer generated picture of the portions of the monolayer lipids inside the membrane. This transmembrane structure was obtained after the annealed dynamic simulations. Intra- and interdigitation of the acyl chains were shown. The total change of the membrane shape, *i.e.*, contraction of the membrane was due to the enhanced inter- and intradigitation of the acyl chains.

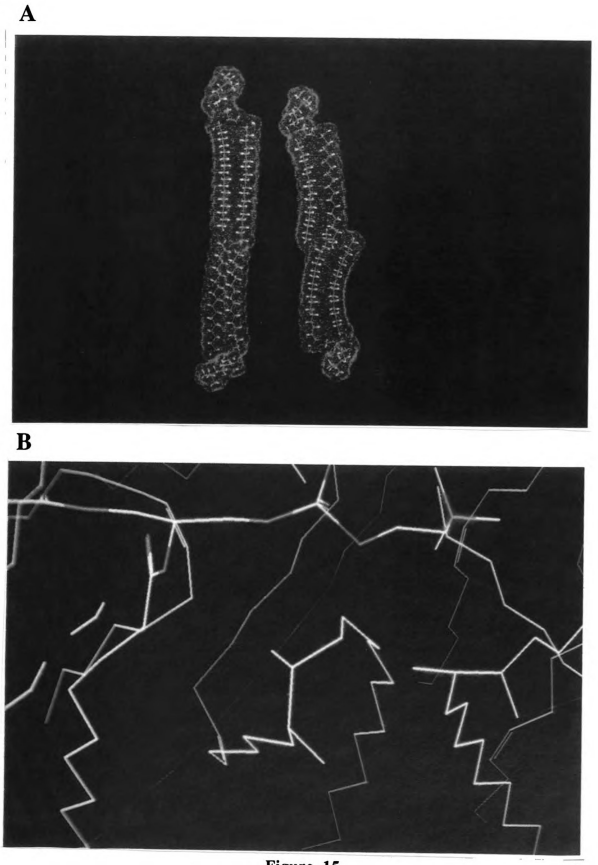

Figure 15

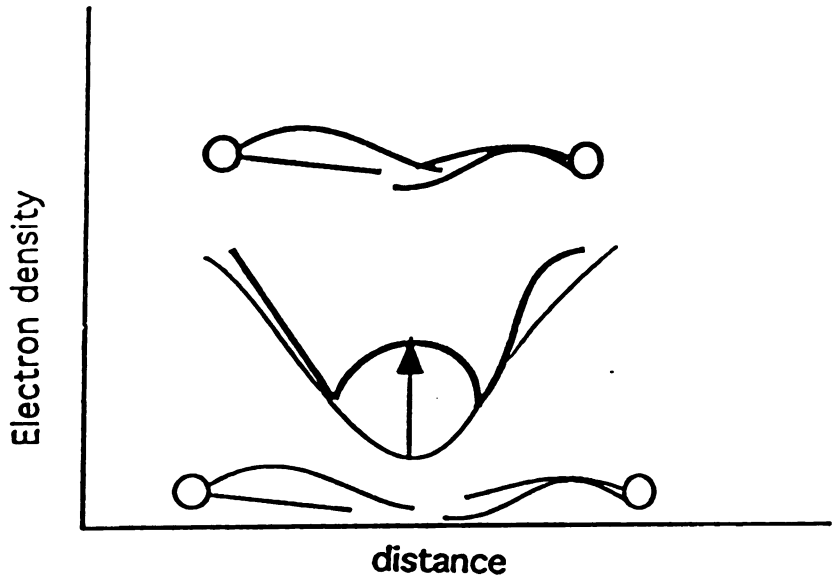

Figure 16. Electronic distributions of the lipids before and after the transition to the monolayer form. The change of electronic distribution of the middle of the lipids would be expected. This changed electronic distribution in the middle made a serious effect on the electronic interactions such as van der Waals interaction (chain-chain interactions).

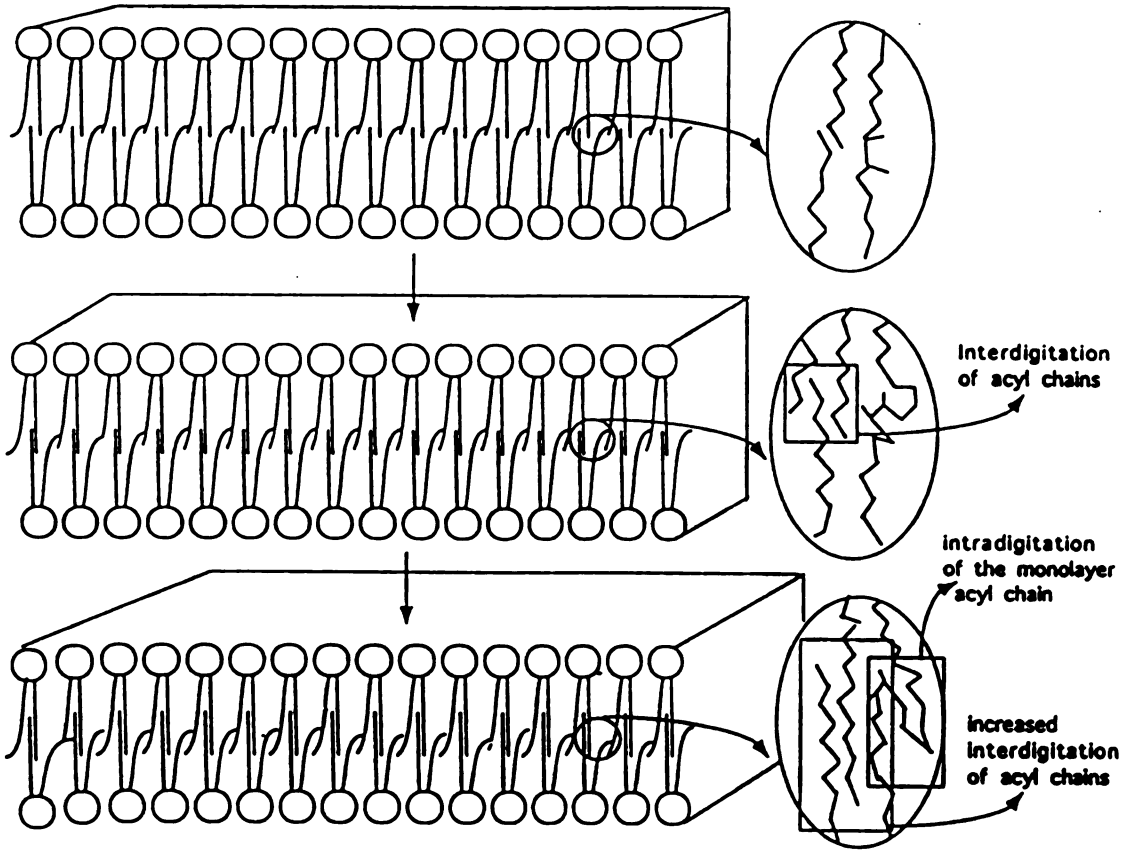

Figure 17. Progressive intra- and interdigitation of the acyl chains in the transmembrane during the simulated annealing calculations. Contraction of the membrane after the transition to monolayer could be explained by intra- and interdigitation of the acyl chains.

CONCLUSIONS

The effects of transmembrane (ω-1 linked hydrocarbon chains) on the molecular motions of model systems from the free hydrocarbon chains to whole membrane model (64 lipids) were studied using molecular mechanics and molecular dynamics simulation methods. RMS (Root Mean Square) distance fluctuation and angle parameters were used for the indices for the description and characterization of the molecular motions. The molecular motional parameters of the lipid in the typical bilayer form and monolayer form (ω-1 linked form) were compared during a 10 ps dynamic simulation. A dramatic decrease in the degree of the motional freedom was observed on going from the bilayer to the bipolar monolayer form. This change of the motional dynamics appears to induce the favorable interdigitation of the tails of the chains thus enhancing van der Waals attraction. Simulated annealing method was used for the general prediction of the membrane structures before and after the transition from the bilayer to monolayer systems. After the transition to the monolayer form, the interdigitation of the acyl chains of the membrane resulted in compaction of the membrane structure. These findings have special significance in light of the recent discovery of the structural transition from bilayer to bipolar monolayer in *Sarcina ventriculi*.

REFERENCES

1. Jung, S., Lowe E.S., Hollingsworth I. R ., and Zeikus, J. G. (1993) *J. Biol. Chem.* **268**, 2828-2835
2. Jung, S. and Hollingsworth I. R .(1993) in preparation (*JBC* submitted)
3. Jung, S. and Hollingsworth I. R .(1993) in preparation (*JBC* submitted)
4. Ingram, L. O. (1982) *J. Bacteriol.* **149**, 166-172
5. Ingram, L. O. (1990) *Crit. Rev. Biotechnol.* **9**, 305-319
6. Ingram, L. O., and N. S. Vreeland. (1980) *J. Bacteriol.* **144**, 481-488
7. Schreir, S., Polnaszek, C. F., and Smith, I.C. (1978) *Biochim. Biophys. Acta* **515**, 395- 436
8. Campbell, I.D., and Dwek, R.A. (1984) In *Biological Spectroscopy* Benjamin/Comming Publishing Co., Menlo Park, California
9. McCammon, J.A., and Harvey,S.C. (1987) In *Dynamics of Proteins and Nucleic Acids*, Cambridge University Press, Cambridge
10. Brooks, C.L. III, Karplus, M., and Pettitt, M. (1988) *Adv. Chem. Phys.* **LXXI**
11. Scott, H.L. (1984) *Chem. Phys. Lett.* **109**. 570 - 577
12. Raghavan, K., Rami, R.M.and Berkowitz, M.L. (1992) *Langmuir* **8**, 233 -240
13. Kirkpatrick, S., Gelatt, C.D., and Vecchi, M.P. (1983) *Science* **220**, 671- 680
14. Bounds, D.G. (1987) *Nature* **329**, 215 - 219
15. Mayo, S.L., Olafson, B.D., and Goddard, W.A. III (1990) *J. Phys. Chem.* **94**, 8897- 8909
16. Gasteiger, J., and Marsili, M (1980) *Tetrahedron* **36**, 3219 - 3226
17. Fletcher, R., and Reeves, C.M. (1964) *Comput, J.* **7**, 149 -156
18. Verlet, L. *Phys. Rev.* 1967, **159**, 98 -105
19. Gennis, R.B. (1989) In *Biomembrane* (Cantor, C.R Eds.) pp166-198, Springer-Verlag, New York, NY

20. Keough, K. M.W. and Davis, P.J. (1979) *Biochemistry* **18**, 1453-1459

21. Huang, C. and Mason, J.T. (1986) *Biochim. Biophys. Acta* **864**, 423-470

22. Mattai, J., Sripada, P.K. and Shipley, G.G. (1987) *Biochemistry* **26**, 3287-3297

23. McGibbon, L., Cossins, A.R., Quinn, P.J., and Russell, N.J. (1985) *Biochim. Biophys. Acta* **820**, 115-121